THE UNIVERSITY *of* EDINBURGH

Satellite Based Estimation of Global Biogenic Methane Emissions

A. Anthony Bloom

Doctor of Philosophy
University of Edinburgh
2011

Abstract

Atmospheric CH_4 is derived from both natural and anthropogenic sources, and the rapid increase in atmospheric CH_4 levels over the past two centuries has predominantly been a result of increased anthropogenic emissions. Nonetheless, natural sources have also changed as a result of global change, and quantifying the fluxes of CH_4 from these sources, and their associated climatic feedbacks, is of paramount importance. In this thesis I have developed a method to upscale the global CH_4 emissions from UV irradiation of foliar pectin (chapter 2). I have quantified the magnitude and distribution of CH_4 emissions from wetlands on a global scale and determined the sensitivity of wetlands to temporal changes in water volume and temperature (chapters 3 and 4). Finally I determine that tropical wetland organic matter decomposition on a global scale behaves non-linearly over seasonal timescales. This implies a substantially different seasonality in CH_4 emissions from wetlands (chapter 5). I show that (i) satellites such as MODIS and GRACE can be used to improve the understanding of individual CH_4 sources and sinks, and (ii) the newly available satellite observations of CH_4 can be effectively used for more than constraining atmospheric chemistry and transport model inversions. Moreover, the work shown in this thesis has contributed new biogenic CH_4 source estimates, but has also posed new questions which will ultimately help guide new projects in the atmospheric CH_4 research area.

Declaration

I declare that this thesis was composed by myself and that the work contained therein is my own, except where explicitly stated otherwise in the text.

A. Anthony Bloom

Acknowledgements

I am indebted to my PhD supervisor Paul Palmer, for his excellent supervision, his keenness in helping me pursue new ideas and his willingness to engage with every stage of the PhD process. I would like to thank Dave Reay, Andy Mcleod, Christian Frankenberg and Annemarie Fraser for their support, regular feedback and participation in my work, and members of the UoE School of GeoSciences staff for their support and feedback on several occasions. The Paul Palmer Earth Observation Chemistry group, including Mike Barkley, James Barlow, Eddy Barratt, Claire Bulgin, Silvia Caldararu, Xuefeng Cui, Liang Feng, Annemarie Frasier, Siegfried Gonzi, James Howie, Catherine Hardacre, Qian Li, Stephan Matthiesen, Mark Parrington, Rob Trigwell and Win Trivitayanurak, have all been incredible source of help and support throughout my PhD. I would like to acknowledge the UoE School of GeoSciences for giving me the opportunity to teach throughout my studies and NERC for funding this PhD.

It's been hard to remember when it was I first decided to undertake a PhD, but I do remember as a five-year-old at the UC Berkeley campus I noticed academics had occasional access to free food, and I suppose my first academic ambitions manifested themselves there. Ever since, countless people have provided help and support throughout the years in many ways, and I thank each and every one of them. Here I will try to acknowledge many of those who provided support and encouragement in the somewhat less distant past. My thanks to all who helped me acquire the knowledge and skills through higher education: from UCL, Phillip Meredith and Frederik Simmons who were endlessly supportive of my decision to pursue a career in academia, Tom Newman for his encouragment and particular enthusiasm for Earth Sciences, Ian Brooks and Jurgen Neuberg from Leeds for their support through the MRes in Physics of the Earth and Atmosphere course. The fantastic work environment in the Attic of the Crew Building has always been a limitless source of inspiration. A big thanks to Silvia Caldararu, Theresa Meacham, Jonny Atherton and Lucy Rowland for bouncing around ideas and for all the constructive criticism. A big thanks to Giorgos Xenakis, whose latex thesis template has saved many PhD students many hours of thesis writing and formatting. A PhD would potentially be more productive and a lot less enjoyable without the animosity of the office environment, so a big thanks to Sigrid Dengel, Stephen Carr (rubberband wars, summer 2008), Nancy Burns and Emily Woollen and Jenny Wright (the coffee room arguements and the eventual confiscation of the cow-bell), Mack Saraswat (for the endless yet enlightening debates) and everyone else I have shared the crew attic with. The crew attic white board must also get an acknowledgement, for so many ideas have been exchanged there. Many thanks to Leon Kapetas (for trying and ultimately failing to be a teacher and mentor in backgammon), as well as Romain, Jamesy, Lorna, Oliver Sus, for the meals, the mushrooms excursions, all the support, and Settlers of Catan. And of course it would have not been the same without flatmates, Beavis the cat, the parents, the twins, Παπού and Γιαγιά . And I cannot

thank the Dunya Ensemble enough, for our performances, and for bringing the magic of music into everyday life. Alice you are wonderful.

“The Earth is round, like an orange.”

Gabriel García Márquez, *One Hundred Years of Solitude*, 1967

Contents

List of Figures

Preface

Methane is the third most important atmospheric greenhouse gas after H_2O and CO_2. Over the past decade we have made some big leaps in our understanding of the role of CH_4 in the Earth's atmosphere. Some of the most significant events in the field include the quantification of the long-term radiative forcing of CH_4 over decadal timescales, the stagnation of atmospheric CH_4 levels during 2000-2007, and the discovery of CH_4 emissions from vegetation.

The last decade has seen significant advances in our understanding on the sources, sinks and distribution of CH_4 on a global scale. Most notable is our ability to observe lower tropospheric CH_4 from space, thus providing us with a continuous and global coverage of the atmosphere's CH_4 concentration. Nonetheless, many questions remain unanswered: Why did the atmospheric CH_4 growth rate slow down at the start of the millenium? How much does each source and sink of CH_4 contribute to the global CH_4 cycle, and how will this change in the coming years? Are plants a significant source of CH_4? The aim of my thesis is to help address these questions by improving the understanding of the spatial distribution and temporal behaviour of natural CH_4 sources from wetlands, bogs, fens, rice paddies and aerobic foliar emissions from terrestrial vegetation on a global scale.

To improve our understanding and ultimately quantify these CH_4 sources, I develop process-based models which I constrain by amalgamating satellite-derived observations of CH_4 and other related datasets, such as gravity derived equivalent water height from the Gravity Recovery and Climate Experiment (GRACE) twin satellites, meteorological surface temperature re-analyses and Moderate-Resolution Imaging Spectroradiometer (MODIS) leaf area. Finally I show how the combination of these datasets can also be used to determine the CH_4 source mechanisms as well as an improved quantification of the global atmospheric CH_4 budget.

Chapter 1

Introduction: Methane in the Earth's Atmosphere

1.1 A History of Atmospheric Methane

Throughout the Earth's history, methane (CH_4) has played a prominent role in the Earth's atmosphere as a potent greenhouse gas. During the first half of the Earth's history, the atmospheric concentration of CH_4 may have been up to 20,000 times greater than present day levels, due to the absense of atmospheric O_2 and the potential biogenic production of CH_4 by early life forms (e.g. Kasting et al., 2001; Kharecha et al., 2005; Haqq-Misra et al., 2008). The gradual appearance of oxygen-producing cyanobacteria occured over hundreds of millions of years (Kasting and Siefert, 2002), and as a result oxygen became a significant component of the Earth's atmosphere. About 2.3 million years ago, the accumulation of oxygen in the atmosphere lead the loss of atmospheric CH_4 (Kasting and Ono, 2006). In part, the oxygen reacted with the atmospheric CH_4: the Earth's cooling due to the atmospheric CH_4 depletion potentially caused one of Earth's major "Snowball Earth" episodes (Kump, 2008). But more significantly, the presence of O_2 in the atmosphere caused one of Earth's first mass extinctions (Schirrmeister et al., 2011), and as a result almost all of anaerobic life became extinct.

Although the great oxygenation event resulted in a dramatic reduction in atmospheric CH_4 abundance, CH_4 continued to play a significant role throughout geological time

as a prominent greenhouse gas. Wetlands, currently the single largest source of CH_4 in the atmosphere, have been the dominant source of CH_4 throughout geological time (e.g. Weber et al., 2010). Global wetland CH_4 production is determined largely by temperature and global wetland area (Gedney et al., 2004). The extent and temperature of wetlands changed with climate (e.g. van Huissteden, 2004), and hence stong climatic feedbacks are associated with wetland CH_4 emissions. The close relationship between temperature and CH_4 has been observed in paleo-atmospheric CH_4 concentrations, such as those derived from trapped air-bubbles in the Vostok ice core (e.g. Petit et al., 1999). The retrieved isotopic temperature, CO_2 and CH_4 have all covaried during this time period. Causality between these quantities is a subject of speculation, and it has been proposed that CH_4 may have triggered rapid climatic changes in the past (e.g. Etiope et al., 2008).

Through agriculture and livestock rearing, humans may have begun to alter the atmospheric CH_4 budget from as far back as 3000 B.C. (Ruddiman, 2001, 2003). Prior to the industrial revolution, anthropogenic emissions (including rice cultivation, ruminants and biomass burning) may have contributed up to an additional 50% higher atmospheric CH_4 concentration to background CH_4 levels (Ruddiman, 2001). Nonetheless, until the onset of the industrial revolution, CH_4 concentrations in the atmosphere were relatively constant at around 700ppb, and as the impact of human beings on the Earth's biosphere became more prominent, anthropogenic emissions dramatically increased over the past 250 years (Wuebbles and Hayhoe, 2002). As a result, atmospheric CH_4 concentrations have more than doubled over the past two centuries. Figure 1.1 shows the concentrations of CH_4 derived from air bubbles trapped in three Antarctic ice cores since 1000 A.D. (Etheridge et al., 1998).

The exponential growth of CH_4 continued uninterrupted, until a slowdown in the CH_4 growth became clear in the 1980s (Steele et al., 1992). Due to a change in the balance of CH_4 sources and sinks, the growth of atmospheric CH_4 halted at the turn of the millenium. Steele et al. (1992) predicted that by 2006 atmospheric CH_4 would reach a maximum. This prediction appeared to be accurate until 2007 (see Figure 1.2), where the atmospheric CH_4 concentration began to show a renewed growth rate (Rigby

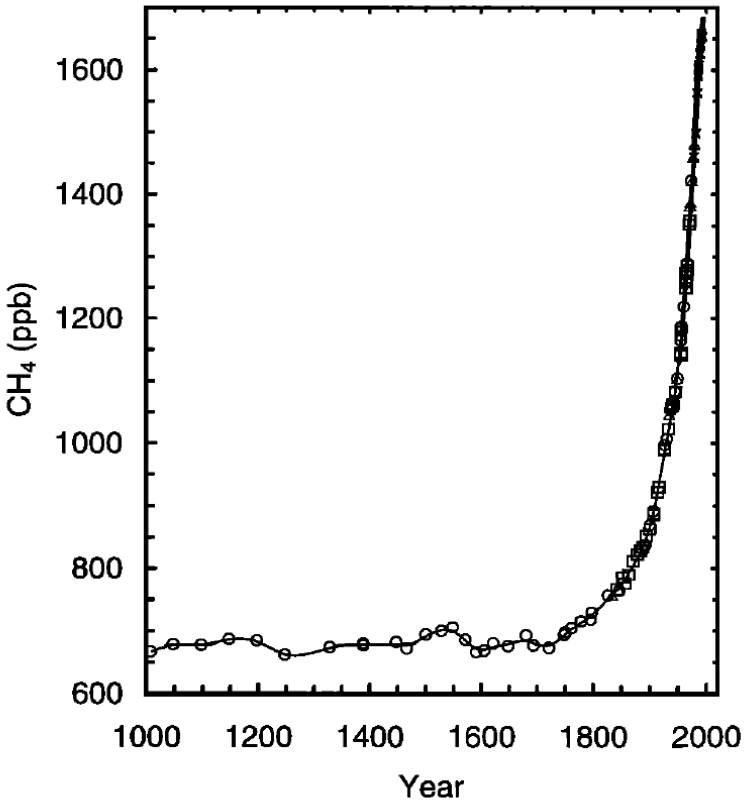

Figure 1.1: Atmospheric CH_4 concentrations (ppb) between 1000 - 2000 A.D. derived from trapped air bubbles in three ice cores taken from Antarctica. Figure adapted from Etheridge et al. (1998).

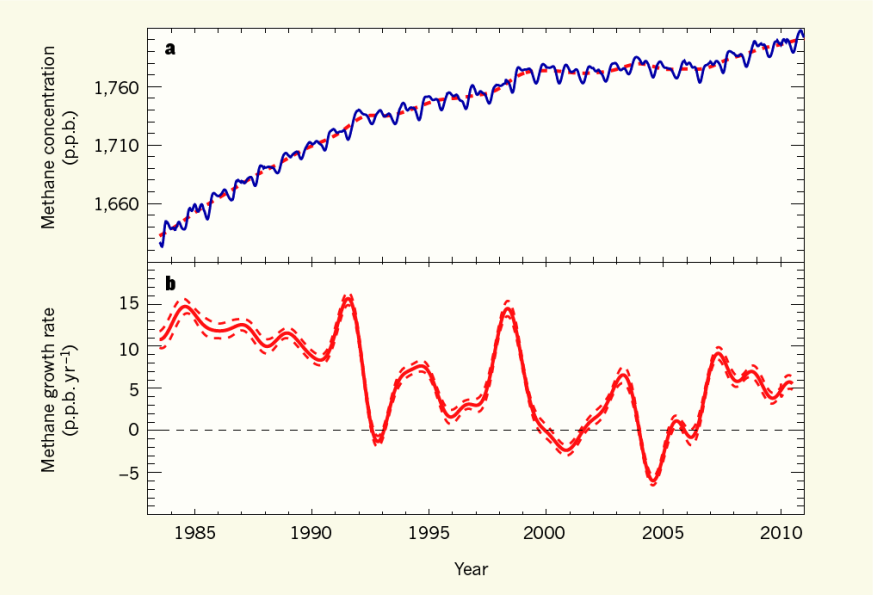

Figure 1.2: Atmospheric CH_4 concentrations (ppb) from 1984 to 2010 (top) and atmospheric CH_4 growth rate (ppb yr^{-1}) during the same period. Figure taken from Heimann (2011).

et al., 2008; Dlugokencky et al., 2009). It is currently unclear which individual CH_4 sources and sinks have been responsible for the alteration of the atmospheric CH_4 balance over the past 30 years, although it has been suggested that a combination of a reduction in rice paddy and wetland emissions in the Northern Hemisphere resulted in a reduced CH_4 growth rate over the past 30 years (Kai et al., 2011). More recently, an increase in boreal and tropical wetland CH_4 emissions in 2007 and 2008 may have lead to the renewed atmospheric CH_4 growth (Dlugokencky et al., 2009). It is therefore of paramount importance to improve our understanding of the spatial behaviour and temporal distribution of CH_4 sources and sinks on a global scale.

1.2 Observing Atmospheric CH_4 on a Global Scale

The first identification of CH_4 was made in 1776 by an Italian scientist who noticed bubbles rising from the bottom of a lake, which he identified as “combustible air” (Balch, 1979; Reay et al., 2007). By mapping out the solar spectrum, Migeotte (1948) discovered the presence of CH_4 in the atmosphere. From the 1960s onwards the scientific community began to grasp the complexity of CH_4 production, transport and

destruction in the Earth's atmosphere (Bainbridge and Heidt, 1966). Although the warming effect of CH_4 in the atmosphere had been addressed (e.g. Wang et al., 1976), CH_4 was assumed to be constant in the atmosphere (e.g. Fowler et al., 1995), until Rasmussen and Khalil (1981) observed a steady growth and determined the warming effect on the Earth's atmosphere as a result of a steady increase of atmospheric CH_4. The first CH_4 air concentration measurements at a global scale were performed by the NOAA Climate Monitoring and Diagnostics laboratory. Measurements were taken from both fixed sites and ships, and span continuously from May 1983 (Steele et al., 1992) to the present day (Dlugokencky et al., 2009).

With an ever expanding network of ground-based measurements our knowledge of atmospheric CH_4 distributions has been steadily improving over the past decades. Nonetheless, some of the largest advances in spatially deciphering the atmosphere's composition have been made through satellite observations of CH_4. By measuring the atmosphere's electromagnetic spectrum from space it is now possible to retrieve information on the atmosphere's CH_4 concentration: this is essentially the space-borne equivalent of the method employed by Migeotte (1948), with the advantage of sounding the atmosphere at regular spatial and temporal intervals. Frankenberg et al. (2005) published the first atmospheric CH_4 map of the Earth's atmosphere. The SCIAMACHY instrument onboard the European Space Agency's ENVISAT measures the solar radiation from the Earth's surface. By comparing the sun's and the atmosphere's absorption spectrum, Frankenberg et al. (2005) and subsequently others have retrieved the concentration of CH_4 in the Earth's Atmosphere. Figure 1.3 shows a map of mean atmospheric CH_4 concentrations during 2004, with a spatial resolution of 30km $\times$ 60km and a claimed precision of roughly 1.8 % (Frankenberg et al., 2006). As expected, the CH_4 concentrations were elevated over areas with known high CH_4 emissions, such as South Asia, East Asia, Europe and the North American east coast. Low concentrations were found in the Southern Hemisphere, where the total CH_4 source is an order of magnitude lower. The original SCIAMACHY retrievals have since been revised as a water-vapour related bias was found to persist over tropical areas (Frankenberg et al., 2008a,b). Other satellites capable of retrieving CH_4 concentrations in the atmosphere include the Tropospheric Emission Spectrometer (TES) on

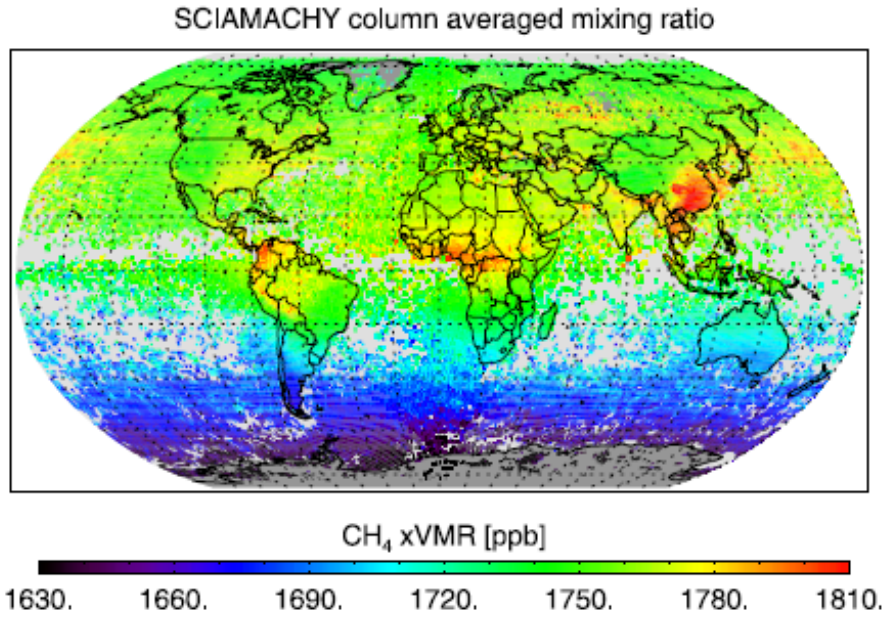

Figure 1.3: Mean atmospheric CH_4 volume mixing ratio at a 1° x 1° resolution during 2004. Figure adapted from **?**.

board the NASA Aura Mission, the ESA Infrared Atmospheric Sounding Interferometer (IASI) and the JAXA Global Greenhouse Gas Observation by Satellite (GOSAT) satellites (Beer, 2006; Razavi et al., 2009; Yokota et al., 2009). While the IASI and TES retrievals are sensitive to the upper troposphere, SCIAMACHY and GOSAT are sensitive to the lower troposphere and hence contain more information on surface CH_4 sources.

As satellite CH_4 retrievals provide the mean volume mixing ratio (VMR) of the atmospheric column, satellite observations of atmospheric CH_4 VMR are only an indicator of the local source/sink strength at a given place and time. Moreover, satellite observations of CH_4 VMR are only available for daytime cloud-free conditions (e.g. Frankenberg et al., 2005). In order to infer the magnitude of sources and sinks, a relationship must be established to link the available column CH_4 VMR and the CH_4 sources and sinks. Such a bridging relationship needs to account for the effects of atmospheric transport, tropospheric chemistry, the sensitivity of CH_4 VMR retrievals to different altitudes, and the lack of data during night-time or cloudy conditions (e.g. Bergamaschi et al., 2009). An example of such a relationship is an atmospheric chemistry and

transport model (ACTM) inversion (e.g. Bousquet et al., 2006). Overall, a variety of inversions methods can now be used to infer greenhouse gas (GHG) sources and sinks from satellite observations of atmospheric GHG concentrations (e.g. Bousquet et al., 2006; Bergamaschi et al., 2009; Feng et al., 2009, 2011).

1.3 Methane Sources and Sinks in the 21^{st} Century

The balance between CH_4 sources and sinks determines the concentration of CH_4 and ultimately the lifetime of CH_4 in the Earth's atmosphere. It is crucial to determine the anthropogenic contribution to atmospheric CH_4 and the ever-changing emissions from natural CH_4 sources in order to understand the global CH_4 budget, mitigate human CH_4 emissions, and improve projections of future levels of atmospheric CH_4. While we have a rough quantitative understanding of the magnitude of individual natural and anthropogenic sources, there is an urgent need to increase the spatial and temporal resolution and reduce the uncertainty associated with individual CH_4 sources and sinks. In this section I will cover the sources and sinks of CH_4, introduce wetland and foliar CH_4 emissions to provide a background for chapters 3 - 5.

1.3.1 Natural Sources of Methane

Natural sources account for approximately 40% of the global atmospheric methane source (Denman et al., 2007). In turn, biogenic sources of CH_4 account for the majority of the natural methane source (Wuebbles and Hayhoe, 2002). In biogenic CH_4 production, methanogens produce CH_4 in anoxic environments, such as the digestive track of ruminants and termites (Wuebbles and Hayhoe, 2002). Overall, wetlands, fens, bogs and and all flooded soil expanses account for the bulk of the natural source (100-231 Tg CH_4 yr^{-1}). The remaining natural biogenic sources include oceans (4-15 Tg CH_4 yr^{-1}), wild animals and termites (35-44 Tg CH_4 yr^{-1}). Non biogenic sources include geological sources (4-14 Tg CH_4 yr^{-1}), hydrates (4-5 Tg CH_4 yr^{-1}) and wildfires (2-5 Tg Tg CH_4 yr^{-1}) (Denman et al., 2007).

Recent findings have identified the aerobic emission of CH_4 from plant leaves (Keppler et al., 2006), estimated to account for 62 - 236 Tg CH_4 $yr^{-1}$of the atmospheric CH_4 source. Laboratory measurements of CH_4 emissions from UV-irradiated pectin (McLeod et al., 2008) confirm that an aerobic pathway for CH_4 emissions exists. Nonetheless, recent revisions to the upscaling method used by Keppler et al. (2006) indicate that the aerobic plant CH_4 emission source was over-estimated. I examine the recent developments of this work in section 1.4.1.

1.3.2 Anthropogenic CH_4 Emissions

Due to the rapid industrialisation over the past two centuries, new anthropogenic sources of CH_4 became significant contributors to the atmospheric CH_4 budget. Total anthropogenic sources account for 264 - 428 Tg CH_4 yr^{-1}. Major sources include livestock rearing (76-189 Tg CH_4 yr^{-1}), rice agriculture (31-112 Tg CH_4 yr^{-1}), energy production (74-77 Tg CH_4 yr^{-1}), coal mining (30-48 Tg CH_4 yr^{-1}), landfills and waste (35-69 Tg CH_4 yr^{-1}) and biomass burning (14-88 Tg CH_4 yr^{-1}) (Denman et al., 2007).

1.3.3 Methane Sinks

The CH_4 sink is mostly accounted for by the reaction of CH_4 with the hydroxyl radical (OH). Methane reaction with tropospheric OH is estimated to account for a 428-511 Tg CH_4 yr^{-1} sink, which accounts for up to 85% of the atmospheric CH_4 loss. Other sinks include CH_4 consumption by methanotrophs in unsaturated soils (26-34 Tg CH_4 yr^{-1}) and the atmospheric transport of CH_4 into the stratosphere (30-45 Tg CH_4 yr^{-1}) (Denman et al., 2007).

1.4 The Role of Wetlands in the Global Methane Cycle

The world's land surface is riddled with more than 10 million square kilometres of wetlands (Figure 1.5); wetlands, which include bogs, fens, swamps and any significant body of flooded soil, constitute essential components of the water cycle, and their role

Figure 1.4: Flamingos foraging in a wetland in Kos, Greece (photograph by George Papapostolou).

in ecology and human welfare is of fundamental importance (Lehner and Doll, 2004). As a result wetland carbon exchanges are complex: while wetlands are net emitters of CH_4 in the atmosphere (e.g. Reay et al., 2007), they also act as one of the largest biological CO_2 sinks (Altor and Mitsch, 2008). It is therefore imperative to expand our knowledge of wetland distributions, their sensitivity to climatic change and the overall wetland-climate feedback.

Methane is produced in freshwater anoxic environments, and is the end product of the decomposition of organic matter. Thauer (1998) summarize the process as follows:

Glucose ($C_6\ O_6\ H_{12}$) $\rightarrow 3CO_2 + 3CH_4$

In reality anoxic plant matter decomposition is more complex, and methanogenesis can occur through either the hydrogen or the acetate pathways (Whalen, 2005). In short, hydrogenotrophic methanogens consume hydrogen and CO_2 to produce CH_4 and H_2O, while acetotrophic methanogens break down acetate to CO_2 and CH_4, and the two methanogenic communities are dependent on each other (Whalen, 2005).

On a global scale, CH_4 emissions from wetlands vary by several orders of magnitude

(e.g. Whalen, 2005). In an anoxic, water-logged soil, the magnitude of the CH_4 emissions depend on a variety of environmental constraints, including substrate availability, vegetation and wetland fauna (e.g. Wuebbles and Hayhoe, 2002; Dingemans et al., 2011). Nonetheless, temperature and water table depth are the prominent variables controlling overall wetland CH_4 emissions (Wuebbles and Hayhoe, 2002). Moreover changes in temperature and wetland hydrology will influence wetland emissions over seasonal and year-to-year timescales (Gedney et al., 2004).

The two main groups of wetlands are boreal and tropical wetlands (e.g. Cao et al., 1996; Riley et al., 2011). Boreal wetland emissions peak during the summer season where the process of methanogenesis is accelerated by temperature. The flood fraction of boreal wetlands also increases during the summer months (Prigent et al., 2007), hence both the volume and temperature of soils results in seasonally increased emissions. On the other hand, the magnitude, seasonal dynamics and climatic sensitivity of tropical wetland emissions remains poorly understood (Mitsch et al., 2010). In-situ observations of methane emissions over tropical regions are sparse (e.g. Marani and Alval, 2007), and there are even fewer long-term observations. The use of satellite observations of inundation fractions (Prigent et al., 2007) was a significant advancement in the efforts to quantify tropical wetland CH_4 emissions (e.g. Ringeval et al., 2010; Hodson et al., 2011; Melack et al., 2004).

On a global scale, CH_4 emissions from wetlands have been calculated using bottom-up methods, were wetland properties such as soil temperature, wetland extent and substrate availability are used to upscale CH_4 emissions globally (e.g. Matthews and Fung, 1987; Cao et al., 1996; Walter et al., 2001; Petrescu et al., 2010). Wetland methane emissions have also been estimated using global flux and/or parameter optimization (top-down) approaches, where atmospheric inverse modelling has been performed to determine the wetland emission contributions to atmospheric CH_4 observations (e.g. Hein et al., 1997; Wang et al., 2004; Bousquet et al., 2006). Overall, the global annual CH_4 emission rates are within the range of 100-231 Tg CH_4 yr^{-1} (Denman et al., 2007). While top-down estimates use global observations of CH_4 to determine the magnitude of wetland emissions, the resulting CH_4 flux estimates will bear low spa-

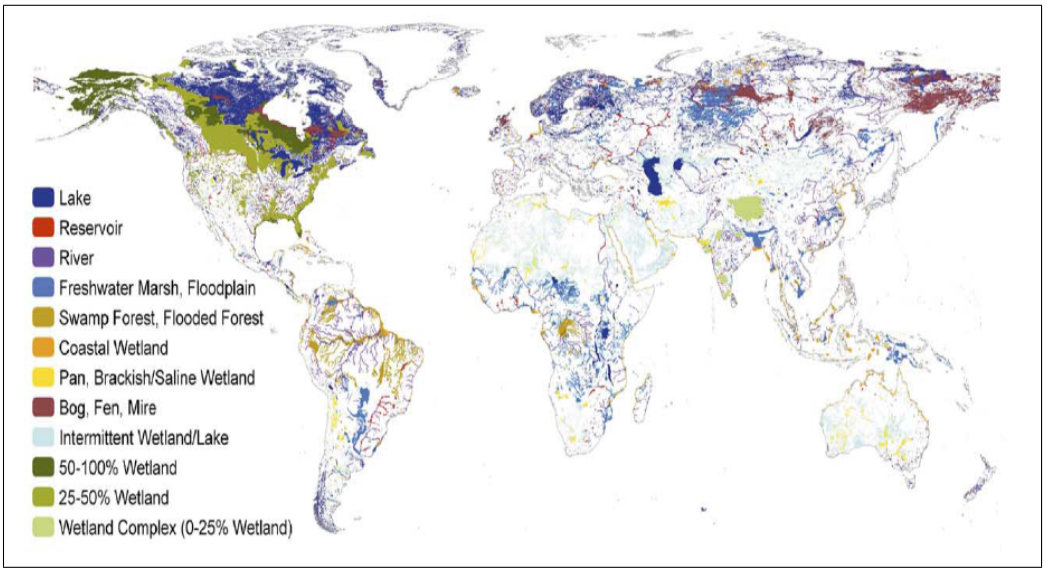

Figure 1.5: Global distribution of wetland areas and wetland types from the Global Wetland and Lakes Database (GWLD). Figure from Lehner and Doll (2004).

tial and temporal resolutions. Nonetheless, top-down approaches will determine the magnitude of wetlands in the context of the global CH_4 budget. Conversely, although bottom-up emission estimates are spatially and temporally better informed and processes controlling CH_4 emissions are better defined, the derivation of wetland CH_4 emission estimates is not constrained by global CH_4 observations.

1.4.1 The Foliar CH_4 Source

Although the magnitude, distribution and temporal behaviour of individual CH_4 sources and sinks often remain poorly understood, it was assumed that all major terms of the contemporary CH_4 budget have been identified. This assumption was recently contested when Keppler et al. (2006) published a controversial paper identifying a new major source of atmospheric CH_4. The controversy arised as no pathway through which globally significant CH_4 emissions can be biogenically produced in aerobic environments had previously been identified. Keppler et al. (2006) determined the existense of CH_4 emissions from plant material under aerobic conditions from observed CH_4 fluxes from both living plant material and dried plant material. Emissions from living plants were found to be at least one order of magnitude greater than dried plant material. Moreover, CH_4 emissions from living plants were found to be positively cor-

related with temperature and sunlight. These observations in conjuncture with global net primary productivity (NPP) values were used to upscale CH_4 emissions of plants to a global scale: results indicate a 62-236 Tg CH_4 yr^{-1}source. In the context of global CH_4 emissions, this implies 10-40% of the source is attributed to the foliar methane source. The magnitude of this previously unidentified CH_4 source was supported by elevated atmospheric CH_4 observations over the tropics (Frankenberg et al., 2005).

The methods employed by Keppler et al. (2006), especially the upscaling approach, have attracted extensive criticism. For example, Parsons et al. (2006) suggest the method by Keppler et al. (2006) is flawed, and suggest the use of leaf mass as opposed to NPP, and Dueck et al. (2007) found insignificant CH_4 emissions from plants when using a ^{13}C labelling approach to quantify CH_4 fluxes. Nonetheless, the Keppler et al. (2006) findings renewed the interest in global atmospheric CH_4 budget. Subsequent quantifications of the global foliar aerobic CH_4 source have mostly been at least half of the Keppler et al. (2006) estimated source (e.g. Kirschbaum et al., 2006; Parsons et al., 2006). In particular, Houweling et al. (2006) determine whether the bottom up estimate by Keppler et al. (2006) explains the atmospheric observations of CH_4 over the tropics, and place an upper limit of 85 Tg CH_4 yr^{-1} on the aerobic CH_4 emission source. The SCIAMACHY data used by Houweling et al. (2006) is the version prior to the water vapour correction (e.g. Frankenberg et al., 2008b), hence the reconciliation between the Keppler et al. (2006) foliar CH_4 emissions estimate and atmospheric CH_4 observations needs to be revised.

The observed CH_4 emissions from purified apple pectin by Keppler et al. (2006) led McLeod et al. (2008) to examine the CH_4 production from pectin. In particular, McLeod et al. (2008) found a strong relationship between UV irradiance of pectin and production of CH_4. The high concentration of pectin in plant cell walls implies that aerobic CH_4 emissions in terrestrial vegetation may nonetheless be a significant source of CH_4.

1.5 Research Summary

Although we have a good understanding of CH_4 sources, sinks and their relative magnitude, many fundamental questions about the CH_4 cycle remain unanswered: what is the role of methane in rapid global change? What led to the stagnation and renewed CH_4 growth during the past decade? How will major biogenic CH_4 sources respond to future climatic variability? In order to better understand the past, present and future of CH_4 in the atmosphere there is an urgent need to improve our understanding of the magnitude, distribution and temporal behaviour of the key CH_4 sources and sinks. In this thesis I will answer a few aspects of these questions by developing satellite based estimation methods for biogenic CH_4 emissions at a global scale.

In chapter 2, I determine whether laboratory measurements of CH_4 from UV-irradiated pectin add up to a significant global CH_4 source. In doing so test the following hypothesis:

- H1: UV irradiated pectin is a significant source of CH_4 on a global scale

I elaborate on the recent findings concerning the much-debated aerobic CH_4 source from terrestrial vegetation. I combine laboratory measurements of CH_4 emissions from pectin under UV irradiation with a global UV irradiance model and MODIS leaf area index (LAI) to upscale foliar CH_4 emissions on a global scale, in order to determine annual foliar CH_4 emissions rates. The work in this chapter has been published in the *New Phytologist* journal (Bloom et al., 2010a).

In chapters 3 and 4, I approach the subject of global wetland CH_4 emissions from a remote-sensing point of view: I use SCIAMACHY CH_4 VMR, GRACE equivalent water height data and NCEP/NCAR surface skin temperature to determine the seasonal controls on wetland CH_4 emissions. I put forward and test the following hypotheses:

- H2: Seasonal variability in spaceborne CH_4 observations is largely driven by wetland CH_4 emissions variability

- H3: Seasonal variability in spaceborne CH_4 observations can be used to estimate CH_4 emissions and complement other global wetland CH_4 emissions estimates

To test these hypotheses I develop a top-down method to quantify wetland and rice paddy CH_4 emissions at a global scale. I use my findings to then infer the sensitivity of wetlands to water and temperature and quantify the change in annual CH_4 emissions between 2003 and 2007. The work in these chapters has been published in *Science* (Bloom et al., 2010b).

In chapter 5, I re-assess the current understanding of the seasonal dynamics of tropical wetland CH_4 emissions. Satellite observations of CH_4 peak 1-3 months before the water table peaks over the Amazon river basin. Laboratory measurements of anaerobic decomposition show rapidly decaying CH_4 emission rates from tropical biomass (e.g. Miyajima et al., 1997; Bianchini Jr. et al., 2010). In this section I test the following hypotheses:

- H4: Carbon availability for CH_4 emissions is seasonally variable in tropical wetlands
- H5: Seasonal variability in tropical wetland carbon results in a lag between observed CH_4 and water table height

I test these hypotheses by developing a process-based model to describe wetland CH_4 emissions as a temporal function of water, temperature and carbon available for methanogenesis. I use SCIAMACHY CH_4 VMR between 2003-2009 to constrain our model parameters. The work in this chapter is currently being prepared for publication.

In chapter 6, I examine the overall significance and the potential impact of my results towards the current understanding of the global CH_4 budget. I examine the prospects of future research in this area, and conclude with a summary of the work carried out in this thesis.

References

Altor, A. E. and W. J. Mitsch, 2008: Methane and carbon dioxide dynamics in wetland mesocosms: Effects of hydrology and soils. *Ecological Applications*, **18**, pp. 1307–1320.

Bainbridge, A. E. and L. E. Heidt, 1966: Measurements of methane in the troposphere and lower stratosphere. *Tellus*, **18**, 221–225.

Balch, W. E., 1979: Methanogens : Reevaluation of a unique biological group. *Microbiology Review*, **43**, 260–296.

Beer, R., 2006: TES on the Aura Mission: Scientific Objectives, Measurements, and Analysis Overview. *IEEE Transactions on Geoscience and Remote Sensing*, **44**, 1102–1105, doi:10.1109/TGRS.2005.863716.

Bergamaschi, P., C. Frankenberg, J. F. Meirink, M. Krol, M. G. Villani, S. Houweling, F. Dentener, E. J. Dlugokencky, J. B. Miller, L. V. Gatti, A. Engel, and I. Levin, 2009: Inverse modeling of global and regional CH_4 emissions using SCIAMACHY satellite retrievals. *Journal of Geophysical Research (Atmospheres)*, **114**, D22301, doi:10.1029/2009JD012287.

Bianchini Jr., I., M. B. d. Cunha-Santino, F. Romeiro, and A. L. Bitar, 2010: Emissions of methane and carbon dioxide during anaerobic decomposition of aquatic macrophytes from a tropical lagoon (São Paulo, Brazil). *Acta Limnologica Brasiliensia (Online)*, **22**, 157–164.

Bloom, A. A., J. Lee-Taylor, S. Madronich, D. J. Messenger, P. I. Palmer, D. S. Reay, and A. R. McLeod, 2010a: Global methane emission estimates from ultraviolet irradiation of terrestrial plant foliage. *New Phytologist*, **187**, 417–425.

Bloom, A. A., P. I. Palmer, A. Fraser, D. S. Reay, and C. Frankenberg, 2010b: Large-Scale Controls of Methanogenesis Inferred from Methane and Gravity Spaceborne Data. *Science*, **327**, 322–325.

Bousquet, P., P. Ciais, J. B. Miller, E. J. Dlugokencky, D. A. Hauglustaine, C. Prigent, G. R. van der Werf, P. Peylin, E.-G. Brunke, C. Carouge, R. L. Langenfelds, J. Lathière, F. Papa, M. Ramonet, M. Schmidt, L. P. Steele, S. C. Tyler, and J. White, 2006: Contribution of anthropogenic and natural sources to atmospheric methane variability. *Nature*, **443**, 439–443, doi:10.1038/nature05132.

Cao, M., S. Marshall, and K. Gregso, 1996: Global carbon exchange and methane emissions from natural wetlands: Application of a process-based model. *Journal of Geophysical Research*, **101**, 14399–14414.

Denman, K., G. Brasseur, A. Chidthaisong, P. Ciai, P. Cox, R. Dickinson, D. Hauglustaine, C. Heinze, E. Holland, D. Jacob, U.Lohmann, S. Ramachandran, P. da Silva Dias, S. Wofsy, and X. Zhang, 2007: *Couplings Between Changes in the Climate System and Biogeochemistry. In: Climate Change 2007: The Physical Science Basis. Contribution of Working Group I to the Fourth Assessment Report of the Intergovernmental Panel on Climate Change [Solomon, S., D. Qin, M. Manning, Z. Chen, M. Marquis, K.B. Averyt, M.Tignor and H.L. Miller (eds.)].*. Cambridge University Press, Cambridge, United Kingdom and New York, NY, USA.

Dingemans, B., E. Bakker, and P. Bodelier, 2011: Aquatic herbivores facilitate the emission of methane from wetlands. *Ecology*, **92**, 1166–1173.

Dlugokencky, E. J., L. Bruhwiler, J. W. C. White, L. K. Emmons, P. C. Novelli, S. A. Montzka, K. A. Masarie, P. M. Lang, A. M. Crotwell, J. B. Miller, and L. V. Gatti, 2009: Observational constraints on recent increases in the atmospheric CH_4 burden. *Geophysical Research Letters*, **36**, L18803, doi:10.1029/2009GL039780.

Dlugokencky, E. J., P. Lang, and K. Masarie, 2009: Atmospheric methane dry air mole fractions from the NOAA ESRL carbon cycle cooperative global air sampling network, 1983-2007, version: 2008-07-02.

Dueck, T. A., R. De Visser, H. Poorter, S. Persijn, A. Gorissen, W. De Visser, A. Schapendonk, J. Verhagen, J. Snel, F. J. M. Harren, A. K. Y. Ngai, F. Verstappen, H. Bouwmeester, L. A. C. J. Voesenek, and A. Van Der Werf, 2007: No evidence for

substantial aerobic methane emission by terrestrial plants: a 13c-labelling approach. *New Phytologist*, **175**, 29–35, doi:10.1111/j.1469-8137.2007.02103.x.

Etheridge, D. M., L. P. Steele, R. J. Francey, and R. L. Langenfelds, 1998: Atmospheric methane between 1000 A.D. and present: Evidence of anthropogenic emissions and climatic variability. *Hournal of Geophysical Research*, **103**, 15979–15994, doi:10.1029/98JD00923.

Etiope, G., A. V. Milkov, and E. Derbyshire, 2008: Did geologic emissions of methane play any role in Quaternary climate change? *Global and Planetary Change*, **61**, 79–88, doi:10.1016/j.gloplacha.2007.08.008.

Feng, L., P. I. Palmer, H. Bösch, and S. Dance, 2009: Estimating surface CO_2 fluxes from space-borne CO_2 dry air mole fraction observations using an ensemble Kalman Filter. *Atmospheric Chemistry & Physics*, **9**, 2619–2633.

Feng, L., P. I. Palmer, Y. Yang, R. M. Yantosca, S. R. Kawa, J.-D. Paris, H. Matsueda, and T. Machida, 2011: Evaluating a 3-D transport model of atmospheric CO_2 using ground-based, aircraft, and space-borne data. *Atmospheric Chemistry & Physics*, **11**, 2789–2803, doi:10.5194/acp-11-2789-2011.

Fowler, D., K. J. Hargreaves, U. Skiba, R. Milne, M. S. Zahniser, J. B. Moncrieff, I. J. Beverland, and M. W. Gallagher, 1995: Measurements of CH_4 and N_2O fluxes at the landscape scale using micrometeorological methods. *Royal Society of London Philosophical Transactions Series A*, **351**, 339–355, doi:10.1098/rsta.1995.0038.

Frankenberg, C., P. Bergamaschi, A. Butz, S. Houweling, J. F. Meirink, J. Notholt, A. K. Petersen, H. Schrijver, T. Warneke, and I. Aben, 2008a: Tropical methane emissions: A revised view from SCIAMACHY onboard ENVISAT. *Geophysical Research Letters*, **35**, 15811, doi:10.1029/2008GL034300.

Frankenberg, C., J. F. Meirink, P. Bergamaschi, A. P. H. Goede, M. Heimann, S. Körner, U. Platt, M. van Weele, and T. Wagner, 2006: Satellite chartography of atmospheric methane from SCIAMACHY on board ENVISAT: Analysis of the years 2003 and 2004. *Journal of Geophysical Research (Atmospheres)*, **111**, D07303, doi:10.1029/2005JD006235.

Frankenberg, C., J. F. Meirink, M. van Weele, U. Platt, and T. Wagner, 2005: Assessing methane emissions from global space-borne observations. *Science*, **308**, 1010–1014.

Frankenberg, C., T. Warneke, A. Butz, I. Aben, F. Hase, P. Spietz, and L. R. Brown, 2008b: Pressure broadening in the $2\nu_3$ band of methane and its implication on atmospheric retrievals. *Atmospheric Chemistry & Physics*, **8**, 5061–5075.

Gedney, N., P. M. Cox, and C. Huntingford, 2004: Climate feedback from wetland methane emissions. *Geophysical Research Letters*, **31**, L20503, doi:10.1029/2004GL020919.

Haqq-Misra, J. D., S. D. Domagal-Goldman, P. J. Kasting, and J. F. Kasting, 2008: A Revised, Hazy Methane Greenhouse for the Archean Earth. *Astrobiology*, **8**, 1127–1137, doi:10.1089/ast.2007.0197.

Heimann, M., 2011: Enigma of the recent methane budget. *Nature*, **476**, 157–158.

Hein, R., P. J. Crutzen, and M. Heimann, 1997: An inverse modeling approach to investigate the global atmospheric methane cycle. *Global Biogeochemical Cycles*, **11**, 43–76, doi:10.1029/96GB03043.

Hodson, E. L., B. Poulter, N. E. Zimmermann, C. Prigent, and J. O. Kaplan, 2011: The El Niño-Southern Oscillation and wetland methane interannual variability. *Geophysical Research Letters*, **38**, L08810, doi:10.1029/2011GL046861.

Houweling, S., T. Röckmann, I. Aben, F. Keppler, M. Krol, J. F. Meirink, E. J. Dlugokencky, and C. Frankenberg, 2006: Atmospheric constraints on global emissions of methane from plants. *Geophysical Research Letters*, **33**, L15821, doi:10.1029/2006GL026162.

Kai, F. M., S. C. Tyler, J. T. Randerson, and D. R. Blake, 2011: Reduced methane growth rate explained by decreased northern hemisphere microbial sources. *Nature*, **476**, 194–197.

Kasting, J. F. and S. Ono, 2006: Palaeoclimates: the first two billion years. *Philosphical Transactions of the Royal Society B: Biological Sciences*, **361**, 917–929.

Kasting, J. F., A. A. Pavlov, and J. L. Siefert, 2001: A Coupled Ecosystem-Climate Model for Predicting the Methane Concentration in the Archean Atmosphere. *Origins of Life and Evolution of the Biosphere*, **31**, 271–285, doi:10.1023/A:1010600401718.

Kasting, J. F. and J. L. Siefert, 2002: Life and the Evolution of Earth's Atmosphere. *Science*, **296**, 1066–1068, doi:10.1126/science.1071184.

Keppler, F., J. T. G. Hamilton, M. Braß, and T. Röckmann, 2006: Methane emissions from terrestrial plants under aerobic conditions. *Nature*, **439**, 187–191, doi:10.1038/nature04420.

Kharecha, P., J. Kasting, and J. Siefert, 2005: A coupled atmosphere-ecosystem model of the early archean earth. *Geobiology*, **3**, 53–76, doi:10.1111/j.1472-4669.2005.00049.x.

Kirschbaum, M. U. F., D. Bruhn, D. Etheridge, E. J.R., G. Farquhar, G. R.M., P. K.I., and W. A.J., 2006: A comment on the quantitative significance of aerobic methane release by plants. *Functional Plant Biology*, **33**, 521–530.

Kump, L. R., 2008: The rise of atmospheric oxygen. *Nature*, **451**, 277–278, doi:10.1038/nature06587.

Lehner, B. and P. Doll, 2004: Full title page pp iii Development and validation of a global database of lakes, reservoirs and wetlands. *Journal of Hydrology*, **296**, 1–22, doi:10.1016/j.jhydrol.2004.03.028.

Marani, L. and P. Alval, 2007: Methane emissions from lakes and floodplains in pantanal, brazil. *Atmospheric Environment*, **41**, 1627–1633, doi:10.1016/j.atmosenv.2006.10.046.

Matthews, E. and I. Fung, 1987: Methane emissions from natural wetlands: Global distribution, area and environmental characteristics of sources. *Global Biochemical Cycles*, **1**, 61–86.

McLeod, A. R., S. C. Fry, G. J. Loake, D. J. Messenger, D. S. Reay, K. A. Smith, and B.-W. Yun, 2008: Ultraviolet radiation drives methane emissions

from terrestrial plant pectins. *New Phytologist*, **180**, 124–132, doi:10.1111/j.1469-8137.2008.02571.x.

Melack, J. M., L. L. Hess, M. Gastil, B. R. Forsberg, S. K. Hamilton, I. B. T. Lima, and E. M. L. M. Nova, 2004: Regionalization of methane emissions in the Amazon basin with microwave remote sensing. *Global Change Biology*, **10**, 530–544.

Migeotte, M. V., 1948: Spectroscopic Evidence of Methane in the Earth's Atmosphere. *Physical Review*, **73**, 519–520, doi:10.1103/PhysRev.73.519.2.

Mitsch, W., A. Nahlik, P. Wolski, B. Bernal, L. Zhang, and L. Ramberg, 2010: Tropical wetlands: seasonal hydrologic pulsing, carbon sequestration, and methane emissions. *Wetlands Ecology and Management*, **18**, 573–586, doi:doi:10.1007/s11273-009-9164-4.

Miyajima, T., E. Wada, Y. T. Hanba, and P. Vijarnsorn, 1997: Anaerobic mineralization of indigenous organic matters and methanogenesis in tropical wetland soils. *Geochimica et Cosmochimica Acta*, **61**, 3739–3751, doi:10.1016/S0016-7037(97)00189-0.

Parsons, A. J., P. C. Newton, H. Clark, and F. M. Kelliher, 2006: Scaling methane emissions from vegetation. *Trends in Ecology and Evolution*, **21**, 423 – 424, doi:DOI: 10.1016/j.tree.2006.05.017.

Petit, J. R., J. Jouzel, D. Raynaud, N. I. Barkov, J. Barnola, I. Basile, M. Bender, J. Chappellaz, M. Davis, G. Delaygue, M. Delmotte, V. M. Kotlyakov, M. Legrand, V. Y. Lipenkov, C. Lorius, L. Pépin, C. Ritz, E. Saltzman, and M. Stievenard, 1999: Climate and atmospheric history of the past 420,000 years from the Vostok ice core, Antarctica. *Nature*, **399**, 429–436, doi:10.1038/20859.

Petrescu, A. M. R., L. P. H. van Beek, J. van Huissteden, C. Prigent, T. Sachs, C. A. R. Corradi, F. J. W. Parmentier, and A. J. Dolman, 2010: Modeling regional to global CH_4 emissions of boreal and arctic wetlands. *Global Biogeochemical Cycles*, **24**, GB4009, doi:10.1029/2009GB003610.

Prigent, C., F. Papa, F. Aires, W. B. Rossow, and E. Matthews, 2007: Global inundation dynamics inferred from multiple satellite observations, 1993-2000. *Journal of Geophysical Research (Atmospheres)*, **112**, D12107, doi:10.1029/2006JD007847.

Rasmussen, R. A. and M. A. K. Khalil, 1981: Atmospheric methane (CH_4): Trends and seasonal cycles. *Journal of Geophysical Research*, **86**, 9826–9832, doi:10.1029/JC086iC10p09826.

Razavi, A., C. Clerbaux, C. Wespes, L. Clarisse, D. Hurtmans, S. Payan, C. Camy-Peyret, and P. F. Coheur, 2009: Characterization of methane retrievals from the IASI space-borne sounder. *Atmospheric Chemistry & Physics*, **9**, 7889–7899.

Reay, D. S., C. N. Hewitt, K. A. Smith, and J. Grace, 2007: *Greenhouse Gas Sinks*, CABI, Wallingford, UK, chapter CH_4: Importance, Sources and Sinks. 143–151, iSBN 978 1 84593 189 6.

Rigby, M., R. G. Prinn, P. J. Fraser, P. G. Simmonds, R. L. Langenfelds, J. Huang, D. M. Cunnold, L. P. Steele, P. B. Krummel, R. F. Weiss, S. O'Doherty, P. K. Salameh, H. J. Wang, C. M. Harth, J. Mühle, and L. W. Porter, 2008: Renewed growth of atmospheric methane. *Geophy. Res. Letter*, **35**, L22805, doi:10/1029/2008GL036037.

Riley, W. J., Z. M. Subin, D. M. Lawrence, S. C. Swenson, M. S. Torn, L. Meng, N. M. Mahowald, and P. Hess, 2011: Barriers to predicting changes in global terrestrial methane fluxes: analyses using CLM4Me, a methane biogeochemistry model integrated in CESM. *Biogeosciences*, **8**, 1925–1953, doi:10.5194/bg-8-1925-2011.

Ringeval, B., N. de NobletDucoudr, P. Ciais, P. Bousquet, C. Prigent, F. Papa, and W. B. Rossow, 2010: An attempt to quantify the impact of changes in wetland extent on methane emissions on the seasonal and interannual time scales. *Global Biogeochemical Cycles*, **24**, GB2003.

Ruddiman, W., 2001: The case for human causes of increased atmospheric CH4 over the last 5000 years. *Quaternary Science Reviews*, **20**, 1769–1777, doi:10.1016/S0277-3791(01)00067-1.

Ruddiman, W. F., 2003: The anthropogenic greenhouse era began thousands of years ago. *Climatic Change*, **61**, 261–293, 10.1023/B:CLIM.0000004577.17928.fa.

Schirrmeister, B. E., A. Antonelli, and H. C. Bagheri, 2011: The origin of multicellularity in cyanobacteria. *BMC Evolutionary Biology*, **11**, 45.

Steele, L. P., E. J. Dlugokencky, P. M. Lang, P. P. Tans, R. C. Martin, and K. A. Masarie, 1992: Slowing down of the global accumulation of atmospheric methane during the 1980s. *Nature*, **358**, 313–316, doi:10.1038/358313a0.

Thauer, R. K., 1998: Biochemistry of methanogenesis: a tribute to marjory stephenson. 1998 marjory stephenson prize lecture. *Microbiology*, **144 (Pt 9)**, 2377–2406.

van Huissteden, J., 2004: Methane emission from northern wetlands in Europe during Oxygen Isotope Stage 3. *Quaternary Science Reviews*, **23**, 1989–2005, doi:10.1016/j.quascirev.2004.02.015.

Walter, B. P., M. Heimann, and E. Matthews, 2001: Modelling modern methane emissions form natural wetlands 1. model description and results. *Journal of Geophysical Research*, **106**, 34189–34206.

Wang, J. S., J. A. Logan, M. B. McElroy, B. N. Duncan, I. A. Megretskaia, and R. M. Yantosca, 2004: A 3-D model analysis of the slowdown and interannual variability in the methane growth rate from 1988 to 1997. *Global Biogeochemical Cycles*, **18**, GB3011, doi:10.1029/2003GB002180.

Wang, W. C., Y. L. Yung, A. A. Lacis, T. Mo, and J. E. Hansen, 1976: Greenhouse Effects due to Man-Made Perturbations of Trace Gases. *Science*, **194**, 685–690, doi:10.1126/science.194.4266.685.

Weber, N., A. Drury, W. Toonen, and M. van Weele, 2010: Glacial wetland distribution and methane emissions estimated from PMIP2 climate simulations. *EGU General Assembly 2010, held 2-7 May, 2010 in Vienna, Austria, p.3529*, **12**, 119–124.

Whalen, S. C., 2005: Biogeochemistry of methane exchange between natural wetlands and the atmosphere. *Environmental Engineering Science*, **22**, 73–95.

Wuebbles, D. J. and K. Hayhoe, 2002: Atmospheric methane and global change. *Earth Science Reviews*, **57**, 177–210, doi:10.1016/S0012-8252(01)00062-9.

Yokota, T., Y. Yoshida, N. Eguchi, Y. Ota, T. Tanaka, H. Watanabe, and S. Maksyutov, 2009: Global concentrations of CO_2 and CH_4 retrieved from gosat: First preliminary results. *SOLA*, **5**, 160–163.

Chapter 2

Global Methane Emission Estimates from Ultraviolet Irradiation of Terrestrial Plant Foliage

New Phytologist

Research

Global methane emission estimates from ultraviolet irradiation of terrestrial plant foliage

A. Anthony Bloom[1], Julia Lee-Taylor[2], Sasha Madronich[2], David J. Messenger[1,3], Paul I. Palmer[1], David S. Reay[1] and Andy R. McLeod[1]

[1]School of GeoSciences, The University of Edinburgh, Crew Building, West Mains Road, Edinburgh EH9 3JN, UK; [2]National Center for Atmospheric Research (NCAR), Atmospheric Chemistry Division, PO Box 3000, Boulder, CO 80305, USA; [3]Institute of Molecular Plant Sciences, School of Biological Sciences, The University of Edinburgh, Daniel Rutherford Building, Mayfield Road, Edinburgh EH9 3JH, UK

Author for correspondence:
Andy McLeod
Tel: +44 131 650 5434
Email: andy.mcleod@ed.ac.uk

Received: *24 December 2009*
Accepted: *5 March 2010*

New Phytologist (2010)
doi: 10.1111/j.1469-8137.2010.03259.x

Key words: foliage, methane (CH_4), pectin, ultraviolet radiation, vegetation.

Summary

- Several studies have reported *in situ* methane (CH_4) emissions from vegetation foliage, but there remains considerable debate about its significance as a global source. Here, we report a study that evaluates the role of ultraviolet (UV) radiation-driven CH_4 emissions from foliar pectin as a global CH_4 source.
- We combine a relationship for spectrally weighted CH_4 production from pectin with a global UV irradiation climatology model, satellite-derived leaf area index (LAI) and air temperature data to estimate the potential global CH_4 emissions from vegetation foliage.
- Our results suggest that global foliar CH_4 emissions from UV-irradiated pectin could account for 0.2–1.0 Tg yr^{-1}, of which 60% is from tropical latitudes, corresponding to < 0.2% of total CH_4 sources.
- Our estimate is one to two orders of magnitude lower than previous estimates of global foliar CH_4 emissions. Recent studies have reported that pectin is not the only molecular source of UV-driven CH_4 emissions and that other environmental stresses may also generate CH_4. Consequently, further evaluation of such mechanisms of CH_4 generation is needed to confirm the contribution of foliage to the global CH_4 budget.

Introduction

Methane (CH_4) is a long-lived greenhouse gas with a 100 yr global warming potential 25 times that of CO_2, and its current atmospheric concentration of 1.8 ppm makes a significant contribution to climatic warming (Solomon *et al.*, 2007). While the main components of the global CH_4 budget have been identified and the total global CH_4 source is relatively well known (Forster *et al.*, 2007), the individual sources and sinks and the recent changes in the growth rate of atmospheric CH_4 concentration and its interannual variability are far from comprehensively understood (Bousquet *et al.*, 2006; Solomon *et al.*, 2007); recent findings have questioned both the identity and magnitude of several important source terms (Beerling *et al.*, 2007). New estimates of marine CH_4 sources have recently been reported for deep-water geological seeps (Solomon *et al.*, 2009) and for surface phytoplankton in oceanic waters (Karl *et al.*, 2008), while a new and controversial terrestrial source of CH_4 was also proposed by Keppler *et al.* (2006), who observed emissions from vegetation foliage under aerobic experimental conditions.

Hitherto, terrestrial CH_4 emissions from biogenic sources were attributed solely to methanogenic microorganisms growing under anaerobic conditions in wetland soils, rice paddies, the gastrointestinal tract of ruminants and termites, and landfills (Keppler *et al.*, 2009; Bloom *et al.*, 2010). However, Keppler *et al.* (2006) observed CH_4 emissions into CH_4-free air from detached leaves, air-dried leaves, intact plants and the plant structural component pectin. They reported emission rates from air-dried leaves of C_3 and C_4 plants in the range 0.2–3 ng g^{-1} leaf DW h^{-1} at 30°C, but these increased to much higher rates of 12–370 ng g^{-1} leaf DW h^{-1} for intact plants. Their emission rates increased by a factor of 3–5 when experimental chambers were exposed to natural sunlight and they also

increased over the range 30–70°C. This suggested a nonenzymatic mechanism as they occurred above the threshold of 50–60°C at which plant enzymes are denatured (Berry & Raison, 1981), but they knew of no mechanism to explain their observations (Keppler *et al.*, 2006). Although these rates of emission were small, Keppler *et al.* (2006) completed a rough extrapolation of the total annual global emission of CH_4 from live vegetation by using mean sunlit and dark emission rates for leaf biomass scaled by day length, duration of growing season, and total net primary productivity (NPP) in each biome. Their estimate of between 62 and 236 Tg (1 Tg = 10^{12} g) CH_4 yr^{-1}, with the largest contribution of 46–169 Tg CH_4 yr^{-1} from tropical forests and grassland, was observed to equate to 10–40% of the known annual CH_4 source strength. Plant litter was estimated to contribute 0.5–6.6 Tg CH_4 yr^{-1}. Consequently, these first observations of Keppler *et al.* (2006) caused intense interest, considerable debate and some scepticism among the scientific community and the media (Schiermeier, 2006a,b), leading to further experimental studies and a wider consideration of their implications for the global CH_4 budget and greenhouse gas mitigation options (Lowe, 2006; NIEPS, 2006).

An early indication that the upscaling approach of Keppler *et al.* (2006) contained methodological inconsistencies came from Kirschbaum *et al.* (2006), who used two different methods to estimate global CH_4 emissions based on leaf biomass (rather than NPP) and on photosynthesis. Both approaches suggested much lower global emissions from vegetation than originally proposed by Keppler *et al.* (2006). Subsequently, further analyses using a variety of methods (Houweling *et al.*, 2006; Parsons *et al.*, 2006; Butenhoff & Khalil, 2007; Ferretti *et al.*, 2007; Megonigal & Guenther, 2008) also suggested substantially lower global emissions from a vegetation source (Table 1). Most recently, Rice *et al.* (2010) have estimated the global transfer of soil-derived CH_4 to the atmosphere by trees in flooded forest regions.

Several recent studies were unable to detect any CH_4 emissions from vegetation foliage (Beerling *et al.*, 2007; Dueck *et al.*, 2007; Kirschbaum & Walcroft, 2008; Megonigal & Guenther, 2008; Nisbet *et al.*, 2009), but other studies have reported CH_4 emissions (Cao *et al.*, 2008; McLeod *et al.*, 2008; Vigano *et al.*, 2008; Wang *et al.*, 2008; Brüggemann *et al.*, 2009; Bruhn *et al.*, 2009) and some have proposed that ultraviolet (UV) generation of reactive oxygen species (ROS) is a component of the mechanism for CH_4 formation (Messenger *et al.*, 2009a,b). Following the suggestion by Keppler *et al.* (2006) that the methyl esters (methoxyl groups) of pectin were a potential source of CH_4, Vigano *et al.* (2008), McLeod *et al.* (2008) and Bruhn *et al.* (2009) all demonstrated that CH_4 emissions from the structural component pectin, as well as fresh and dried leaf tissue, depend on UV radiation. The studies of Dueck *et al.* (2007), Beerling *et al.* (2008) and Kirschbaum & Walcroft (2008) did not include UV wavelengths, which might

Table 1 Estimates of global aerobic methane (CH_4) emissions by vegetation (after Megonigal & Guenther (2008) and Keppler *et al.* (2009))

Scaling method	Range of global CH_4 production (Tg yr^{-1})	Source
Sunlit and dark leaf emission rate scaled by day length, season length and biome net primary production	62–236	Keppler *et al.* (2006)
Leaf emission rates (Keppler *et al.*, 2006) scaled by biome leaf biomass: range 15–60 Tg yr^{-1}; or by leaf photosynthesis, 10 Tg yr^{-1}	10–60	Kirschbaum *et al.* (2006)
Leaf emission rates (Keppler *et al.*, 2006) scaled by biome leaf biomass: leafy biomass alone, 42 Tg yr^{-1}; plus nonleafy biomass, 11 Tg yr^{-1}	42–53	Parsons *et al.* (2006)
Atmospheric transport model, isotope ratios, mass balance. Pre-industrial plausible value, 85 Tg yr^{-1}, to maximum present-day upper limit, 125 Tg yr^{-1}	85–125	Houweling *et al.* (2006)
Leaf emission rates (Keppler *et al.*, 2006) scaled using model of cloud cover and canopy shading. Scaled using LAI, 36 Tg yr^{-1}; scaled using foliage biomass, 20 Tg yr^{-1}, maximum expected, 69 Tg yr^{-1}	20–69	Butenhoff & Khalil (2007)
Mass balance, ice core isotope ratios using: pre-industrial, 'best estimate' 0–46 Tg yr^{-1}, 'maximum estimate' 9–103 Tg yr^{-1}; modern source, 'best estimate' 0–176 Tg yr^{-1}, 'maximum estimate' 0–213 Tg yr^{-1}	0–213	Ferretti *et al.* (2007)
Global VOC emissions model assuming VOCs and CH_4 have similar biochemical origin. Range dependent on land cover and weather data	34–56	Megonigal & Guenther (2008)
Foliar CH_4 emission from UV irradiation of pectin (McLeod *et al.*, 2008), 2 m air temperature, MODIS LAI and UV climatology. Scaled using leaf biomass and 5% pectin content, 0.2–0.8 Tg yr^{-1}; scaled using leaf area and 5% pectin content, 0.3–1.0 Tg yr^{-1}	0.2–1.0	This study

LAI, leaf area index; MODIS, Moderate Resolution Image Spectroradiometer ; VOC, volatile organic compound.

explain the absence of CH_4 emissions in their experiments. McLeod *et al.* (2008) and Bruhn *et al.* (2009) also demonstrated that prior removal of methyl esters from pectin stopped CH_4 production under UV irradiation, while Keppler *et al.* (2008) used isotopically labelled pectin to demonstrate that pectin methyl esters are a source of the emitted CH_4. These studies clearly demonstrate that pectin can be a source of CH_4 under the influence of UV irradiation, including natural sunlight (McLeod *et al.*, 2008). We therefore decided to estimate the potential global production of CH_4 from plant pectin under appropriate spectrally weighted UV radiation. In this study we used the spectral weighting function for UV-driven CH_4 emission from pectin (McLeod *et al.*, 2008) to provide a first estimate of the potential global emission of CH_4 from foliar pectin and we compare this with other published estimates of the contribution of vegetation to the global CH_4 budget.

Materials and Methods

We estimate monthly CH_4 emissions per unit ground area (F_{CH4}) from the UV irradiation of terrestrial plant foliage using a CH_4 emission rate per unit leaf DW (K_{LEAF}) with a global distribution of leaf DW estimated from the mean biome specific leaf area (SLA) and the global distribution of leaf area index (LAI). We assume that where LAI > 1, the total incident UV radiation is intercepted by unit LAI and that all its foliar pectin is irradiated. We extrapolate short-term (2 h) experimental emission rates from McLeod *et al.* (2008) to a monthly timescale, thus providing an upper estimate of global emissions but with assumptions that are discussed later.

We estimate F_{CH4} using the following relationship:

$$F_{CH4}(t) = C(t)K_{LEAF}UV_{CH4}(t)M_{LEAF}(t), \qquad \text{Eqn 1}$$

where t refers to a particular month; $C(t)$ describes the temperature dependence of the emission rate on monthly timescales; K_{LEAF} is the CH_4 production per unit leaf DW (kg CH_4 kg^{-1} leaf DW) per unit of spectrally weighted UV irradiation (J m^{-2}); UV_{CH4} is the monthly total UV irradiation spectrally weighted for methanogenesis (J m^{-2}); and M_{LEAF} (kg m^{-2}) is the irradiated leaf DW calculated from the product of leaf area (with LAI ≤ 1) and mean biome SLA. We evaluate monthly F_{CH4} on a spatial scale of 1.25° longitude by 1.00° latitude resolution, from which we determine global mean annual F_{CH4}. In the following sections we describe the details of all terms involved in calculating F_{CH4} along with their respective uncertainties.

Rate of foliar CH_4 emission (K_{LEAF})

We calculate the foliar CH_4 emission (K_{LEAF}) from the leaf content of pectin, a structural component of plant cell walls, and a CH_4 emission rate from pectin (K_{PECTIN}) that was found in previous work to be linearly related to spectrally weighted UV irradiance (UV_{CH4}) at 30°C (McLeod *et al.*, 2008), where $K_{PECTIN} = 3.09 \times 10^{-11}$ kg CH_4 kg^{-1} pectin DW per unit of spectrally weighted UV irradiation (J m^{-2}). The spectral weighting, described later, was determined by finding the best-fit straight-line logarithmic relationship between weighted irradiance and CH_4 emission using three types of polychromatic UV lamps and sunlight (McLeod *et al.*, 2008). An independent study found a linear relationship between unweighted UV irradiance and CH_4 emission from pectin and living leaves (Vigano *et al.*, 2008) that extended up to five times ambient irradiance, and demonstrated persistent emissions over 35 d. Similar results were observed over a 1 wk period by Bruhn *et al.* (2009). We therefore apply laboratory measurements of K_{PECTIN} to larger spatial and temporal scales, as these measurements showed that UV-driven K_{PECTIN} was constant over long periods of time, and changed linearly with the UV irradiance. We assume a constant rate of 3.09×10^{-11} kg CH_4 kg^{-1} pectin per unit irradiation (J m^{-2}) for the UV-driven CH_4 emission from pectin as an upper limit in our calculations and discuss the limitations of this approach later in the paper.

Published estimates of the pectin and cell wall content of vegetation vary between species and between plant organs, with the cell wall content averaging 15–20% of organ DW. Approximately 30% of the DW of the primary cell wall of dicots (flowering plants, angiosperms, with two cotyledons) is composed of pectins, while monocots (angiosperms with only one cotyledon) are generally thought to have very small amounts of pectin (McNeil *et al.*, 1984; Voragen *et al.*, 2009). However, Jarvis *et al.* (1988) found a large variability in pectin content between different monocot species, some containing similar amounts to the dicots. We therefore use a value for pectin content of 5% leaf DW as a representative upper value of the reported range. Assuming a foliar pectin content of 5% leaf DW provides a CH_4 emission rate from UV irradiance of foliage, K_{LEAF}, of 1.54×10^{-12} kg CH_4 kg^{-1} leaf DW per unit of spectrally weighted UV irradiation (J m^{-2}). This value for K_{LEAF} is similar to the value reported previously for spectrally weighted UV-driven CH_4 emissions from tobacco (McLeod *et al.*, 2008).

We describe the temperature dependence of K_{PECTIN}, C, as a power law:

$$C = Q_{10}^{(T-T_0)/10}, \qquad \text{Eqn 2}$$

where T is leaf temperature approximated using 2 m air temperature, T_0 is 30°C, and Q_{10} = 2 (i.e. a factor of 2 variation for a 10°C change in temperature), as suggested by Bruhn *et al.* (2009). We use monthly mean 2 m air temperature values from the 6-hourly analyses of NCEP/NCAR

New Phytologist

(National Centers for Environmental Prediction/National Center for Atmospheric Research) (Kalnay *et al.*, 1996) to evaluate C and spatially interpolate 2 m air temperature onto a regular 1.25° longitude by 1.00° latitude grid. We fit a sine curve to the 6-hourly values and use the average temperature during the warmest 12 h as a proxy for daylight leaf temperature, which we use to determine monthly mean daylight leaf temperature.

Monthly spectrally weighted UV irradiance (UV_{CH4})

We calculate the CH_4-effective irradiance for pectin (UV_{CH4}) by combining an annual climatology of UV spectral irradiance $I(\lambda)$ at the Earth's surface with a spectral sensitivity function for UV production of CH_4 from pectin $B(\lambda)$ (McLeod *et al.*, 2008):

$$UV_{CH4} = \int \int_{280\,nm}^{400\,nm} I(\lambda)B(\lambda)d\lambda dt. \quad \text{Eqn 3}$$

We evaluate UV_{CH4} every 30 min in 1 nm steps from 280 to 400 nm using the NCAR radiative transfer TUV (tropospheric ultraviolet–visible) model (Madronich, 1993; Madronich & Flocke, 1997), and determine the monthly total irradiation on a geographical resolution of 1.25° longitude by 1.00° latitude.

We use the TUV model with satellite-based (Nimbus-7, Meteor-3 and Earth Probe) total ozone mapping spectrometer (TOMS) observations of column O_3 (Herman *et al.*, 1996; McPeters *et al.*, 1996, 1998) averaged over 11 yr (1990–2000) to calculate $I(\lambda)$. We account for scattering from aerosols and clouds by using TOMS reflectivity measurements at 380 nm and a cloud adjustment factor following the method of Lee-Taylor *et al.* (2010).

The spectral weighting function for UV production of CH_4 from pectin, $B(\lambda)$, determined by McLeod *et al.* (2008), which decays by a factor of 10 every 80 nm and is normalized to unity at 300 nm, is given by

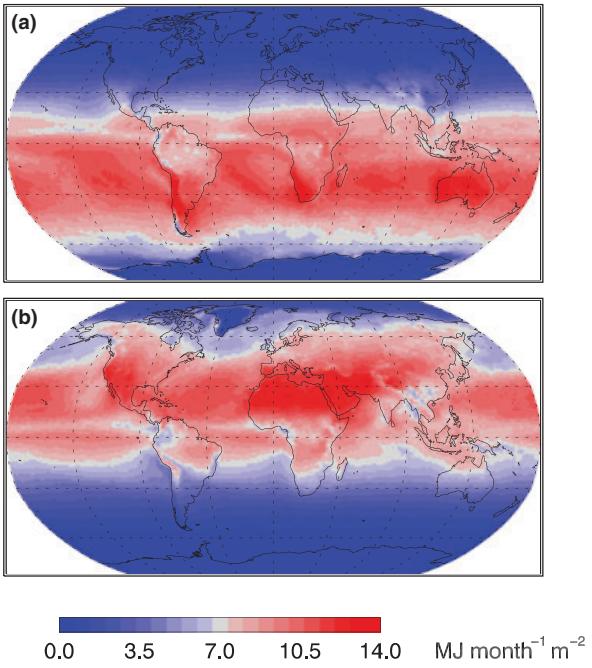

Fig. 1 Ultraviolet radiation climatology between 1990 and 2000 for January (a) and July (b), spectrally weighted for methane (CH_4) production from pectin according to McLeod *et al.* (2008).

$$B(\lambda) = 10^{(300-\lambda)/80}. \quad \text{Eqn 4}$$

Notably, this function is similar to that determined for CO emissions from plant leaves by Schade *et al.* (1999). Fig. 1 shows the monthly distribution of UV_{CH4} for January and July, accounting for mean column O_3 and cloud cover between 1990 and 2000. We also calculate the UV climatology without correction for cloud cover (data not shown) for comparative calculations (described later).

Dry weight of UV-irradiated leaves (M_{LEAF})

We estimate the biomass of UV-irradiated leaves, M_{LEAF} (kg m^{-2}), by

Table 2 Specific leaf area (SLA) of biomes (from Parsons *et al.*, 2006) and corresponding Global Land Cover 2000 categories (GLC, 2003) for each biome

Biome	SLA (m^2 kg^{-1})	GLC2000 land cover groups
Tropical forests	12.0	All forests between 23.5°N and 23.5°S
Temperate forests	8.5	All forests between 23.5–50°N and 23.5–50°S
Boreal forests	7.7	All forests between 50–90°N and 50–90°S
Mediterranean shrublands	6.9	All shrub mosaics between 23.5–45°N and 23.5–45°S
Tropical savannas and grassland	16.9	All grass cover and shrub mosaics between 23.5°N and 23.5°S
Temperate grasslands	16.9	All grass cover outside 23.5°N–23.5°S and all shrub mosaics outside 45°S–45°N
Deserts	6.9	Deserts
Crops	24.5	All cultivated/managed areas and cropland mosaics

$$M_{LEAF} = LAI L_w, \quad \text{Eqn 5}$$

where L_w is the leaf DW per unit area (kg m^{-2}). The monthly mean LAI is determined from the Moderate Resolution Image Spectroradiometer (MODIS) Terra 0.25° × 0.25° LAI product (Knyazikhin *et al.*, 1999). We interpolate LAI to the regular 1.25° longitude by 1.00° latitude grid. Then, as UV transmittance of leaves and complete leaf canopies is generally very low (McLeod & Newsham, 1997), with most UV radiation absorbed by the top 25% of forest canopies (Brown *et al.*, 1994), we assume a maximum LAI value of 1 with total absorbance of incident UV.

L_w is the reciprocal of SLA (m^2 kg^{-1}). In order to determine biome SLA values (Parsons *et al.*, 2006) for each grid square, we use the Global Land Cover 2000 product (GLC, 2003) by matching biome categorizations (Table 2).

Results and Discussion

Our estimates of methane emissions based on leaf DW are shown in Fig. 2 as the magnitude and distribution of the total annual F_{CH4} (a), the maximum monthly emission (b) and the minimum monthly emission (c). F_{CH4} is larger over the tropics, where temperature and UV irradiance are highest. We find the largest values (15 mg m^{-2} yr^{-1}) over the equatorial African rainforest belt and over northern Australia. Values over the Amazon and Southeast Asia are more diffuse, with a magnitude of, typically, 10 mg m^{-2} yr^{-1} as a result of lower UV radiation (see Fig. 1).

We determine uncertainties associated with F_{CH4} by propagating the uncertainties associated with C, K_{LEAF}, UV_{CH4}, and M_{LEAF}. Errors associated with the gridded 2 m air temperature analyses were assumed to be spatially uncorrelated, and were attributed an uncertainty of 0.5°C, resulting in a 3% average uncertainty for C. K_{PECTIN} and pectin content errors are globally correlated. K_{PECTIN} has an associated uncertainty of 3.7%, as determined from the uncertainty of the gradient between the empirical relationship between UV irradiance and CH_4 emissions (McLeod *et al.*, 2008). We assign an uncertainty of 50% for pectin content, reflecting sparse information about variations within the full range of species and ecosystems. As a result, the uncertainty of K_{LEAF} (51%) is dominated by the pectin uncertainty. We attribute a random error of 5% to UV_{CH4} (Lee-Taylor & Madronich, 2007). Systematic error associated with UV_{CH4} data can be up to 25%, being largest where absorbing aerosols are present, such as industrial or heavily urbanized areas: these are significant but within the uncertainty range for F_{CH4} (see later discussion). Although a positive snow-related UV_{CH4} bias is also expected, we anticipate negligible effects on F_{CH4} as a result of low coinciding air temperature.

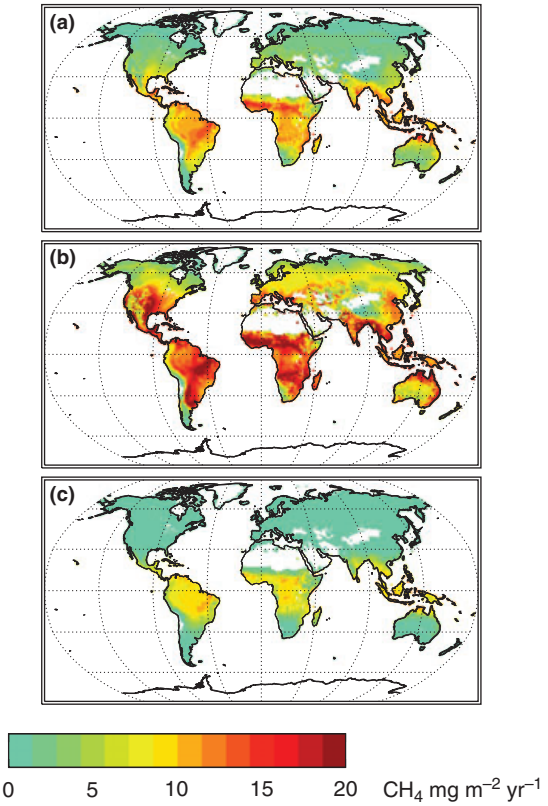

Fig. 2 (a) Total annual foliar methane (CH_4) emissions determined from spectrally weighted global ultraviolet irradiance, MODIS (Moderate Resolution Image Spectroradiometer) leaf area index (LAI) and 2 m air temperature. (b) Maximum and (c) minimum monthly foliar CH_4 emissions.

The use of an action spectrum and spectral weighting function can have important effects on the experimental determination of UV effects. However, uncertainties in CH_4 emissions resulting from our choice of weighting function are not expected to be large, because the same function is used to quantify determination of K_{PECTIN} and to compute the global climatology of weighted UV radiation. Using data from McLeod *et al.* (2008), we estimate the uncertainty in F_{CH4} resulting from our choice of $B(\lambda)$ by using a range of slopes for $B(\lambda)$, within 90% of the maximum correlation of the experimental relationship between weighted irradiance and CH_4 emission (i.e. $10^{(300-\lambda)/66} > B(\lambda) > 10^{(300-\lambda)/95}$). We estimate an uncertainty of 9.5% for the product $UV_{CH4} \times K_{PECTIN}$ by integrating the range of $B(\lambda)$ in K_{PECTIN} using an example solar spectrum from McLeod *et al.* (2008) representative of UV_{CH4}.

We assume spatially uncorrelated errors associated with MODIS LAI and attribute an uncertainty of 5% to LAI values ≤ 1. Errors in SLA are correlated within each biome and uncorrelated between different biomes: we attribute an

uncertainty of 20% for each SLA. The overall uncertainty of M_{LEAF} is 55%. We find an average grid-scale emission uncertainty of 56.5% by summing the uncertainties of all terms in quadrature. Uncertainties associated with pectin content and biome SLA make the largest contributions to the overall uncertainty of F_{CH4}.

Fig. 3 shows the contributions and uncertainties of F_{CH4} from the eight biomes used (Table 2). The global annual total for F_{CH4}, using corrections for cloud cover and air temperature, was estimated to be 0.49 ± 0.27 Tg yr^{-1}. Emissions from tropical latitudes account for 63% of the total values, with tropical forests representing the single largest contribution to F_{CH4}, as expected. Crops (20%), tropical savannas and grassland (14%) and temperate forests (10%) also represent significant contributions to F_{CH4}.

Fig. 3 also shows the sensitivity of these results to the UV_{CH4} fields if the effects of clouds and temperature are included separately and in combination. The largest effect for many of the biomes results from the temperature correction C, particularly extra-tropical biomes where there is a large seasonal cycle in surface air temperature, resulting in a 37% decrease in global emissions compared with uncorrected values (data not shown) and a 50% decrease over extra-tropical biomes. Neglecting the cloud correction of UV irradiance would result in a 29–34% increase in emissions.

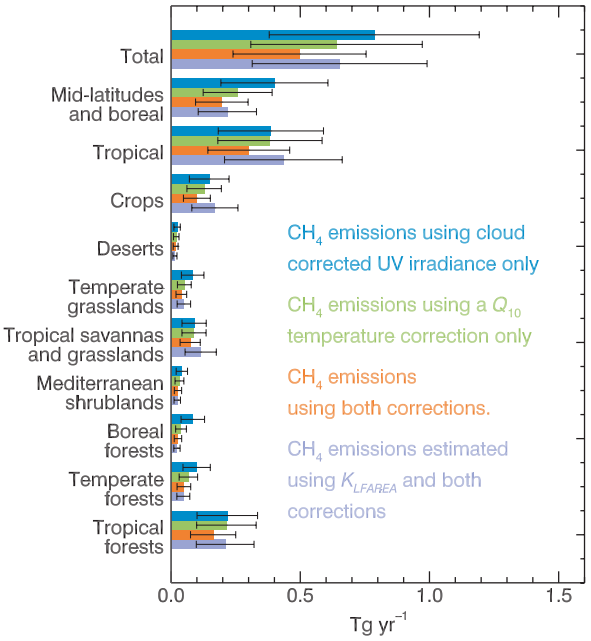

Fig. 3 Mean annual foliar methane (CH_4) emissions from eight individual biomes (tropical forests, temperate forests, boreal forests, Mediterranean shrublands, tropical savannas and grassland, temperate grasslands, deserts and crops); all tropical biomes combined (tropical); all extra-tropical biomes combined (mid-latitudes and boreal); and all biomes (total). The error bars on each estimate represent the uncertainty range. Contributions of each biome are calculated from the CH_4 emission per unit leaf DW (K_{LEAF}) and spectrally weighted UV irradiance with the following corrections: corrected only for cloud cover; corrected only for temperature using a Q_{10}-dependent air temperature; using both corrections; and by using the CH_4 emission per unit leaf area (K_{LFAREA}) with both cloud and temperature corrections.

Leaf structure and its internal distribution of pectin (plus other factors described later) will affect the emission of CH_4, so that resulting emission may be more related to leaf surface area than to leaf DW. We therefore perform a second CH_4 emission calculation based on leaf area, instead of leaf DW, assuming that the experimental pectin sheets used to generate K_{PECTIN} (McLeod *et al.*, 2008) are representative of all foliage. This method of calculation assumes that the density of pectin and its UV absorbance on experimental sheets is representative of pectin in foliage and has its own caveats. However, assuming a pectin content of 5% DW for leaves, the pectin sheets (20.3 × 25.4 cm) containing 250 mg pectin would have an equivalent leaf SLA value of 10.3 m^2 kg^{-1}, which is within the range of average values for biome SLA (Table 2). We therefore apply the equivalent CH_4 emission rate per unit leaf area to K_{LEAF}, which we redefine as K_{LFAREA} (kg CH_4 m^{-2} leaf area) per unit spectrally weighted UV irradiation (J m^{-2}), and recalculate F_{CH4} using the formula:

$$F_{CH4}(t) = C(t)K_{LFAREA}UV_{CH4}(t)LAI(t), \qquad \text{Eqn 6}$$

where LAI ≤ 1 and assuming a constant SLA value of 10.3 m^2 kg^{-1} for all biomes. Estimating the value of F_{CH4} by scaling with leaf area yields a total CH_4 source of 0.65 ± 0.34 Tg, which is also shown in Fig. 3 as global and individual biome contributions. Although this method gives a global CH_4 source 37% higher than the value scaled using leaf DW and biome specific SLA, the spatial distributions of CH_4 emissions remain relatively unchanged.

Assuming global CH_4 sources of 550 Tg yr^{-1}, we find that F_{CH4} emissions scaled by leaf DW account for 0.04–0.15% of the global source. Table 1 shows our estimate to be at least one to two orders of magnitude smaller than previously reported F_{CH4} emissions. Our analysis explicitly accounts for the part of the UV spectrum where pectin emission is most responsive; accounts for the temperature dependence of F_{CH4} emissions; uses the most up-to-date global datasets to account for spatial and temporal changes in LAI, and spatial distributions of biomes; and provides an uncertainty for the F_{CH4} emission estimate related to the input datasets.

Our estimates of F_{CH4} make several assumptions that require further discussion. We extrapolate CH_4 emissions from plant pectin measured over 2 h to calculate monthly means and we assume that the rates of emission do not saturate at high irradiance or decline through time. We justify

this because independently determined experimental rates of UV-driven CH_4 emission were linear, with UV irradiance up to five times ambient values of unweighted UV, and persisted over 35 d (Vigano *et al.*, 2008). The emission rate of CH_4 from irradiating experimental pectin sheets (McLeod *et al.*, 2008) at the global maximum irradiation of 1.27×10^8 J yr^{-1} m^{-2} from our spectrally weighted UV climatology (including cloud correction) corresponds to yearly conversion of only *c.* 9.6% of the pectic methyl groups on the pectin. However, it is likely that CH_4 emission rates would fall through time and our calculations should therefore be regarded as upper estimates.

We expect that the CH_4 emissions from foliar pectin will be proportional to the UV radiation absorbed but will also be influenced by leaf structure, pectin distribution, UV-photosensitizing compounds, UV-screening compounds, and chemical and biochemical processes for quenching ROS (McLeod *et al.*, 2008; Messenger *et al.*, 2009b). These factors will vary between plant species and influence both the spectral response and magnitude of K_{LEAF}. While our calculations may provide an upper estimate for the potential global emission of CH_4 from UV irradiation of foliar pectin, there remain additional questions arising from published experimental work and potential refinements to the calculations. For instance, it would be possible to estimate UV irradiation within a leaf canopy using a model with a detailed canopy environment component (e.g. MEGAN: Model of Emissions of Gases and Aerosols from Nature as described by Megonigal & Guenther, 2008) and to refine the calculation of F_{CH4} based upon canopy architecture and UV-irradiated leaf area. We omit night-time emissions from our global estimate of F_{CH4}, as negligible emissions were observed in the absence of UV (McLeod *et al.*, 2008). We do not include potential CH_4 emissions derived from nonleafy biomass and other plant structural compounds in foliage. Vigano *et al.* (2008) observed UV-driven CH_4 emissions from plant cellulose and lignin in addition to pectin and the significance of these emissions remains unquantified. Most recently, Vigano *et al.* (2009) reported that studies using stable isotopes revealed that only some of the CH_4 emissions detected from plants originated from pectin methyl groups. Additionally, it has been suggested that other environmental stresses (both biotic and abiotic) and cellular signalling processes that produce ROS may all generate some CH_4 from plant material (Keppler *et al.*, 2009; Messenger *et al.*, 2009a,b). Qaderi & Reid (2009) reported that temperature and water stress increased a subsequent CH_4 emission using six plant species, and Z. P. Wang *et al.* (2009) showed that physical injury also elicits CH_4 emissions.

The transport of CH_4 from anaerobic processes in soil to the atmosphere via internal plant tissues, such as aerenchyma, is well known in aquatic vascular plants (especially grasses and sedges) of wetlands and rice paddies (Schütz *et al.*, 1991). However, several studies have suggested that soil-derived CH_4 can be transferred to the atmosphere via the transpiration stream of vegetation (Nisbet *et al.*, 2009) or via internal tissues of trees (Rusch & Rennenberg, 1998; Terazawa *et al.*, 2007; Rice *et al.*, 2010), and several field observations of vegetation emissions (do Carmo *et al.*, 2006; Crutzen *et al.*, 2006; Sanhueza & Donoso, 2006; Sinha *et al.*, 2007; Cao *et al.*, 2008; Wang *et al.*, 2008; S. Wang *et al.*, 2009) have an unexplained CH_4 source. Consequently, further studies are still required to complete the understanding of the mechanisms and magnitude of plant CH_4 emissions.

Acknowledgements

The authors acknowledge the helpful comments of three anonymous referees. This work was supported by research awards from the Natural Environment Research Council (to A.R.M. and D.S.R.), the Moray Endowment Fund (to A.R.M.), the University of Edinburgh Development Trust (to D.J.M.), the University of Edinburgh Donald Mackenzie Scholarship (to D.J.M.) and by UK Natural Environmental Research Council studentships NE/F007973/1 and NER/S/A/2006/14236 (to A.A.B. and D.J.M., respectively) with financial support from Forest Research (to D.J.M.). A.R.M. acknowledges the support of a Royal Society Leverhulme Trust Senior Research Fellowship. The National Center for Atmospheric Research is sponsored by the National Science Foundation.

References

Beerling DJ, Gardiner T, Leggett G, McLeod A, Quick WP. 2008. Missing methane emissions from leaves of terrestrial plants. *Global Change Biology* **14**: 1821–1826.

Beerling DJ, Hewitt CN, Pyle JA, Raven JA. 2007. Critical issues in trace gas biogeochemistry and global change. *Philosophical Transactions of the Royal Society of London. Series A: Mathematical Physical Sciences* **365**: 1629–1642.

Berry JA, Raison JK. 1981. Responses of macrophytes to temperature. In: Lange OL, Nobel PS, Osmond CB, Ziegler H, eds. *Physiological plant ecology I. Responses to the physical environment, Encyclopedia of Plant Physiology, New Series Vol. 12A*. Berlin, Germany, 277–338.

Bloom AA, Palmer PI, Fraser A, Reay DS, Frankenberg C. 2010. Large-scale controls of methanogenesis inferred from methane and gravity spaceborne data. *Science* **327**: 322–325.

Bousquet P, Ciais P, Miller JB, Dlugokencky EJ, Hauglustaine DA, Prigent C, Van der Werf GR, Peylin P, Brunke EG, Carouge C *et al.* 2006. Contribution of anthropogenic and natural sources to atmospheric methane variability. *Nature* **443**: 439–443.

Brown MJ, Parker GG, Posner NE. 1994. A survey of ultraviolet-B radiation in forests. *Journal of Ecology* **82**: 843–854.

Brüggemann N, Meier R, Steigner D, Zimmer I, Louis S, Schnitzler JP. 2009. Nonmicrobial aerobic methane emission from poplar shoot cultures under low-light conditions. *New Phytologist* **182**: 912–918.

Bruhn D, Mikkelsen TN, Øbro J, Willats WGT, Ambus P. 2009. Effects of temperature, ultraviolet radiation and pectin methyl esterase on aerobic methane release from plant material. *Plant Biology* **11**: 43–48.

Butenhoff CL, Khalil MAK. 2007. Global methane emissions from terrestrial plants. *Environmental Science & Technology* **41**: 4032–4037.

Cao G, Xu X, Long R, Wang Q, Wang C, Du Y, Zhao X. 2008. Methane emissions by alpine plant communities in the Qinghai–Tibet Plateau. *Biology Letters* **4**: 681–684.

do Carmo JB, Keller M, Dias JD, de Camargo PB, Crill P. 2006. A source of methane from upland forests in the Brazilian Amazon. *Geophysical Research Letters* **33**: L04809.

Crutzen PJ, Sanhueza E, Brenninkmeijer CAM. 2006. Methane production from mixed tropical savanna and forest vegetation in Venezuela. *Atmospheric Chemistry and Physics Discussions* **6**: 3093–3097.

Dueck TA, de Visser R, Poorter H, Persijn S, Gorissen A, de Visser W, Schapendonk A, Verhagen J, Snel J, Harren FJM *et al.* 2007. No evidence for substantial aerobic methane emission by terrestrial plants: a ^{13}C-labelling approach. *New Phytologist* **175**: 29–35.

Ferretti DF, Miller JB, White JWC, Lassey KR, Lowe DC, Etheridge DM. 2007. Stable isotopes provide revised global limits of aerobic methane emissions from plants. *Atmospheric Chemistry and Physics* **7**: 237–241.

Forster P, Ramaswamy V, Artaxo P, Berntsen T, Betts R, Fahey DW, Haywood J, Lean J, Lowe DC, Myhre G *et al.* 2007. Changes in atmospheric constituents and in radiative forcing. In: Solomon S, Qin D, Manning M, Chen Z, Marquis M, Averyt KB, Tignor M, Miller HL, eds. *Climate change 2007: the physical science basis. Contribution of working group I to the fourth assessment report of the intergovernmental panel on climate change*. New York, NY, USA: Cambridge University Press, 129–234.

GLC. 2003. *Global Land Cover 2000 database*. European Commission, Joint Research Centre. http://bioval.jrc.ec.europa.eu/products/glc2000/glc2000.php.

Herman JR, Bhartia PK, Krueger AJ, McPeters RD, Wellemeyer CG, Seftor CJ, Jaross G, Schlesinger BM, Torres O, Labow G *et al.* 1996. *Meteor-3 total ozone mapping spectrometer (TOMS) Data Products User's Guide. NASA Reference Publication 1393*. Greenbelt, MD, USA: Goddard Space Flight Center.

Houweling S, Rockmann T, Aben I, Keppler F, Krol M, Meirink JF, Dlugokencky EJ, Frankenberg C. 2006. Atmospheric constraints on global emissions of methane from plants. *Geophysical Research Letters* **33**: L15821.

Jarvis MC, Forsyth W, Duncan HJ. 1988. A survey of the pectic content of nonlignified monocot cell walls. *Plant Physiology* **88**: 309–314.

Kalnay E, Kanamitsu M, Kistler R, Collins W, Deaven D, Gandin L, Iredell M, Saha S, White G, Woollen J *et al.* 1996. The NCEP/NCAR 40-year reanalysis project. *Bulletin of the American Meteorological Society* **77**: 437–471.

Karl DM, Beversdorf L, Bjorkman KM, Church MJ, Martinez A, DeLong EF. 2008. Aerobic production of methane in the sea. *Nature Geoscience* **1**: 473–478.

Keppler F, Boros M, Frankenberg C, Lelieveld J, McLeod A, Pirttilä AM, Röckmann T, Schnitzler JP. 2009. Methane formation in aerobic environments. *Environmental Chemistry* **6**: 459–465.

Keppler F, Hamilton JTG, Brass M, Röckmann T. 2006. Methane emissions from terrestrial plants under aerobic conditions. *Nature* **439**: 187–191.

Keppler F, Hamilton JTG, McRoberts WC, Vigano I, Brass M, Röckmann T. 2008. Methoxyl groups of plant pectin as a precursor of atmospheric methane: evidence from deuterium labelling studies. *New Phytologist* **178**: 808–814.

Kirschbaum MUF, Bruhn D, Etheridge DM, Evans JR, Farquhar GD, Gifford RM, Paul KI, Winters AJ. 2006. A comment on the quantitative significance of aerobic methane release by plants. *Functional Plant Biology* **33**: 521–530.

Kirschbaum MUF, Walcroft A. 2008. No detectable aerobic methane efflux from plant material, nor from adsorption/desorption processes. *Biogeosciences* **5**: 1551–1558.

Knyazikhin Y, Glassy J, Privette JL, Tian Y, Lotsch A, Zhang Y, Wang Y, Morisette JT, Votava T, Myneni RB *et al.* 1999. *MODIS leaf area index (LAI) and fraction of photosynthetically active radiation absorbed by vegetation (FPAR) product (MOD15) algorithm theoretical basis document*. http://eospso.gsfc.nasa.gov/atbd/modistables.html.

Lee-Taylor J, Madronich S. 2007. *Climatology of UV-A, UV-B, and erythemal radiation at the earth's surface, 1979–2000. NCAR technical note NCAR/ TN-474+STR*. Boulder, CO, USA: Atmospheric Chemistry Division, National Center for Atmospheric Research.

Lee-Taylor J, Madronich S, Fischer C, Mayer B. 2010. A climatology of UV radiation, 1979–2000, 65S-65N. In: Gao W, Schmoldt D, Slusser JR, eds. *UV radiation in global climate change: measurements, modeling and effects on ecosystem*. Heidelberg, Germany: Springer-Verlag and Beijing, China: Tsinghua University Press, 1–22.

Lowe DC. 2006. Global change: a green source of surprise. *Nature* **439**: 148–149.

Madronich S. 1993. UV radiation in the natural and perturbed atmosphere. In: Tevini M, ed. *Environmental effects of UV (ultraviolet) radiation*. Boca Raton, FL, USA: Lewis Publisher, 17–69.

Madronich S, Flocke S. 1997. Theoretical estimation of biologically effective UV radiation at the Earth's surface. In: Zerefos C, ed. *Solar ultraviolet radiation – modeling, measurements and effects*. Berlin, Germany: Springer-Verlag, 23–48.

McLeod AR, Fry SC, Loake GJ, Messenger DJ, Reay DS, Smith KA, Yun BW. 2008. Ultraviolet radiation drives methane emissions from terrestrial plant pectins. *New Phytologist* **180**: 124–132.

McLeod AR, Newsham KK. 1997. Impacts of elevated UV-B on forest ecosystems. In: Lumsden PJ, ed. *Plants and UV-B*. Cambridge, UK: Cambridge University Press, 247–281.

McNeil M, Darvill AG, Fry SC, Albersheim P. 1984. Structure and function of the primary cell walls of plants. *Annual Review of Biochemistry* **53**: 625–663.

McPeters RD, Bhartia PK, Krueger AJ, Herman JR, Schlesinger BM, Wellemeyer CG, Seftor CJ, Jaross G, Taylor SL, Swissler T *et al.* 1996. *Nimbus-7 total ozone mapping spectrometer (TOMS) Data Products User's Guide. NASA Reference Publication 1384*. Washington, DC, USA: National Aeronautics and Space Administration.

McPeters RD, Bhartia PK, Krueger AJ, Herman JR, Wellemeyer CG, Seftor CJ, Jaross G, Torres O, Moy L, Labow G *et al.* 1998. *Earth Probe total ozone mapping spectrometer (TOMS) Data Products User's Guide. NASA Technical Publication 1998-206895*. Greenbelt, MD, USA: Goddard Space Flight Center.

Megonigal JP, Guenther AB. 2008. Methane emissions from upland forest soils and vegetation. *Tree Physiology* **28**: 491–498.

Messenger DJ, McLeod AR, Fry SC. 2009a. Reactive oxygen species in aerobic methane formation from vegetation. *Plant Signaling and Behavior* **4**: 1–2.

Messenger DJ, McLeod AR, Fry SC. 2009b. The role of ultraviolet radiation, photosensitizers, reactive oxygen species and ester groups in mechanisms of methane formation from pectin. *Plant, Cell & Environment* **32**: 1–9.

NIEPS. 2006. *Do recent scientific findings undermine the climate benefits of carbon sequestration in Forests? An expert review of recent studies on methane emissions and water tradeoffs*. Durham, NC, USA: Nicholas Institute for Environmental Policy Solutions, Duke University.

Nisbet RER, Fisher R, Nimmo RH, Bendall DS, Crill PM, Gallego-Sala AV, Hornibrook ERC, Lopez-Juez E, Lowry D, Nisbet PBR *et al.* 2009. Emission of methane from plants. *Proceedings of the Royal Society of London. Series B, Biological Sciences* **276**: 1347–1354.

Parsons AJ, Newton PCD, Clark H, Kelliher FM. 2006. Scaling methane emissions from vegetation. *Trends in Ecology & Evolution* **21**: 423–424.

Qaderi MM, Reid DM. 2009. Methane emissions from six crop species exposed to three components of global climate change: temperature, ultraviolet-B radiation and water stress. *Physiologia Plantarum* **137**: 139–147.

Rice AL, Butenhoff CL, Shearer MJ, Teama D, Rosenstiel TN, Khalil MAK. 2010. Emissions of anaerobically produced methane by trees. *Geophysical Research Letters* **37**: L03807.

Rusch H, Rennenberg H. 1998. Black alder (*Alnus glutinosa* (L.) Gaertn.) trees mediate methane and nitrous oxide emission from the soil to the atmosphere. *Plant and Soil* **201**: 1–7.

Sanhueza E, Donoso L. 2006. Methane emission from tropical savanna *Trachypogon* sp. grasses. *Atmospheric Chemistry and Physics* **6**: 5315–5319.

Schade GW, Hofmann RM, Crutzen PJ. 1999. CO emissions from degrading plant matter (I). Measurements. *Tellus. Series B, Chemical and Physical Meteorology* **51**: 889–908.

Schiermeier Q. 2006a. Methane finding baffles scientists. *Nature* **439**: 128.

Schiermeier Q. 2006b. The methane mystery. *Nature* **442**: 730–731.

Schütz H, Schröder P, Rennenberg H. 1991. Role of plants in regulating the methane flux to the atmosphere. In: Sharkey TD, Holland EA, Mooney HA, eds. *Trace gas emissions by plants*. San Diego, CA, USA: Academic Press, 29–63.

Sinha V, Williams J, Crutzen PJ, Lelieveld J. 2007. Methane emissions from boreal and tropical forest ecosystems derived from *in-situ* measurements. *Atmospheric Chemistry and Physics Discussions* 7: 14011–14039.

Solomon EA, Kastner M, MacDonald IR, Leifer I. 2009. Considerable methane fluxes to the atmosphere from hydrocarbon seeps in the Gulf of Mexico. *Nature Geoscience* **2**: 561–565.

Solomon S, Qin D, Manning M, Alley RB, Berntsen T, Bindoff NL, Chen Z, Chidthaisong A, Gregory JM, Hegerl GC *et al.* 2007. Technical summary. In: Solomon S, Qin D, Manning M, Chen Z, Marquis M, Averyt KB, Tignor M, Miller HL, eds. *Climate change 2007: the physical science basis. Contribution of working group I to the fourth assessment report of the intergovernmental panel on climate change*. New York, NY, USA: Cambridge University Press, 20–92.

Terazawa K, Ishizuka S, Sakatac T, Yamada K, Takahashi M. 2007. Methane emissions from stems of *Fraxinus mandshurica* var. *japonica* trees in a floodplain forest. *Soil Biology & Biochemistry* **39**: 2689–2692.

Vigano I, Holzinger R, van Weelden H, Keppler F, McLeod A, Röckmann T. 2008. Effect of UV radiation and temperature on the emission of methane from plant biomass and structural components. *Biogeosciences* **5**: 937–947.

Vigano I, Röckmann T, Holzinger R, van Dijk A, Keppler F, Greule M, Brand WA, Geilmann H, van Weelden H. 2009. The stable isotope signature of methane emitted from plant material under UV irradiation. *Atmospheric Environment* **43**: 5637–5646.

Voragen AGJ, Coenen GJ, Verhoef RP, Schols HA. 2009. Pectin, a versatile polysaccharide present in plant cell walls. *Structural Chemistry* **20**: 263–275.

Wang S, Yang X, Lin X, Hu Y, Luo C, Xu G, Zhang Z, Su A, Chang X, Chao Z *et al.* 2009. Methane emission by plant communities in an alpine meadow on the Qinghai-Tibetan Plateau: a new experimental study of alpine meadows and oat pasture. *Biology Letters* **5**: 535–538.

Wang ZP, Gulledge J, Zheng JQ, Liu W, Li LH, Han XG. 2009. Physical injury stimulates aerobic methane emissions from terrestrial plants. *Biogeosciences* **6**: 615–621.

Wang ZP, Han XG, Wang GG, Song Y, Gulledge J. 2008. Aerobic methane emission from plants in the Inner Mongolia Steppe. *Environmental Science & Technology* **42**: 62–68.

Chapter 3

Large-Scale Controls of Methanogenesis Inferred from Methane and Gravity Spaceborne Data

methanol (*29*), there are strong arguments against such a contribution. First, the major product on Ag is formaldehyde (*30*). Second, high temperatures are needed for the reaction [>250°C (*31*)]; the industrial process that uses Ag as a catalyst works at over 600°C in order to achieve sufficiently high yields (*25*). Third, the overall catalytic activity of np-Au does not increase but decreases as the residual Ag content increases.

The conclusion that the observed coupling reactivity and selectivity is due to Au surface sites as reactive sites is also confirmed by experiments in which an aldehyde was co-dosed to the methanol stream. According to our reaction model, the coupling product methyl formate is formed by the reaction of formaldehyde with methoxy groups. Thus, the formation of mixed coupling products can be expected when a different aldehyde is added to the reactant mixture—a result that was recently obtained in model studies on O/Au(111) (*32*). Thus, selective cross-coupling of different alcohols and aldehydes should also be feasible on np-Au. In fact, the mechanistic model predicts that the methyl esters will selectively form because co-feeding the aldehyde circumvents the rate-determining β-C-H activation step in the reaction. As an example, we chose the reaction of methanol and acetaldehyde, which is expected to produce methyl acetate. When adding acetaldehyde to the gas stream (1 volume % H_3C_2HO + 2 volume % CH_3OH + 10 volume % O_2), methyl acetate—the coupling product between methoxy and the co-fed acetaldehyde—is the only product (except for small amounts of CO_2). No methyl formate is detected, as is anticipated from the molecular-scale mechanism. Thus, the reactivity of the aldehyde causes the selectivity to change toward the new coupling product and opens the door to a rich coupling chemistry on np-Au.

Application of np-Au as a large-scale catalyst will depend on the economical viability, which is strongly connected to an economic use of the precious metal. One approach is to crush the material; another one is to coat the alloy on templates working as a backbone for catalyst pellets before dealloying. In this way, mass transport limitation because of pore diffusion can also be largely avoided. The feasibility of the latter approach was already proven, resulting in np-Au material with a relative density in the range of only 1.5% (*33*), which lies in the range of metal loadings of supported commercial catalysts. Future investigations will focus on an expansion of the scope of reactions to larger primary and secondary alcohols, such as ethanol or *tert*-butanol.

References and Notes

1. United Nations World Commission on Environment and Development (WCED), "Our Common Future (The Brundtland Report)" (Annex to General Assembly document A/42/427, Oxford Univ. Press, Oxford, 1987).
2. M. Poliakoff, P. Licence, *Nature* **450**, 810 (2007).
3. V. Gewin, *Nature* **440**, 378 (2006).
4. A. Abad, P. Concepcion, A. Corma, H. Garcia, *Angew. Chem. Int. Ed.* **44**, 4066 (2005).
5. T. Ishida, M. Haruta, *Angew. Chem. Int. Ed.* **46**, 7154 (2007).
6. B. Jorgensen, S. E. Christiansen, M. L. D. Thomsen, C. H. Christensen, *J. Catal.* **251**, 332 (2007).
7. A. K. Sinha, S. Seelan, S. Tsubota, M. Haruta, *Top. Catal.* **29**, 95 (2004).
8. M. D. Hughes *et al.*, *Nature* **437**, 1132 (2005).
9. R. J. Madix, *Science* **233**, 1159 (1986).
10. B. J. Xu, X. Y. Liu, J. Haubrich, R. J. Madix, C. M. Friend, *Angew. Chem. Int. Ed.* **48**, 4206 (2009).
11. X. Y. Deng, B. K. Min, A. Guloy, C. M. Friend, *J. Am. Chem. Soc.* **127**, 9267 (2005).
12. X. Y. Liu, B. J. Xu, J. Haubrich, R. J. Madix, C. M. Friend, *J. Am. Chem. Soc.* **131**, 5757 (2009).
13. J. Gong, D. W. Flaherty, R. A. Ojifinni, J. M. White, C. B. Mullins, *J. Phys. Chem. C* **112**, 5501 (2008).
14. M. Haruta, T. Kobayashi, H. Sano, N. Yamada, *Chem. Lett.* **16**, 405 (1987).
15. G. J. Hutchings, *Catal. Today* **100**, 55 (2005).
16. J. Schwank, S. Galvagno, G. Parravano, *J. Catal.* **63**, 415 (1980).
17. H. Falsig *et al.*, *Angew. Chem. Int. Ed.* **47**, 4835 (2008).
18. B. Hvolbaek *et al.*, *Nano Today* **2**, 14 (2007).
19. G. C. Bond, D. T. Thompson, *Gold Bull.* **33**, 41 (2000).
20. M. Haruta, *ChemPhysChem* **8**, 1911 (2007).
21. V. Zielasek *et al.*, *Angew. Chem. Int. Ed.* **45**, 8241 (2006).
22. H. M. Yin *et al.*, *J. Phys. Chem. C* **112**, 9673 (2008).
23. J. T. Zhang, P. P. Liu, H. Y. Ma, Y. Ding, *J. Phys. Chem. C* **111**, 10382 (2007).
24. R. Zeis, T. Lei, K. Sieradzki, J. Snyder, J. Erlebacher, *J. Catal.* **253**, 132 (2008).
25. *Ullmann's Encyclopedia of Industrial Chemistry* (Wiley, New York, ed. 7, 2009); www.wiley-vch.de/vch/software/ullmann/index.php?page=home.
26. I. E. Marko, P. R. Giles, M. Tsukazaki, S. M. Brown, C. J. Urch, *Science* **274**, 2044 (1996).
27. T. Mallat, A. Baiker, *Chem. Rev.* **104**, 3037 (2004).
28. A. Wittstock *et al.*, *J. Phys. Chem. C* **113**, 5593 (2009).
29. X. Y. Liu, R. J. Madix, C. M. Friend, *Chem. Soc. Rev.* **37**, 2243 (2008).
30. W. S. Sim, P. Gardner, D. A. King, *J. Phys. Chem.* **99**, 16002 (1995).
31. C. B. Wang, G. Deo, I. E. Wachs, *J. Phys. Chem. B* **103**, 5645 (1999).
32. B. J. Xu, X. Y. Liu, J. Haubrich, C. M. Friend, *Nat. Chem.*, published online 29 November 2009 (doi:10.1038/nchem.467).
33. G. W. Nyce, J. R. Hayes, A. V. Hamza, J. H. Satcher, *Chem. Mater.* **19**, 344 (2007).

34. We are grateful to R. Schlögl (Fritz-Haber-Institute, Berlin) for critically reading the manuscript. Work at LLNL was performed under the auspices of the U.S. Department of Energy (DOE) by LLNL under contract DE-AC52-07NA27344. C.M.F. acknowledges a Senior Research Award from the Alexander von Humboldt Foundation and a fellowship from the Hanse-Wissenschaftskolleg in Germany as well as research support from the U.S. DOE under contract DE-FG02-84-ER13289. M.B. acknowledges financial support from the University of Bremen.

Supporting Online Material

www.sciencemag.org/cgi/content/full/327/5963/319/DC1
Materials and Methods
Figs. S1 to S4

20 October 2009; accepted 17 November 2009
10.1126/science.1183591

Large-Scale Controls of Methanogenesis Inferred from Methane and Gravity Spaceborne Data

A. Anthony Bloom,[1] Paul I. Palmer,[1]* Annemarie Fraser,[1] David S. Reay,[1] Christian Frankenberg[2]

Wetlands are the largest individual source of methane (CH_4), but the magnitude and distribution of this source are poorly understood on continental scales. We isolated the wetland and rice paddy contributions to spaceborne CH_4 measurements over 2003–2005 using satellite observations of gravity anomalies, a proxy for water-table depth Γ, and surface temperature analyses T_S. We find that tropical and higher-latitude CH_4 variations are largely described by Γ and T_S variations, respectively. Our work suggests that tropical wetlands contribute 52 to 58% of global emissions, with the remainder coming from the extra-tropics, 2% of which is from Arctic latitudes. We estimate a 7% rise in wetland CH_4 emissions over 2003–2007, due to warming of mid-latitude and Arctic wetland regions, which we find is consistent with recent changes in atmospheric CH_4.

The atmospheric concentration of methane (CH_4), an important greenhouse gas, is determined by a balance between natural and anthropogenic sources and sinks (*1*), leading to an atmospheric lifetime of approximately 9 years (*2*). Renewed interest in global budget calculations of CH_4 levels is due to (i) the largely unexplained stability of CH_4 concentrations during 1999–2006 and the renewed growth since early 2007 (*3*); (ii) laboratory and field measurements that support a small, previously unidentified, aerobic source of CH_4 from terrestrial vegetation (*4*); and (iii) new satellite observations that provide additional constraints on current understanding (*5*). Concentration measurements of CH_4 provide global constraints for emission estimates, but without additional, independent information it is difficult to attribute observed variability to individual sources and sinks.

Emissions from wetlands are the largest single source of CH_4, representing 20 to 40% of the total CH_4 emissions budget (*1*), of which 70% is estimated to originate from southern and tropical latitudes (*6*). Rice cultivation accounts for 6 to 20% of global CH_4 emissions (*1*), the majority of which originates from south and southeast Asia (*7*). Methanogenesis, the biogenic

[1]School of GeoSciences, University of Edinburgh, Edinburgh, UK. [2]SRON Netherlands Institute for Space Research, Utrecht, Netherlands.

*To whom correspondence should be addressed. E-mail: pip@ed.ac.uk

production of CH_4, occurs in natural wetlands and rice paddies by the anaerobic degradation of organic matter by methanogenic archaea. Production rates are controlled by the availability of suitable substrates; alternative electron acceptors for competing redox reactions, such as sulfate reduction (*8*); temperature; and soil salinity (*9*). Aerobic oxidation of CH_4 by methanotrophs is a key factor in controlling CH_4 emissions (*10*), with net fluxes to the atmosphere being primarily determined by the balance between CH_4 production and consumption in the wetland soils. Emergent wetland vegetation can also increase the transport of CH_4 between the soil and atmosphere (*11*). Although the controls on methanogenesis from wetlands and rice paddies are similar, the two sources are typically spatially distinct (*12*). Nevertheless, there is substantial uncertainty and regional variation associated with all these controlling factors. Wetland emissions dominated the interannual variability of CH_4 sources over 1984–2003 (*13*). A decrease in wetland emissions over the past decade has reportedly masked a coincident increase in anthropogenic emissions (*13*), leading to stable global mean CH_4 concentrations (*14*). Changes in the OH sink during 2006–2007 were not large enough to explain observed changes in CH_4 concentration (*3*).

We present an approach to understanding the role of wetlands and rice cultivation in producing observed CH_4 concentrations, using spaceborne measurements of gravity and CH_4 over the 3-year period from 2003 to 2005. We used three data sets. First, we used satellite column observations of CH_4 from the Scanning Imaging Absorption Spectrometer for Atmospheric Chartography (SCIAMACHY) instrument (*15*) aboard the Envisat satellite, which have been retrieved from solar-backscattered radiation at wavelengths from 1630 to 1679 nm (*5*), accounting for new water spectroscopic parameters (*16*). Retrieved columns, which are most sensitive to CH_4 in the lower troposphere (*5*), range from 1630 to 1810 parts per billion, with the largest values generally over mid-latitude and tropical continents (*16*).

Second, we used gravity anomaly measurements from the Gravity Recovery and Climate Experiment (GRACE) satellite (*17*). These measurements, used in previous studies to investigate changes in groundwater, have been corrected for geophysical mass variations such as tides, atmo-

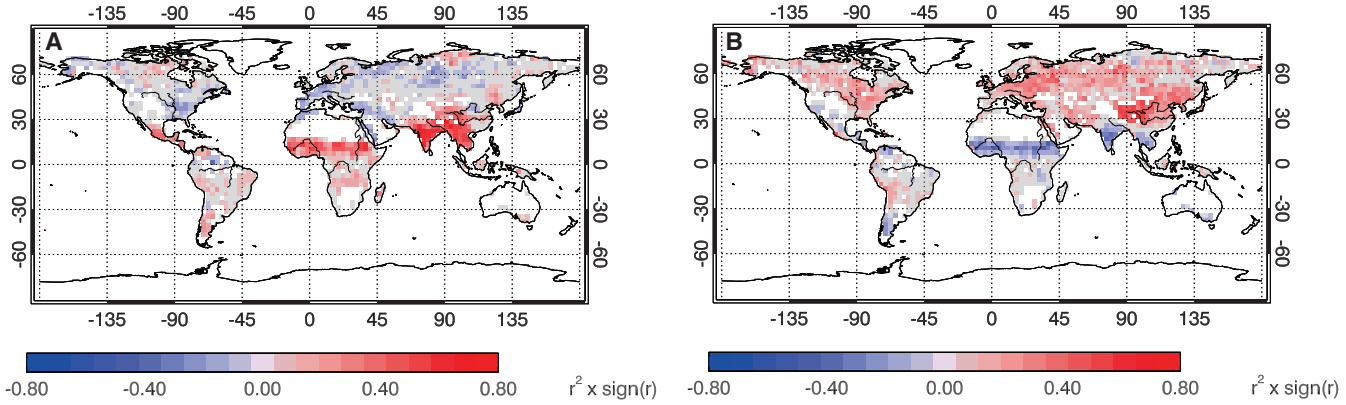

Fig. 1. Correlations (r^2) between cloud-free SCIAMACHY CH_4 column volume mixing ratios (VMRs) (in parts per million) and (**A**) equivalent groundwater depth (in meters), determined from gravity anomaly measurements from the GRACE satellites (*18*) and (**B**) NCEP/NCAR surface skin temperatures (in kelvin), calculated on a 3° × 3° horizontal grid over 2003–2005. The correlation at a given point is determined by at least 15 and typically 60 CH_4, groundwater, and temperature measurements. See SOM for a description of individual data sets.

Fig. 2. Time series of SCIAMACHY CH_4 column VMR and groundwater depth over the (**A**) Ganges, (**B**) Niger, (**C**) South Amazon, and (**D**) South Congo river basins. The correlation (r^2) between the variables is given for each panel. River basins are geographicaly defined with total runoff-integrating pathways (*26*). Vertical lines denote the start and end of each calendar year. A spatial representation of river basin correlations between CH_4 and groundwater is included in the SOM.

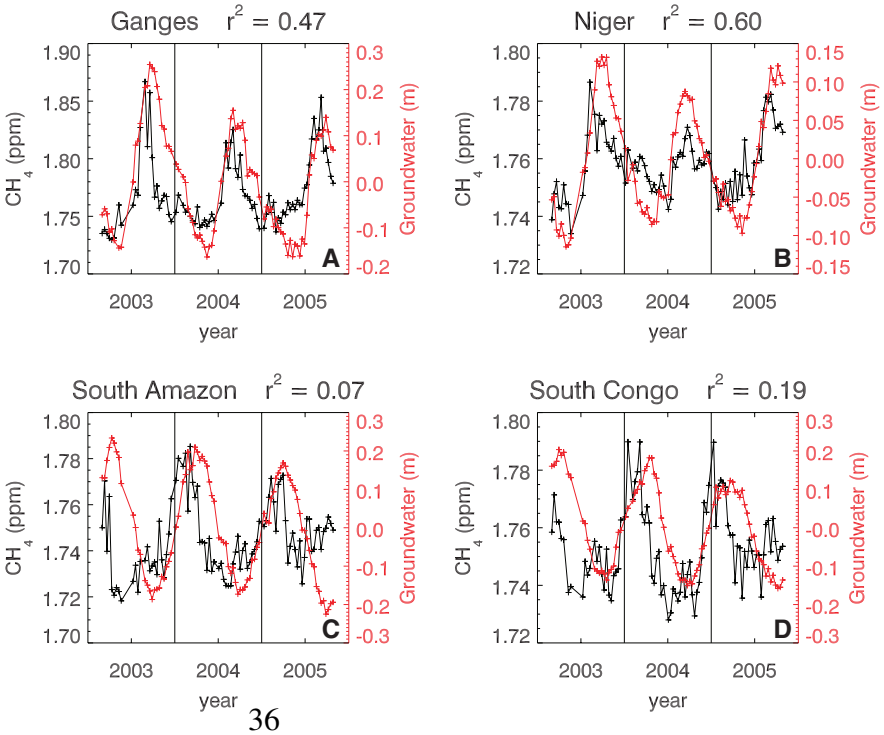

spheric pressure, and wind (*18*). Relative equivalent water height Γ (in meters), inferred from gravity [see supporting online material (SOM)], shows seasonal variability ranging from 5 to 20 cm over major river basins (*19*). We used a Γ data set with a 10-day time step (*18*), which we regridded to 3° × 3°. Finally, we used surface skin temperature fields T_S (in kelvin) from the National Centre for Environmental Prediction/National Centre for Atmospheric Research (NCEP/NCAR) weather analyses (*20*) as a proxy for soil temperature (SOM). We resolved all three data sets at the temporal and spatial resolutions of the Γ data set (SOM).

We find that that changes in wetlands and rice emissions dominate the observed variability of CH_4 columns over wetland regions [square of the correlation coefficient (r^2) = 0.7, SOM], and hence we interpret changes in these columns as changes in surface sources. We find that seasonal variations in the OH sink (*21*) and the CH_4 source from fires (*22*) typically explain <10 and 3% of the observed CH_4 column variability, respectively. CH_4 column data are available only over cloud-free daytime scenes; changes in controls on wetland CH_4 emissions on time scales shorter than 1 or 2 days due to processes such as rainfall, associated with cloudy conditions, are not well described by GRACE or Envisat. We excluded analysis over oceans, deserts, and regions with permanent ice cover.

To quantify the role of wetlands and rice cultivation in determining the observed variability of column CH_4, we correlated these data with concurrent changes in Γ and T_S over 2003–2005 (Fig. 1). We find that changes in Γ explain between 40 and 80% of the observed variability in CH_4 measurements over the tropics. We find high correlations over many major river basins (SOM), with the exception of the Amazon basin, which is described below. We generally find a negative correlation between Γ and CH_4 at high latitudes, which can be explained by high Γ in winter due to snow accumulation and associated low CH_4 emission, and low Γ in spring and summer due to displacement of snow melt and higher CH_4 emission as the exposed wetland is progressively warmed. At higher latitudes, we find that observed variations in CH_4 are mostly explained by changes in T_S (used here as a proxy for soil temperature). Changes in T_S over the tropics explain little of the observed variation in CH_4. Analysis of the deseasonalized time series shows similar but reduced correlations between CH_4 and Γ and T_S (SOM). This analysis provides global observations of the latitude dependence of the controlling factors—water table depth and soil temperature—that determine large-scale variations in wetland and rice paddy CH_4 emissions (*6*). This work supports our model calculations (SOM) that show that wetland and rice paddy emissions are largely responsible for observed CH_4 column variations.

Although variations in methanogenesis are predominantly attributed to variations in either groundwater or temperature, we account for the more complex dependence of methanogenesis with respect to both quantities (*23*). Within tropical latitudes, Γ is expected to be the dominant term in

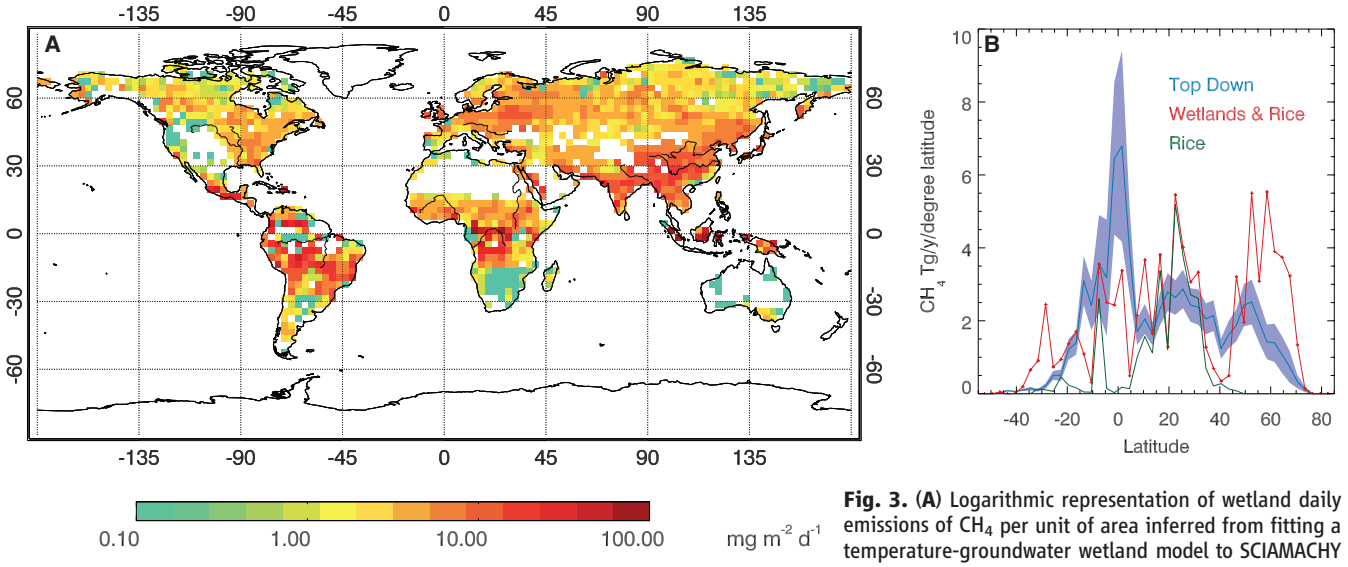

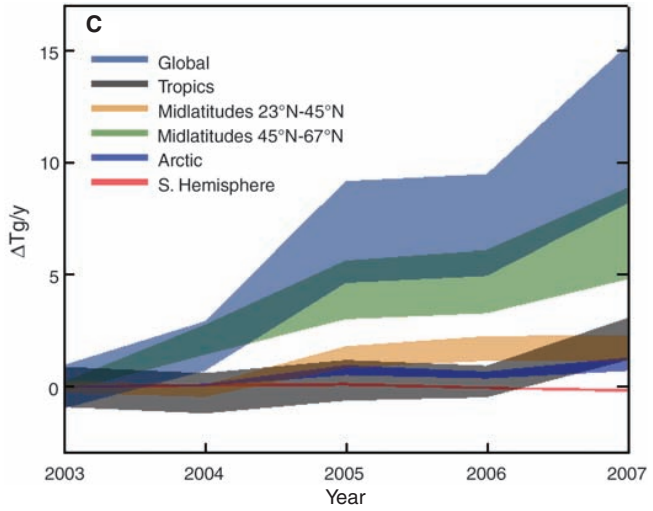

Fig. 3. (**A**) Logarithmic representation of wetland daily emissions of CH_4 per unit of area inferred from fitting a temperature-groundwater wetland model to SCIAMACHY CH_4 concentrations averaged on a 3° × 3° grid over 2003–2005. The normalized wetland and rice paddy emission distribution was scaled to 227 Tg of CH_4 (*1*). (**B**) Zonal integral of bottom-up emission model estimates of CH_4 from wetlands, including bogs and swamps, and rice paddies (*27*) (red); from rice paddies only (green); and from normalized top-down CH_4 emissions over 2003–2005 (blue). The shaded area indicates the uncertainty of our estimates due to systematic and random errors (SOM). (**C**) Predicted changes in annual wetland emissions for global wetlands, the tropics, the mid-latitudes from 23°N to 45°N, the mid-latitudes from 45°N to 67°N, the Arctic latitudes (>67° N), and the Southern Hemisphere. We assume a global wetland CH_4 flux of 170 Tg/year in 2003 (*1*). The line thickness denotes the estimated uncertainty of the predicted changes, including random errors from Γ and T_S measurements, and the error associated with 170 Tg/year, which we estimate as the standard deviation of global wetland CH_4 emission estimates taken from the IPCC Fourth Assessment Report (*1*).

areas with distinct dry and wet seasons. In areas where the preexisting groundwater volume is large with respect to Γ variations, a combined Γ-T_S relationship is expected. Figure 2 shows time series over four regions that exemplify the relationship between changes in Γ and column CH_4. For the Niger and the Ganges basins, changes in Γ coincide closely with the CH_4 variability, as is expected if the CH_4 signal is due to methanogenesis. Over the Amazon basin, the overall correlation between Γ and CH_4 is negligible ($r^2_{Amazon} = 0.01$). Changes in Γ over the Amazon basin are much larger than values observed over other river basins (Fig. 2) and lag behind CH_4 changes by 1 to 3 months in the north of the basin, possibly due to the seasonal migration of the intertropical convergence zone (SOM), but we find a statistically significant correlation over the southern half of the basin (south of 4°S, $r^2 = 0.07$). Although the CH_4 seasonal cycles over the north and south Amazon are synchronous, the seasonal cycle of wetland groundwater over the north Amazon precedes the south Amazon cycle by approximately 2 months; considering the east-west divide of the Amazon basin does not improve the correlation. Wetland emissions over the Amazon basin coincide with the Amazon River system and its varzeas (*24*). We acknowledge that even large temporal changes in wetland groundwater, Γ(t), over this basin will not necessarily represent large changes in surface soil moisture because of the depth of the wetland groundwater, D + Γ(t), where D represents the initial volume of the water column.

To determine the distribution of wetland emissions of CH_4 ($F^{w,\Gamma}_{CH_4}$, in mg/m^2/day), we developed a simple model (SOM) that describes the time-dependent relation between these emissions and T_S, and D + Γ(t)

$$F^{w,\Gamma}_{CH_4}(t) = k[D + \alpha\Gamma(t)]Q_{10}(T_S)^{\frac{T_S(t)-T_0}{10}} \quad (1)$$

where α is the fractional influence of Γ(t) on the total wetland groundwater volume D + Γ(t) (where $0 < \alpha < 1$); $Q_{10}(T_S)$ describes the change in methanogenesis rate with a 10 K increase in temperature, where T_0 is a constant ($T_0 = 273.16$ K) (*23*); and k (mg/m^3/day) incorporates other controlling factors (such as soil pH). The temperature dependence of $Q_{10}(T_S)$ can be approximated by $Q_{10}(T_0)^{[(T_0)/(T_S)]}$ (*23*). We acknowledge that the derived values of $Q_{10}(T_S)$ represent the relation between methanogenesis and T_S as opposed to soil temperature (SOM). We maximized the local linear correlation between $F^{w,\Gamma}_{CH_4}$ and SCIAMACHY CH_4 columns by varying (D/α) on a per grid basis and globally fitting $Q_{10}(T_0)$, where the gradient is proportional to changes in wetland emissions and the intercept is the sum of the remaining sources and sinks (SOM). We expect wetland and rice paddy emissions to follow a similar seasonal cycle, reflecting necessary hydrological and temperature conditions, but acknowledge that rice paddy emissions occur at specific intervals during the rice cultivation process. The global value of $Q_{10}(T_0)$ that best fits the data is 1.65 ± 0.15, although we find that wetland and rice paddy emission distributions remain similar within the range $1 < Q_{10}(T_0) < 2$.

The resulting normalized $F^{w,\Gamma}_{CH_4}$ distribution was then scaled to a total global wetland and rice paddy source of 227 Tg of CH_4/year, using the median value from the Intergovernmental Panel on Climate Change (IPCC) Fourth Assessment Report (*1*) to derive global emission rates shown in Fig. 3A. We find the largest CH_4 fluxes over South America, equatorial Africa, and southeast Asia. Emissions over the extratropical Northern Hemisphere are generally lower, but have elevated values over northern Europe and central Siberia and local peaks over North America. We find that uncertainties associated with extratropical CH_4 fluxes are an order of magnitude smaller than those associated with tropical fluxes (SOM).

We used prior information about rice paddy distributions (*12*) to isolate wetland regions from our emission estimates. The resulting latitudinal distribution of wetland emissions is similar to those produced by independent bottom-up emission estimates (Fig. 3B) and is within the range of the large intermodel differences (*25*). We find that the tropics account for 55.5 ± 2.5% of global wetland emissions, with the Amazon and Congo river basins accounting for 20.0 ± 2.6 Tg of CH_4/year and 25.7 ± 1.7 Tg of CH_4/year, respectively. We find that rice paddy areas account for 29.1 ± 0.6% (66.0 ± 1.4 Tg of CH_4/year) of the total rice plus wetland CH_4 source, acknowledging that a small proportion of this may be attributed to the spatial coincidence of rice paddies and wetlands. We find that rice paddy emissions centered over China and south and southeast Asia account for 32.5 ± 3.7 Tg of CH_4/year of the global rice paddy source, which is in agreement with bottom-up emission estimates (*12*).

We used our $F^{w,\Gamma}_{CH_4}$ model to determine the evolution of wetland CH_4 emissions over 2003–2007 relative to 2003 emissions. The change in annual emissions over that 5-year period was evaluated using the product of the fractional emission change and the wetland CH_4 map in Fig. 3A. We omitted areas of rice cultivation (*12*), where year-to-year changes in CH_4 emissions are determined by irrigation and other management regimes. We find a progressive global increase in CH_4 from wetlands over 2003–2007, due mainly to temperature increases at extratropical latitudes (45° to 67°N). We also find that Arctic wetland emissions (>67°N) increased by 30.6 ± 0.9% over 2003–2007 to approximately 4.2 ± 1.0 Tg of CH_4/year (SOM). We find that emissions from tropical wetlands remained constant over 2003–2006, with the exception of a 2.1 ± 0.7 Tg/year increase during 2007, most of which is accounted for by increased fluxes over the Congo (0.7 ± 0.2 Tg of CH_4/year) and Sahel (0.9 ± 0.2 Tg of CH_4/year) regions, as a result of increasing groundwater volume. The declining groundwater volume over tropical river basins over 2003–2006 did not significantly affect year-to-year changes in global wetland emissions. Our emissions calculations lead to better agreement with observed surface CH_4 anomalies over 2003–2008 than those obtained using bottom-up wetland emissions (SOM), reproducing the observed post-2006 positive anomaly in both the Northern and Southern Hemispheres. This supports the idea that changes in wetland emissions have significantly contributed to recent changes in atmospheric CH_4 concentrations.

There is substantial potential for wetland emissions to feed back positively to changes in climate (*23*), and therefore it is critical that we understand the extent of overlap between wetlands and regions that are most sensitive to projected future warming. We anticipate that the new constraints developed here will ultimately improve model predictions of this feedback.

References and Notes

1. K. Denman *et al.*, in *Climate Change 2007: The Physical Science Basis. Contribution of Working Group I to the Fourth Assessment Report of the Intergovernmental Panel on Climate Change*, S. Solomon *et al.*, Eds. (Cambridge Univ. Press, Cambridge, 2007), pp. 499–588.
2. E. J. Dlugokencky *et al.*, *Geophys. Res. Lett.* **30**, 1992 (2003).
3. M. Rigby *et al.*, *Geophys. Res. Lett.* **35**, L22805 (2008).
4. A. R. McLeod *et al.*, *New Phytol.* **180**, 124 (2008).
5. C. Frankenberg *et al.*, *Atmos. Chem. Phys.* **8**, 5061 (2008).
6. B. P. Walter, M. Heimann, E. Matthews, *J. Geophys. Res.* **106**, 34189 (2001).
7. E. Matthews, I. Fung, J. Lerner, *Global Biogeochem. Cycles* **5**, 3 (1991).
8. D. M. Ward, M. R. Winfrey, *Adv. Aquat. Microbiol.* **3**, 141 (1985).
9. R. Segers, *Biogeochemistry* **41**, 23 (1998).
10. J. Le Mer, P. Roger, *Eur. J. Soil Biol.* **37**, 25 (2001).
11. A. Joabsson, T. R. Christensen, B. Wallén, *Trends Ecol. Evol.* **14**, 385 (1999).
12. I. Fung *et al.*, *J. Geophys. Res.* **96**, (D7), 13033 (1991).
13. P. Bousquet *et al.*, *Nature* **443**, 439 (2006).
14. J. R. Evans, *New Phytol.* **175**, 1 (2007).
15. H. Bovensmann *et al.*, *J. Atmos. Sci.* **56**, 127 (1999).
16. C. Frankenberg *et al.*, *Geophys. Res. Lett.* **35**, L15811 (2008).
17. B. D. Tapley, S. Bettadpur, J. C. Ries, P. F. Thompson, M. M. Watkins, *Science* **305**, 503 (2004).
18. J.-M. Lemoine *et al.*, *Adv. Space Res.* **39**, 1620 (2007).
19. J. L. Chen, C. R. Wilson, J. S. Famiglietti, M. Rodell, *J. Geod.* **81**, 237 (2007).
20. E. Kalnay *et al.*, *Bull. Am. Meteorol. Soc.* **77**, 437 (1996).
21. A. Fiore *et al.*, *J. Geophys. Res. (Atmos.)* **108**, 4787 (2003).
22. G. R. van der Werf *et al.*, *Atmos. Chem. Phys.* **6**, 3423 (2006).
23. N. Gedney, P. M. Cox, C. Huntingford, *Geophys. Res. Lett.* **31**, L20503 (2004).
24. J. M. Melack *et al.*, *Glob. Change Biol.* **10**, 530 (2004).
25. M. Cao, S. Marshall, K. Gregson, *J. Geophys. Res.* **101**, (D9), 14399 (1996).
26. T. Oki, Y. C. Sud, *Earth Interact.* **2**, 1 (1998).
27. E. Matthews, I. Fung, *Global Biogeochem. Cycles* **1**, 61 (1987).

28. We thank J. Melack for providing feedback on the manuscript and R. Hipkin and F. Simons for assistance with GRACE gravity data. This work is funded by United Kingdom Natural Environmental Research Council studentship NE/F007973/1 and the National Centre for Earth Observation.

Supporting Online Material

www.sciencemag.org/cgi/content/full/327/5963/322/DC1
SOM Text
Figs. S1 to S6
Table S1
References

20 April 2009; accepted 11 November 2009
10.1126/science.1175176

Chapter 4

Large-Scale Controls of Methanogenesis Inferred from Methane and Gravity Spaceborne Data: Supplemantary Online Material

www.sciencemag.org/cgi/content/full/327/5963/322/DC1

Supporting Online Material for

Large-Scale Controls of Methanogenesis Inferred from Methane and Gravity Spaceborne Data

A. Anthony Bloom, Paul I. Palmer,* Annemarie Fraser, David S. Reay, Christian Frankenberg

*To whom correspondence should be addressed. E-mail: pip@ed.ac.uk

Published 15 January 2010, *Science* **327**, 322 (2010)
DOI: 10.1126/science.1175176

This PDF file includes:

1 Supporting online material for Large-scale Controls of Methanogenesis Inferred From Methane and Gravity Spaceborne Data by Bloom, Palmer, Fraser, Reay and Frankenberg

1.1 SCIAMACHY CH_4 columns

We use satellite column observations of CH_4 from the SCanning Imaging Absorption spectroMeter for Atmospheric CHartographY (SCIAMACHY) instrument (*1*), aboard ENVISAT, which have been retrieved from solar-backscattered radiation at 1630–1679 nm wavelengths (*2*), accounting for new water spectroscopic parameters (*3*). Retrieved columns, most sensitive to CH_4 in the lower troposphere (*2*), range from 1630 ppb to 1810 ppb, with the largest values generally over midlatitude and tropical continents (*3*). The data consist of CH_4 and CO_2 Vertical Column Densities (VCD) during January 2003 to October 2005 (*2*).

The SCIAMACHY pixel size for CH_4 VCD is 30 km by 120 km while for CO_2 VCD it is 30 km by 60 km (*4*). Although the SCIAMACHY swath is discontinuous along its track, the gaps are filled by subsequent orbits and near-global coverage can be achieved within 7 days. The exclusion of unreliable data, such as measurements over oceans and during cloudy conditions, results in substantial coverage gaps.

The mean column volume mixing ratio (CVMR) of CH_4 within the atmospheric column has been derived using equation 1

$$CH_4^{CVMR} = (\frac{CH_4^{VCD}}{CO_2^{VCD}})CO_2^{CVMR}, \quad (1)$$

where CH_4^{VCD} and CO_2^{VCD} are the vertical column densities of CH_4 and CO_2, and CO_2^{VMR} is the mean column volume CO_2 mixing ratio. We derive CH_4^{CMVR} using mean values of CO_2^{CVMR} obtained from the global CarbonTracker model (*5*). The CH_4^{VMR} data is then interpolated onto a $3^\circ \times 3^\circ$grid.

1.2 GRACE data

The Gravity Recovery and Climate Experiment (GRACE) mission consists of a twin satellite system that measures the temporal change in the Earth's gravitational field. Global coverage by the satellite is achieved every 30 days (*6*), although the effective temporal resolution is equivalent to 10 days with a maximum resolution of 400 km (*7*). The global gravity field is described as a geoidal height, the deviation of the gravitational equipotential surface from a reference, Earth geoid, in spherical harmonics. Equivalent water height, Γ, can be derived as a weighted sum of the geoid spherical harmonics with respect to spherical degree and the Earth's load deformation coefficients (*8*). We use the CNES 10 day 1°x 1°groundwater equivalent product Γ with an effective resolution of 667 km (*8*) which we interpolate to a $3^\circ$by 3°grid.

1.3 NCEP/NCAR surface temperature data

We used surface skin temperature (T_s), the temperature of the surface at radiative equilibrium, from NCEP/NCAR re-analysis data (*9*) as a proxy for soil temperature. We chose to use skin temperature because subsurface temperature estimates may contain additional model error (*10*) and the three-layer soil temperature model used in the NCEP/NCAR re-analysis (*9*) is not globally representative of wetland temperature regimes due to the variable wetland depths. Over 2003–2007, we find that NCEP/NCAR T_s value reproduce 97% of the variability of soil temperature at 10 cm depth in ice free regions; the range of soil temperatures is smaller than the range of surface skin temperatures, which leads to a small underestimate of inferred $Q_{10}(T_0)$.

Surface skin temperature fields are derived from T62 Gaussian grid NCEP re-analysis fields at a temporal resolution of 6 hours. The average grid resolution within latitudes of 60°S and 60°N is approximately 2°. The data was then interpolated to a 3°× 3°resolution. NCEP/NCAR T_s fields agree with satellite data to a level consistent with the 40-year ECMWF reanalysis (*11*).

1.4 GEOS-Chem chemistry transport model of CH_4

We use the GEOS-Chem 3-D global chemical transport model (version v8-01-01), driven by version 4 of the assimilated meteorological fields from NASA's Global Modeling and Assimilation Office. For this study we run the model at a horizontal resolution of 2°×2.5°, with 30 vertical levels. We include anthropogenic sources of CH_4 from ruminant animals, coal mining, oil production, landfills (*12*); biomass burning (*13*); and biofuel burning (*14*). We include natural sources from termites and hydrates, and a soil sink (*15*). Emissions from rice and wetlands were either taken from bottom-up inventories (*15*) or based on results from our study. We use monthly mean 3-D OH fields (*16*) to describe the tropospheric OH sink of CH_4. Loss rates for CH_4 in the stratosphere were adapted from a 2-D stratospheric model (*17*).

1.5 The relationship between wetland emissions and CH_4 columns

We use the GEOS-Chem model to characterise the relationship between wetland emissions (*15*) and CH_4 columns. We run the model for a complete year and analyse daily output. We sample the model between 10-12 local time, the approximate overpass time of ENVISAT. To account for vertical sensitivity of SCIAMACHY we apply a mean instrument averaging kernel to model profiles of CH_4 and vertically integrate the resulting profile to obtain columns. The model columns and wetland emissions were averaged over 10-day periods to be consistent with our data analysis.

We calculate grid point correlations (r^2) between model columns and monthly-varying emissions of rice and wetlands. Figure 1 shows that r^2 correlations are typically >0.7 where bottom-up emission estimates locate rice paddies and wetlands, supporting the idea that variability of these surface emissions determine variability of overlying CH_4 columns. Correlations between model CH_4 columns and integrated OH columns are an order of magnitude less than with rice or wetlands, and spatially more diffuse.

For each grid point, we also calculate the gradient between the peak-to-peak amplitude of wetland and rice paddy emissions and overlying CH_4 columns using a least-squares estimation method (*18*).

We assign a 5% error to the model columns, representing the maximum difference between the model and surface flask measurements. No error was assigned to the emissions. The gradient given here is the global mean with its standard error: 1.9±0.3 (ppb/(mg/m^2/day)), n=1828 for rice+wetlands. Individual gradients more than three standard deviations from the mean were omitted, eliminating grid points with very small emission variation.

1.6 Estimating changes in CH_4 due to seasonal variations in OH sink

We use monthly mean tropospheric OH concentrations calculated using the GEOS-Chem chemistry and aerosol simulation (*16*) to determine the annual variability of CH_4^{VMR} due to changes in oxidation by the OH radical.

We estimate the change in CH_4 concentrations due to seasonal variations of OH by subtracting the loss of CH_4 due to the annual mean OH concentration (ppb/month) from CH_4 loss due to monthly mean OH concentrations (ppb/month) and integrating the residual over a year:

$$[CH_4^{OHcor}] = \int \frac{d[CH_4^{OHloss}]}{dt} - \overline{\frac{d[CH_4^{OHloss}]}{dt}} dt, \quad (2)$$

where $\frac{dCH_4^{OHloss}}{dt} = -k[OH][CH_4^{VMR}]$, CH_4^{VMR} is the zonal mean CH_4^{VMR}, $[OH]$ is the zonal mean boundary layer OH concentration and k is the reaction rate constant between CH_4 and OH.

Figure 2 shows the CH_4 column peak-to-peak amplitude due to seasonal changes in OH oxidation expressed as a percentage of the peak-to-peak amplitude of column CH_4. As described in the main text, variations in column CH_4 due to OH are typically less than 10% of the column variation. This illustrative calculation is supported by the GEOS-Chem calculations described above.

1.7 Gridding data spatially and temporally

The two-dimensional fields of CH_4, Γ and T_s were evaluated on a common 3°× 3°grid between 88.5°S to 88.5°N and 178.5°W to 178.5°E. The datasets are averaged at a temporal resolution of 10 days: the centre days chosen when GRACE data was available. The gridded data provides a global field for each parameter at each sampling point in time. We average all CH_4 measurements at a single grid-point within a certain time frame to create a 3°× 3° CH_4 field at each timestep. Due to the uneven coverage of SCIAMACHY data, as described above, the fields often have substantial gaps.

1.8 Seasonal de-trending

We remove the seasonal cycle from each time series by fitting a fixed period sine curve, $Asin(2\pi t_{years} + \phi)$, allowing us to examine the seasonally independent relationship between these quantities. The seasonal de-trending experiments (Figure 3) show a significant correlation between the de-trended time series of CH_4 and temperature/gravity. We can therefore exclude the possibility of coincident seasonal variations between CH_4 and Γ or T_s as the main contribution of the correlations reported in the main paper.

1.9 River basin timeseries

We use geographical river basin boundaries (*19*) in order to examine the overall variations in CH_4, Γ and T_s associated with 30 major river catchment areas. For each timestep we derive the mean CH_4, Γ and T_s. Correlations between CH_4, Γ and T_s are shown in Figure 4.

1.10 The InterTropical Convergence Zone and CH_4 columns over South America

The ITCZ refers to a region where Northeast and Southeast trade winds converge, resulting in upward motion of air and elevated precipitation. The ITCZ is typically between 5° N and 5° S but meanders on a seasonal scale, sometimes reaching midlatitudes. The ITCZ is an effective barrier for atmospheric mixing between North and South hemisphere.

In the main text, we suggest that the seasonal meandering of the ITCZ might help explain the weak relationship between variations of CH_4 column and Γ over the Amazon basin. During Austral summer, the ITCZ shifts southward over South America which is accompanied by increased precipitation and higher CH_4 concentrations, characteristic of the northern hemisphere. Increased precipitation will lead to an increase in Γ. We acknowledge that a sudden increase in Γ will not instantaneously increase CH_4 emissions: water represents a barrier to CH_4 diffusion from the soil to the atmosphere (due to the low solubility of CH_4). Instead, we expect that CH_4 emissions (and subsequent changes to the atmospheric column) will lag the initial flooding event as anaerobic conditions prevail in the soils and soil CH_4 concentrations build up. Similarly, as the water table decreases we expect a peak in CH_4 soil emission as the diffusion barrier is removed but the methanogenesis conditions continue. The spaceborne columns over South America represent a superposition of (a) the increase of atmospheric CH_4 due to the southward migration of the ITCZ and (b) the increase in CH_4 wetland emissions due to elevated precipitation (and a subsequent increase in Γ) from the presence of the ITCZ. We also acknowledge that the elevated cloud cover associated with the ITCZ will reduce the sampling of this region during the wet season.

1.11 Gravity-temperature methanogenesis dependence

To determine the magnitude of wetland methanogenesis from SCIAMACHY CH_4^{VMR} columns we use equation 3 to describe global wetland methanogenesis (*20*):

$$F^w_{CH4} = k_{CH4} f_w C_s Q_{10}(T)^{\frac{T-T_0}{10}}, \tag{3}$$

where C_s is soil carbon, f_w is the wetland cover fraction, T is the temperature averaged over some depth (K), T_0 is 273.16 K, $Q_{10}(T)$ is the methanogenesis temperature dependence, and k_{CH4} is a calibration constant that ensures the required global emission budget. The value of $Q_{10}(T)$ is dependent on the temperature range so a temperature independent constant $Q_{10}(T_0)$ can be used to define the temperature sensitivity globally (*20*):

$$Q_{10}(T_0) = Q_{10}(T)^{\frac{T_0}{T}}. \tag{4}$$

We adapt equation 3 to describe wetland emissions as a function of Γ and surface temperature:

$$F_{CH4}^{w,\Gamma}(t) = k(D + \alpha\Gamma(t))Q_{10}(T)^{\frac{T(t)-T_0}{10}}, \tag{5}$$

where D is the initial volume of the water column; $\Gamma(t)$ is the water column height change over time t; α, a coefficient between $0 < \alpha < 1$, indicates the fraction of $\Gamma(t)$ affecting the wetland water volume; and k is a constant which absorbs C_s and f_w from equation 3. After factorising α we normalise $F_{CH4}^{w,\Gamma}$ by adjusting k accordingly.

We define the CH_4 column VMR at a surface location at time t as follows:

$$CH_4^{CVMR}(t) = \gamma F_{CH4}^{w,\Gamma}(t) + S(t) + c \tag{6}$$

where $F_{CH4}^{w,\Gamma}(t)$ is the normalised local wetland CH_4 emission; γ is the forward model that describes the relationship between emissions and observed column concentrations; S includes the remaining sources and sinks (including advection); and c is the background CH_4 level. We assume zero covariance between $F_{CH4}^{w,\Gamma}$ and S, allowing us to solve equation 6 as a linear equation:

$$CH_4^{CVMR} = \gamma F_{CH4}^{w,\Gamma}(t) + C, \tag{7}$$

where γ is the gradient, and the intercept $C = (\overline{S} + c)$ is the sum of the remaining sources and sinks. In reality we expect some correlation between S and $F_{CH4}^{w,\Gamma}$: a positive correlation would coincide in an overestimate of γ, and vice versa. Using equation 7, we solve for $\frac{D}{\alpha}$ per grid square and $Q_{10}(T)$ globally in order to maximise the correlation between $F_{CH4}^{w,\Gamma}$ and CH_4^{CVMR}. We exclude oceans, deserts and regions of permanent ice cover.

Equation 7 implies that where $F_{CH4}^{w,\Gamma}$ is zero the mean atmospheric concentration of CH_4 is C, as expected. The wetland contribution to the atmospheric concentration is then:

$$\overline{CH_4^{CVMR}} - C = \overline{\gamma F_{CH4}^{w,\Gamma}}. \tag{8}$$

Because $\overline{F_{CH4}^{w,\Gamma}} = 1$ the wetland contribution to the atmospheric concentration is equal to γ, which is the gradient between $F_{CH4}^{w,\Gamma}$ and CH_4^{CVMR}.

Finally, we scale the spatial distribution of γ ($3° \times 3°$resolution) to a global wetland+rice CH_4 source of 227 Tg y^{-1} (*21*), with a resulting distribution in mg m^{-2} day^{-1}. Oceans, deserts and regions with permanent ice cover are excluded from our global wetland analysis. We also exclude areas with negative correlations between $F_{CH4}^{w,\Gamma}$ and CH_4, but these represent only a small fraction of scenes.

1.12 CH_4 wetland emissions uncertainties

To obtain uncertainties for our wetland emission estimates of CH_4 we propagate systematic errors associated with the method and random errors associated with the GRACE and NCEP/NCAR data. Figure 5 shows the sum of random and systematic uncertainties for the normalised wetland CH_4 emission, representing c15–20% uncertainty globally and c40% over the tropics. Figure 3c from the main paper shows the uncertainty associated with the change in our wetland emission estimates relative to 2003 and so will only include the random errors.

The method includes fitting a wetland emission model to observed CH_4 column from the SCIAMACHY instrument. We account for the uncertainty of CH_4^{CVMR} (ppb) using equation 1, using the mean fitting uncertainties for CH_4 and CO_2 column densities (molec/cm^2) during 2003, and estimating an uncertainty of 1% for CarbonTracker CO_2 concentrations (ppb). We also propagate uncertainty resulting from the linear fit of $F_{CH4}^{w,\Gamma}$ to CH_4^{CVMR} (γ) using a two-step approach. First, by quantifying the error on linear fit per gridpoint and then quantifying the standard error of the mean statistics of the locally-fitted γ and its uncertainty. Using the GEOS-Chem chemistry transport model (see above) we estimate that the uncertainty of the global γ to be 16% (0.3/1.9).

The main sources of random error are GRACE measurements of Γ and NCEP/NCAR surface skin temperature. Uncertainties in GRACE measurements are within the range of 3–6mm (*8*). We assume a global mean uncertainty of 0.5 K for a 10-day mean of surface skin temperature, which is likely to be an overestimate. Total random errors correspond to 0.5 Tg/yr.

1.13 CH_4 wetland emissions over northern high latitudes

In the main paper we report CH_4 wetlands emissions of 4.2±1.0 Tg from Arctic latitudes, defined here as >67° N, which is smaller than the 10 Tg reported by another bottom-up inventory (*22*). We report in Table 1 our results in a manner consistent with other bottom-up wetland emission estimates at high northern latitudes. Generally, our results agree better with more recent studies.

Table 1: Wetland emission estimates at northern high latitudes from bottom-up inventories and our study.

Latitude region	Our Study [Tg]	Previous Studies [Tg]
40–80°N	49±0.6	47 (*23*)
50–70°N	27±0.5	62 (*22*)
>66°N	3±0.2	10 (*22*)
>50°N	28±0.5	45–106 (*24*)
>45°N	41±0.6	38 (*25*)
>40°N	49±0.5	31 (*26*)
>30°N	68±0.8	65 (*27*)

1.14 Wetland CH_4 emissions change between 2003-2007

To model changes in CH_4 emissions over 2003–2007, we drive the wetland emission model adapted in this work and fitted for 2003–2005 (equation 5) with GRACE equivalent water height, Γ, and NCEP surface temperatures over that time period. We drive the model at a one-day temporal resolution in order to avoid seasonal bias due to missing data. To fill in the gap in GRACE data during January–March 2003 we use the adjusted seasonal equivalent for 2004.

We use 2003 as a baseline year and calculate the percentage increase in emission from the baseline. To determine the change in wetland emissions (Δ Tg/y) we multiply the percentage increase to our estimated wetland emission distribution scaled by 170 Tg y^{-1}, the median of bottom-up wetland emission estimates (*21*).

We use the GEOS-Chem chemistry transport model (described above), driven by a) our wetland emissions and b) a bottom-up inventory (*15*), to reproduce the observed CH_4 anomalies from surface flask sites (*28–30*) during 2003–2007. We define the anomaly as the long-term mean for each dataset subtracted from the dataset. Figure 6 shows that the magnitude and variability of CH_4 mole fraction anomalies (ppb) determined using our emission model are more consistent with the observations than the model using the bottom-up inventory. Our emission model is able to capture the positive anomaly since 2006 in both the northern and southern hemisphere (*28–30*), suggesting that changes in wetland emissions are partially responsible for recent changes in the global mean concentration of CH_4.

2 Figures

2.1 Figure 1

Correlations (r^2) between daily GEOS-Chem CH_4 columns (Jan-Dec, 2003), convolved with a mean SCIAMACHY averaging kernel, and the associated (top) rice paddy and (bottom) wetland CH_4 emissions.

2.2 Figure 2

Fractional contribution of CH_4 column variability due to variability in the OH sink, expressed as the ratio between the CH_4 column peak-to-peak amplitude due to seasonal changes in OH and the peak-to-peak amplitude of column CH_4.

2.3 Figure 3

(Top) Signed correlation (r^2) between the seasonally de-trended water table depth Γ (metres) and CH_4 concentration (ppb) during 2003-2005. A best-fit one-year period sine curve was used to remove the seasonal trend from both quantities. (Bottom) Signed correlation between the seasonally de-trended temperature and CH_4 concentration time series during 2003-2005 at each point. A best-fit one-year period sine curve was used to remove the seasonal trend from both quantities. Note the difference in scale from Figure 1 of main paper.

2.4 Figure 4

Signed correlation (r^2) between CH_4 and groundwater (a) and temperature (b) over major river basins. River basin masks (*19*) are used as averaging windows for the CH_4 and groundwater data. Note the difference in scale from Figure 1 of main paper.

2.5 Figure 5

Uncertainties calculated for normalised CH_4 wetland emissions, shown in daily fluxes of CH_4 per unit area. An global uncertainty of 1% was used for CO_2 Carbon Tracker Data. Regions of large uncertainties mostly coincide with large CH_4 wetland emissions (see paper).

2.6 Figure 6

Monthly mean observed and model CH_4 mole fraction anomalies at northern (top) and southern hemisphere (bottom) surface measurement sites, 2003–2008 (*28–30*). Anomalies are calculated by subtracting the 2003–2008 mean concentration from the mole fraction timeseries. The GEOS-Chem chemistry transport model, driven by our wetland emissions (red) and a bottom-up emission inventory (blue) (*15*). Correlation (r) between observed and model anomalies are shown inset.

References

1. H. Bovensmann, *et al.*, *Journal of Atmospheric Sciences* **56**, 127 (1999).
2. C. Frankenberg, *et al.*, *Atmospheric Chemistry & Physics* **8**, 5061 (2008).
3. C. Frankenberg, *et al.*, *Geophysical Research Letters* **35**, L15811 (2008).
4. M. Buchwitz, *et al.*, *Atmospheric Chemistry & Physics* **5**, 941 (2005).
5. W. Peters, *et al.*, *Proc. Nat. Acad. Sci. USA* **104**, 18925 (2007).
6. B. D. Tapley, S. Bettadpur, J. C. Ries, P. F. Thompson, M. M. Watkins, *Science* **305**, 503 (2004).
7. D. D. Rowlands, *et al.*, *Geophysical Reseach Letters* **32**, 4310 (2005).
8. J.-M. Lemoine, *et al.*, *Advances in Space Research* **39**, 1620 (2007).
9. E. Kalnay, *et al.*, *Bulletin of the American Meteorological Society* **77**, 437 (1996).
10. M. E. Mann, G. A. Schmidt, *EGS - AGU - EUG Joint Assembly, Abstracts from the meeting held in Nice, France, 6 - 11 April 2003, abstract #1574* pp. 1574–+ (2003).
11. B.-J. Tsuang, M.-D. Chou, Y. Zhang, A. Roesch, K. Yang, *J. Climate* **21** (2008). Doi:10.1175/2007JCLI1502.1.
12. J. G. J. Olivier, J. A. V. Aardenne, F. Dentener, L. Ganzeveld, J. A. H. W. Peters, *Non-CO2 Greenhouse Gases (NCGG-4)* (Millpress, Rotterdam, 2005), chap. Recent trends in global greenhouse gas emissions: regional trends and spatial distribution of key sources, pp. 325–330. ISBN 90 5966 043 9.
13. G. R. van der Werf, *et al.*, *Atmospheric Chemistry & Physics* **6**, 3423 (2006).

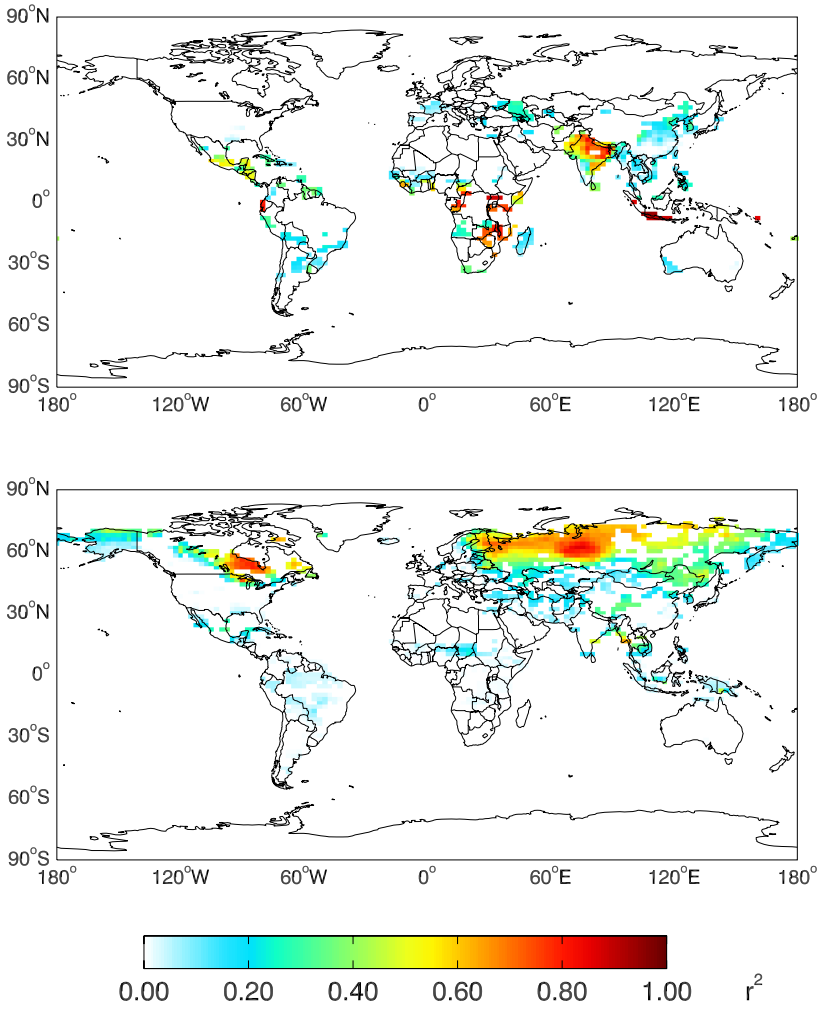

Figure 1: Correlations (r^2) between daily GEOS-Chem CH_4 columns (Jan-Dec, 2003), convolved with a mean SCIAMACHY averaging kernel, and the associated (top) rice paddy and (bottom) wetland CH_4 emissions.

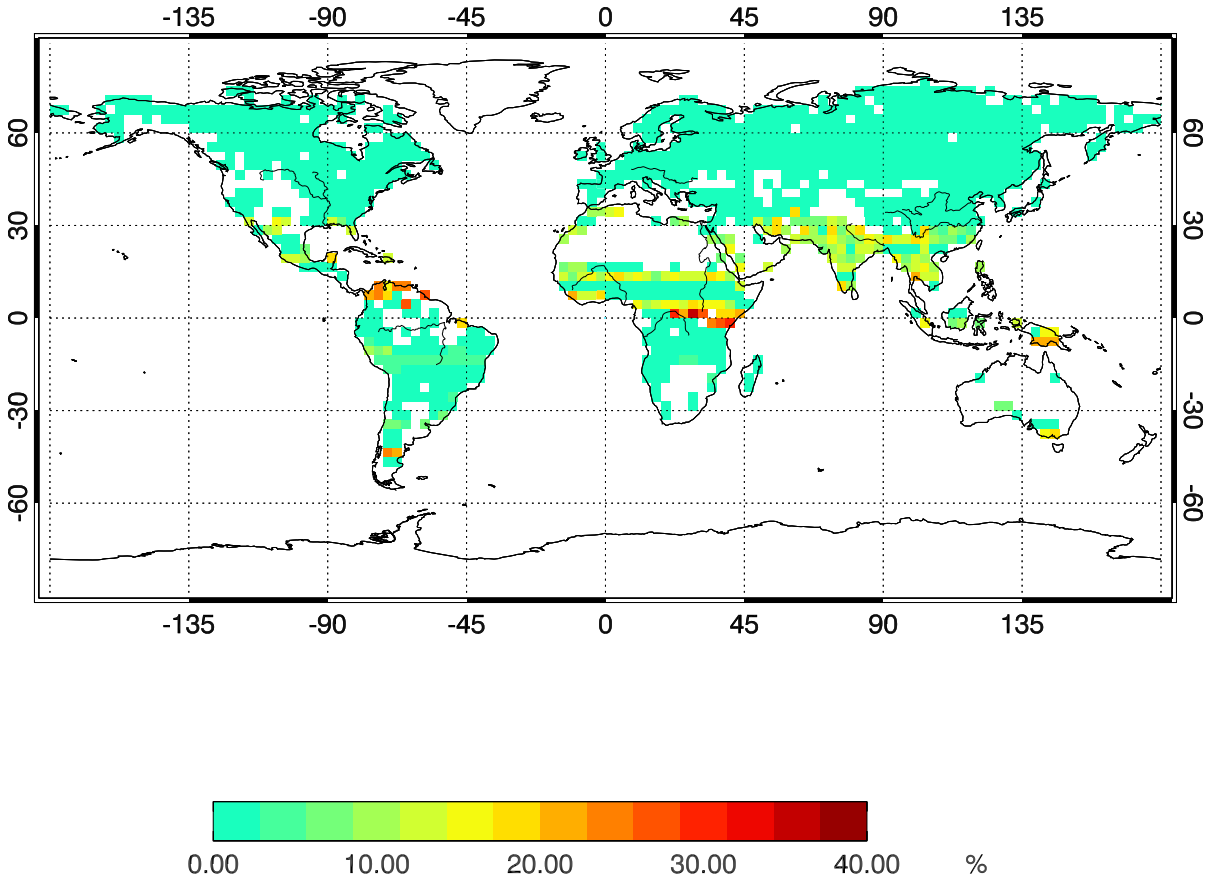

Figure 2: Fractional contribution of CH_4 column variability due to variability in the OH sink, expressed as the ratio between the CH_4 column peak-to-peak amplitude due to seasonal changes in OH and the peak-to-peak amplitude of column CH_4.

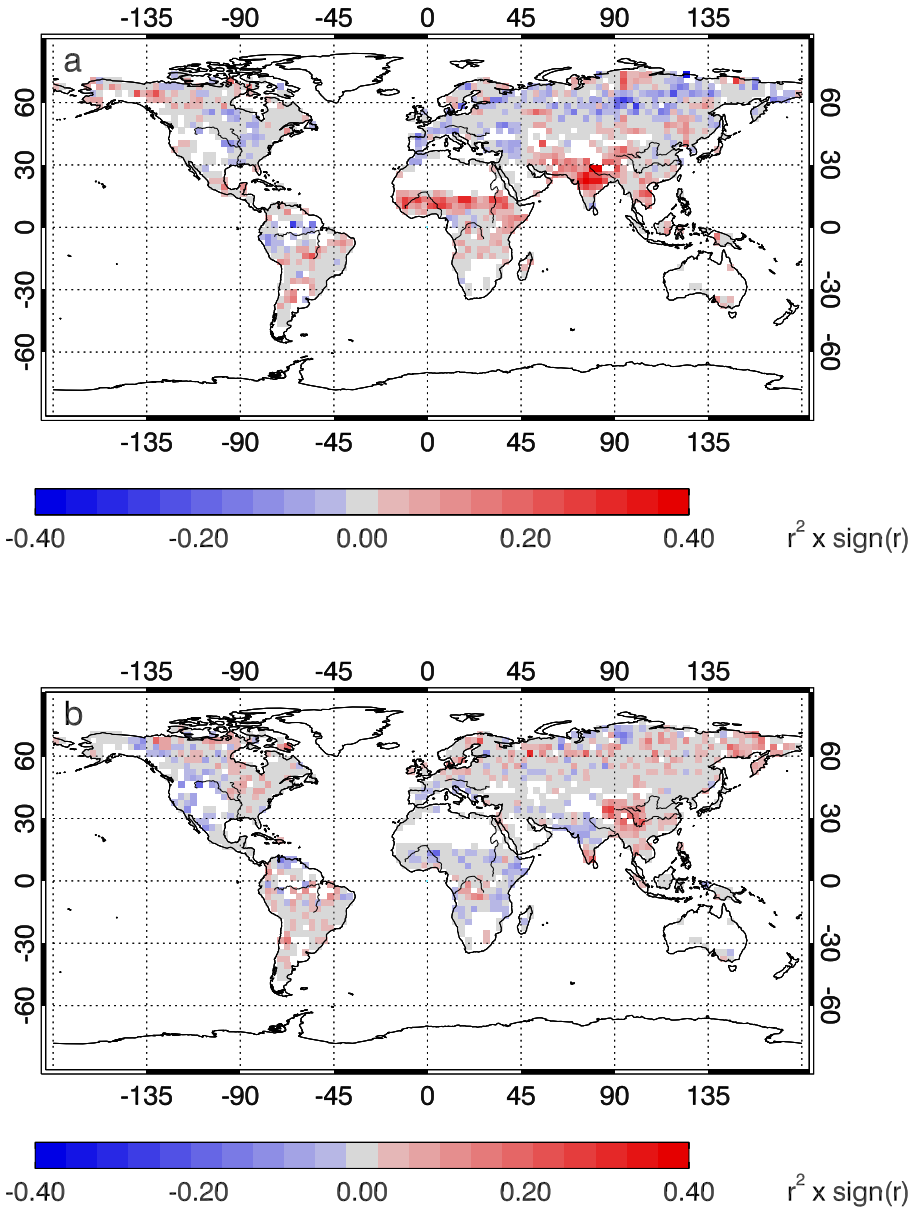

Figure 3: (Top) Signed correlation (r^2) between the seasonally de-trended water table depth Γ (metres) and CH_4 concentration (ppb) during 2003-2005. A best-fit one-year period sine curve was used to remove the seasonal trend from both quantities. (Bottom) Signed correlation (r^2) between the seasonally de-trended temperature and CH_4 concentration time series during 2003-2005 at each point. A best-fit one-year period sine curve was used to remove the seasonal trend from both quantities. Note the difference in scale from Figure 1 of main paper.

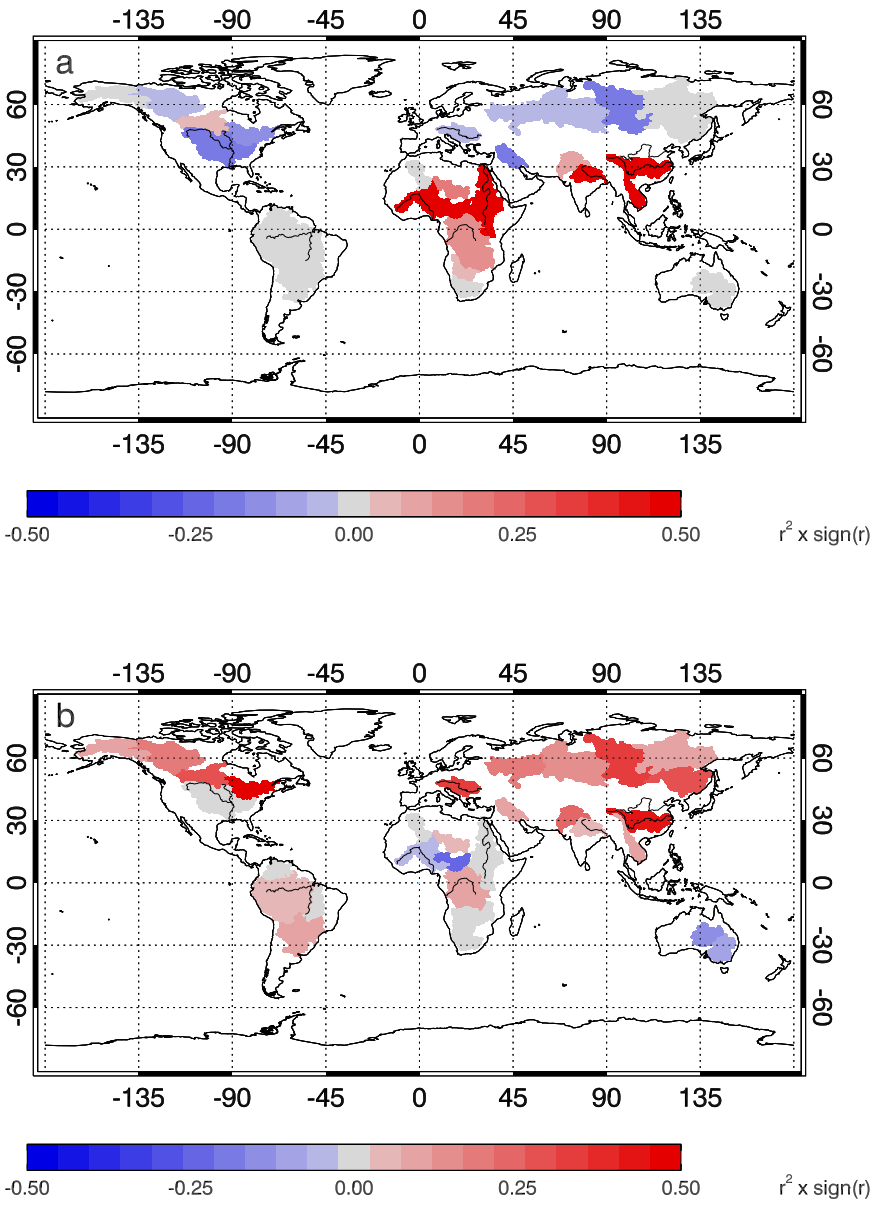

Figure 4: Signed correlation (r^2) between CH_4 and groundwater (a) and temperature (b) over major river basins. River basin masks (*19*) are used as averaging windows for the CH_4 and groundwater data. Note the difference in scale from Figure 1 of main paper.

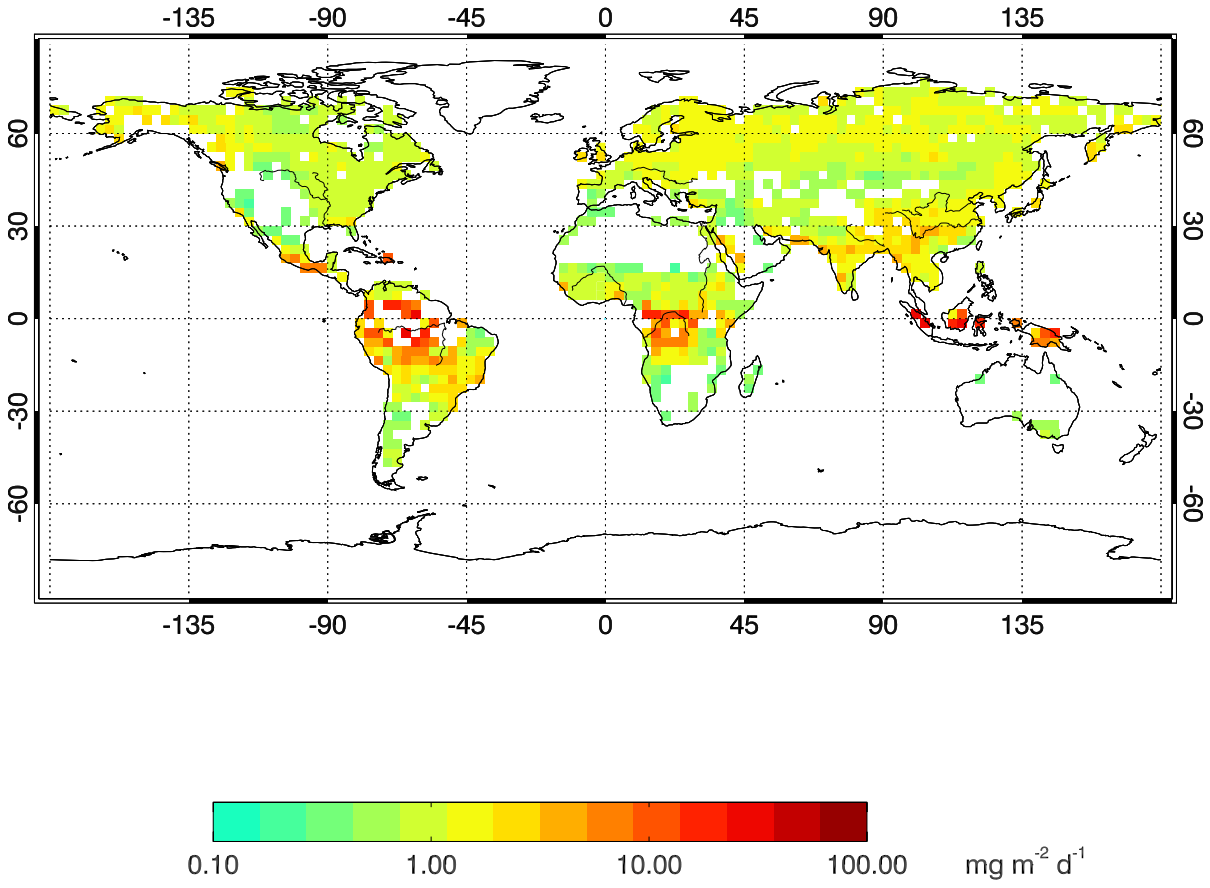

Figure 5: Uncertainties calculated for normalised CH_4 wetland emissions (see text), expressed as daily fluxes of CH_4 per unit area (mg $^{-2}$ d^{-1}).

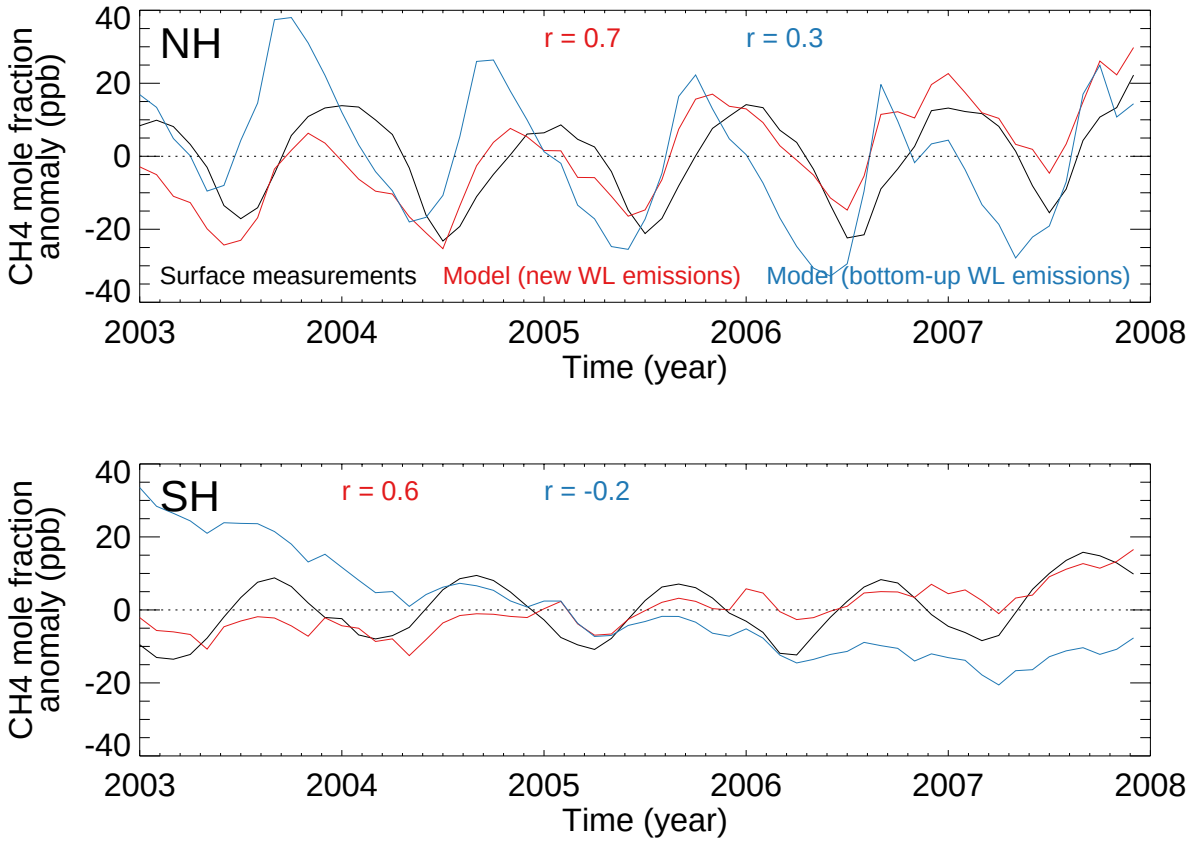

Figure 6: Monthly mean observed and model CH_4 mole fraction anomalies at northern (top) and southern hemisphere (bottom) surface measurement sites, 2003–2008 (*28–30*). Anomalies are calculated by subtracting the 2003–2008 mean concentration from the mole fraction timeseries. The GEOS-Chem chemistry transport model, driven by our wetland emissions (red) and a bottom-up emission inventory (blue) (*15*). Correlation (r) between observed and model anomalies are shown inset.

14. B. N. Duncan, R. V. Martin, A. C. Staudt, R. Yevich, J. A. Logan, *J. Geophys. Res* **108** (2003). Doi:10.1029/2002JD002378.

15. I. Fung, *et al.*, *Journal of Geophysical Research* **96**, 13033 (1991).

16. A. Fiore, *et al.*, *Journal of Geophysical Research (Atmospheres)* **108**, 4787 (2003).

17. J. S. Wang, *et al.*, *Global. Biogeochem. Cycles* **18** (2004). Doi:10.1029/2003GB002180.

18. D. York, N. M. Evensen, M. Lpez-Martnez, J. D. B. Delgado, *Am. J. Phys.* **72**, 367 (2004).

19. T. Oki, Y. C. Sud, *Earth Interactions* **2**, 1 (1998).

20. N. Gedney, P. M. Cox, C. Huntingford, *Geophysical Research Letters* **31**, 20503 (2004).

21. K. Denman, *et al.*, *Couplings Between Changes in the Climate System and Biogeochemistry. In: Climate Change 2007: The Physical Science Basis. Contribution of Working Group I to the Fourth Assessment Report of the Intergovernmental Panel on Climate Change [Solomon, S., D. Qin, M. Manning, Z. Chen, M. Marquis, K.B. Averyt, M.Tignor and H.L. Miller (eds.)].* (Cambridge University Press, Cambridge, United Kingdom and New York, NY, USA., 2007).

22. E. Matthews, I. Fung, *Global Biochemical Cycles* **1**, 61 (1987).

23. Y. Liu, Modeling the emissions of nitrous oxide (N_2O) and methane (CH_4) from the terrestrial biosphere to the atmosphere, Ph.D. thesis, MIT (1996).

24. D. I. Sebacher, R. C. Harriss, K. B. Bartlett, S. M. Sebacher, S. S. Grice, *Tellus Series B Chemical and Physical Meteorology B* **38**, 1 (1986).

25. K. B. Bartlett, R. C. Harriss, *Chemosphere* **26**, 261 (1993).

26. C. Mingkui, K. Gregson, S. Marshall, *Atmospheric Environment* **32**, 3293 (1998).

27. B. P. Walter, M. Heimann, E. Matthews, *Journal of Geophysical Research* **106**, 34189 (2001).

28. R. G. Prinn, *et al.*, *J. Geophys. Res.* **105**, 17751 (2000).

29. E. J. Dlugokencky, P. Lang, K. Masarie, Atmospheric methane dry air mole fractions from the NOAA ESRL carbon cycle cooperative global air sampling network, 1983-2007, version: 2008-07-02 (2009). Ftp://ftp.cmdl.noaa.gov/ccg/ch4/flask/event/.

30. R. L. Francey, *et al.*, Global atmospheric sampling laboratory (GASLAB): supporting and extending the Cape Grim trace gas programs. baseline atmospheric program (Australia) 1993 (1996). Edited by R.J. Francey, A.L. Dick and N. Derek, pp 8-29, Bureau of Meteorology and CSIRO Division of Atmospheric Research, Melbourne, Australia.

Chapter 5

Seasonal Variability of TropicalWetland CH4 Emissions: the role of the methanogen-available carbon pool

Manuscript prepared for Biogeosciences
with version 4.2 of the LaTeX class copernicus.cls.
Date: 18 November 2011

Seasonal Variability of Tropical Wetland CH_4 Emissions: the role of the methanogen-available carbon pool

A. A. Bloom[1], P. I. Palmer[1], A. Fraser[1], and D. S. Reay[1]
[1]School of GeoSciences, University of Edinburgh, Edinburgh, UK.
Correspondence to: A. Anthony Bloom (a.a.bloom@ed.ac.uk)

Abstract.

We develop a dynamic methanogen-available carbon model (DMCM) to quantify the role of the methanogen-available carbon pool in determining the spatial and temporal variability of tropical wetland CH_4 emissions over seasonal timescales. We fit DMCM parameters to satellite observations of CH_4 columns from SCIAMACHY CH_4 and equivalent water height (EWH) from GRACE. Over the Amazon river basin we find substantial seasonal variability of this carbon pool (coefficient of variation = 28 $\pm$ 22%) and a rapid decay constant (ϕ = 0.017 day^{-1}), in agreement with available laboratory measurements, suggesting that plant litter is likely the prominent methanogen carbon source over this region. Using the DMCM we derive global CH_4 emissions for 2003–2009, and determine the resulting seasonal variability of atmospheric CH_4 on a global scale using the GEOS-Chem atmospheric chemistry and transport model. First, we estimate tropical emissions amount to 111.1 Tg CH_4 yr^{-1} of which 24% is emitted from Amazon wetlands. We estimate that annual tropical wetland emissions have increase by 3.4Tg CH_4 yr^{-1} between 2003 and 2009. Second, we find that the model is able to reproduce the observed seasonal lag between CH_4 concentrations peaking 1–3 months before peak EWH values. We also find that our estimates of CH_4 emissions substantially improve the comparison between the model and observed CH_4 surface concentrations (r=0.9). We anticipate that these new insights from the DMCM represent a fundamental step in parameterising tropical wetland CH_4 emissions and quantifying the seasonal variability and future trends of tropical CH_4 emissions.

1 Introduction

Wetlands are the single largest source of methane (CH_4) into the atmosphere and account for 20–40% of the global CH_4 source (Denman et al., 2007), of which tropical wetlands account for 50–60% of this global wetland CH_4 source (e.g. Cao et al., 1996; Bloom et al., 2010). Tropical wetland biogeochemistry is poorly understood compared to boreal peatlands (Mitsch et al., 2010), resulting in large inter-model discrepancies of the magnitude and distribution of tropical wetland CH_4 emission estimates (Riley et al., 2011). Tropical climate variability (e.g., resulting in widespread droughts, Lewis et al., 2011) can lead to large year to year variations in tropical wetland CH_4 emissions and subsequently the global CH_4 budget (Hodson et al., 2011). An improved quantitative understanding of the magnitude, distribution, and variation of tropical wetland CH_4 emissions is therefore essential to further understanding of the global CH_4 cycle. Here, we parameterise tropical wetland CH_4 emissions, and hence introduce a predictive capability that can be used to determine future emissions and to help quantify global CH_4 climate feedbacks.

In wetlands and rice paddies, methanogenesis (the biogenic production of CH_4) occurs as the final step of anoxic organic matter decomposition (Neue et al., 1997). Factors influencing methanogenesis rates include substrate availability, soil pH, temperature, water table position and CH_4 oxidation rates (Whalen, 2005). Wetland vegetation type and aquatic herbivore activity can also affect the transport of CH_4 between the soil and atmosphere (Joabsson et al., 1999; Dingemans et al., 2011). On a global scale, seasonal variations in wetland CH_4 fluxes are mostly determined by temporal changes in wetland water volume and soil temperature (Walter et al., 2001; Gedney et al., 2004), and from seasonal changes in wetland extent and wetland water table depth (Ringeval et al., 2010; Bloom et al., 2010). Recent work that used SCIAMACHY lower tropospheric CH_4 column concentrations and Gravity Recovery And Climate Experiment (GRACE) equivalent water height (EWH) retrievals show that the seasonality of wetland CH_4 emissions can be largely explained by seasonal changes in surface temperature and water volume (Bloom et al., 2010). The Amazon and Congo river basins were the only major exceptions in this study, where CH_4 concentrations peaked several weeks before EWH, highlighting our incomplete understanding of the processes controlling tropical wetland CH_4 emissions over seasonal timescales.

In this paper we focus on the seasonal lag between CH_4 emissions and flooding over the Amazon river basin area (Oki and Sud, 1998). We use SCIAMACHY CH_4 retrievals and GRACE EWH (both described in section 2.2) to determine the seasonal lag between wetland CH_4 emissions and wetland water volume. Figure 1 shows that seasonal flooding of the Amazon basin occurs typically 1–3 months after the peak CH_4 concentrations, and to a lesser extent the lag persists throughout tropical wetland areas. In section 2, we test the hypothesis that this lag is related to the depletion of methanogen-available carbon during the onset of the tropical wet season by explicitly accounting for this carbon pool in a parameterised model of tropical wetland CH_4 emissions (Bloom et al., 2010). We optimise model parameters by fitting them to SCIAMACHY CH_4 column and GRACE

EWH measurements, and use the resulting model to estimate global wetland emission estimates. In section 3 we compare our results to previous estimates of wetland CH_4 emissions and to decomposition rates of methanogen-available carbon in anaerobic environments. Finally, we use our estimated emissions to drive the GEOS-Chem atmospheric chemistry model as an approach to test the consistency between our emission estimates and observed variations of atmospheric CH_4 concentration. We conclude the paper in section 4.

2 Process-based Model and Application

Here, we introduce a methanogen-available carbon pool (C_μ) that typically originates from labile plant litter, recalcitrant organic matter decomposition and root exudates (e.g. Wania et al., 2010). Typically soil carbon pool decay constants are more than an order of magnitude lower than those of leaf litter (Sitch et al., 2003; Wania et al., 2010). Therefore, if C_μ originates mostly from the slow-decomposing recalcitrant carbon pool, then variations in C_μ over seasonal timescales are likely to be small. Conversely, if C_μ is drawn from leaf litter, then large variations in C_μ abundance may arise as a result of rapid litter decomposition in the tropics. Miyajima et al. (1997) measure CH_4 accumulation of anaerobic decomposition of incubated tropical withered tree leaves over a 200 day period. These observations show a rapid decrease in decomposition rates over the incubation period. Bianchini Jr. et al. (2010) found similar results from dried and ground anaerobic decomposition of *Oxycaryum cubense* at 20°C: following a 20-day lag (where no emissions were observed) CH_4 produced from organic carbon decomposition peaked after a 50-day period, and then rapidly decreased. On a tropical river-basin scale, flooded areas expand at the onset of the wet season and engulf newly available plant litter: as a result, CH_4 emissions from plant litter may peak before the height of the water table. The occurrence of anaerobic CH_4 emissions from litter decomposition within sub-seasonal timescales raises the question as to whether C_μ significantly varies in time.

2.1 Model Description

We base our model on previous work (Bloom et al., 2010) that describes the temporal variability of wetland emissions $F^t_{CH_4}$ (mg CH_4 m^{-2} day^{-1}) as a function of EWH and surface temperature:

$$F^t_{CH_4} = k(\Gamma^t_w + D_\alpha)Q_{10}(T^t_s)^{\frac{T^t_s}{10}}, \quad (1)$$

where at time t (days), Γ^t_w is the EWH, T^t_s is the surface temperature (K), D_α is the equivalent depth of the wetland soil (m), $Q_{10}(T^t_s)$ is the temperature dependence function implemented by Gedney et al. (2004), and k is a scaling constant (mg CH_4 m^{-2} day^{-1}) accounting for all temporally constant factors (e.g. Gedney et al., 2004).

Equation 1 assumes an inexhaustible source of methanogen-available carbon. Here we account for the potential seasonal changes in C_μ by substituting k with $\phi_0 C^t_\mu$, where ϕ_0 (day^{-1}) is the

temperature, water and carbon independent decay constant of wetland methanogenesis, and C_μ^t is the value of C_μ (mg CH_4 m^{-2}) at time t:

$$F_{CH_4}^t = \phi_0 C_\mu^t (\Gamma_w^t + D_\alpha) Q_{10} (T_s)^{\frac{T_s^t}{10}}. \quad (2)$$

To determine temporal changes in C_μ, we define C_μ^{t+1} in terms of C_μ^t:

$$C_\mu^{t+1} = C_\mu^t + N_\mu \Delta t - F_{CH_4}^t \Delta t, \quad (3)$$

where Δt is the time interval, $F_{CH_4}^t$ is the carbon loss due to emitted CH_4 (equation 2), N_μ is the net influx of carbon available for methanogenesis from plant litter, root exudates, and breakdown of complex polymers from the recalcitrant carbon pool. We assume N_μ is temporally constant, and we assume wetland carbon stocks are in quasi-equilibrium on annual timescales, hence $\overline{N_\mu}$ = $\overline{F_{CH_4}^t}$. Note that when ϕ_0 is small, the equilibrium $C_\mu \gg N_\mu \Delta t$. In this case, $C_\mu^{t+1} \simeq C_\mu^t$ and equation 2 converges to equation 1 (Bloom et al., 2010), which assumes $\phi_0 C_\mu$ is constant over seasonal timescales. In order to compare derived decay constants with observed and model values (e.g. Miyajima et al., 1997; Wania et al., 2010), we determine the annual mean decay constant of wetlands areas as $\overline{\phi} = \overline{F_{CH_4}^t} / \overline{C_\mu}$ (day^{-1}). Equations 2 and 3 constitute the dynamic methanogen-available carbon model (DMCM).

2.2 Data

For the sake of brevity we only include a brief description of the datasets for our analysis and refer the reader to dedicated papers. Solar backscatter data from the Scanning Imaging Absorption Spectrometer for Atmospheric Cartography (SCIAMACHY) instrument onboard Envisat is used to retrieve the mean column concentrations of CH_4 in the atmosphere (Frankenberg et al., 2005). The spatial resolution of CH_4 retrievals is 30km $\times$ 60km, and the Envisat orbital geometry ensures global coverage at 6-day intervals. CH_4 retrievals are only achievable in daytime cloud-free conditions. The Gravity Recovery and Climate Experiment (GRACE) is a twin satellite system from which the Earth's gravity field is retrieved at 10-day intervals. Tides, atmospheric pressure and wind are included in the applied corrections on GRACE gravity retrievals: the remaining temporal variation in GRACE gravity is dominated by terrestrial water variability (Tapley et al., 2004). We incorporate SCIAMACHY CH_4 concentrations, GRACE EWH and NCEP/NCAR daily 1.9° x 1.88° temperature re-analyses (Kalnay et al., 1996) into a process-based model following Bloom et al. (2010). We use the 2003-2008 SCIAMACHY column CH_4 retrievals (Frankenberg et al., 2008), and the CNES GRACE EWH 1° x 1° 10-day resolution product (Lemoine et al., 2007): we aggregate all three datasets to a daily 3° x 3° horizontal grid (see Bloom et al., 2010).

2.3 Global parameter optimisation

We implement the DMCM on a global 3° $\times$ 3° grid for the period 2003–2009. We drive the DMCM using the aggregated daily values of T_s^t and Γ_w^t. We spin up the DMCM using 2003 T_s^t and Γ_w^t

values until it reaches an annual equilibrium ($\overline{N_\mu} = \overline{F^t_{CH_4}}$). In contrast to Bloom et al. (2010), we supplement the $Q_{10}(T_s)$ function with a gradual linear cut-off for temperatures for 0°C $< T^t_s <$ -10°C, and when $T^t_s <$ -10°C, $F^t_{CH_4} = 0$ as a first order approximation to wintertime CH_4 emission inhibition in boreal wetlands. As the Q_{10} function never reaches zero, this supplementary constraint will effectively suppress winter-time CH_4 emissions, which is broadly consistent with our current understanding of CH_4 emissions in boreal wetlands.

We apply the DMCM globally in order to determine (i) the temporal variability of $\overline{\phi}$ and C_μ in the tropics within each $3^\circ \times 3^\circ$ gridcell (ii) the potential of C_μ temporal variability on extra-tropical wetland environments, and (iii) CH_4 emissions from wetlands and rice paddies at a global scale. We determine the global distribution and seasonal variability of wetland CH_4 emissions by optimising parameters ϕ_0 and D_α at each gridcell by minimising the following cost function (J):

$$J = \sum_{t=1}^{n} (\kappa * \Delta F^t_{CH_4} - \Delta S^t_{CH_4})^2, \tag{4}$$

where $\Delta S^t_{CH_4}$ denotes the SCIAMACHY CH_4 variability after we remove the interannual trend (represented as a 2^{nd} order polynomial); $F^t_{CH_4}$ is derived from equations 2 and 3; and the conversion factor κ (ppm kg^{-1} CH_4 m^{-2} day^{-1}) relates CH_4 emissions to the equivalent column concentration in the lower troposphere (e.g. Bloom et al., 2010). We then implement the global $Q_{10}(T_s)$ optimisation approach of Bloom et al. (2010). Like other top-down parameter optimisation methods of global wetland CH_4 emissions (Gedney et al., 2004; Bloom et al., 2010), our method is unable to distinguish between the seasonality of CH_4 emissions from wetlands and rice paddies due to the concurring fluxes over seasonal timescales, although we anticipate varying fertilisation and irrigation practices will also influence the seasonality in rice paddy CH_4 emissions (Conen et al., 2010). We hence distinguish the sources spatially (Bloom et al., 2010) for which we have more confidence in the distribution of rice paddies. Finally, we use the IPCC global wetland and rice paddy CH_4 emissions median of 227.5 Tg CH_4 yr^{-1} (Denman et al., 2007) as a base value for 2003 emissions.

We propagate the following uncertainties through our global wetland and rice paddy CH_4 emissions estimation (Bloom et al., 2010): (i) SCIAMACHY CH_4 observation errors; (ii) the uncertainty of the linear fit between $F^t_{CH_4}$ and $S^t_{CH_4}$; (iii) the uncertainty $\sigma_\kappa = \pm 16\%$ associated with κ; and (iv) a global wetland and rice paddy uncertainty of $\pm$ 58 Tg CH_4 yr^{-1} (Denman et al., 2007).

3 Results and Discussion

Over the Amazon river basin we find wetland CH_4 fluxes coinciding with small values of C_μ, resulting in a highly variable C_μ over seasonal timescales. Assuming an annual mean inundated fraction of 3.3% (Prigent et al., 2007), the median CH_4 flux over a flooded area is 1.06Mg C ha^{-1}(369 mg CH_4 m^{-2} day^{-1}). The median Amazon wetland C_μ = 0.16Mg C ha^{-1} with a range of 0.02–7.89Mg C ha^{-1} (5^{th}–95^{th} percentile). The large spatial variability of C_μ is consistent with the

complexity of methanogenesis rates in wetlands (Neue et al., 1997; Whalen, 2005). Large temporal changes of C_μ are observed in the Amazon river basin where the mean C_μ coefficient of variation (c_v) is $28 \pm 22\%$ over the period 2003-2009. When we allow C_μ to vary in extra-tropical regions we find a median of $c_v < 0.1\%$, and as a result the relatively small C_μ variability does not influence the seasonality of CH_4 emissions outside the tropics. For rice paddy areas in southeast Asia we find a median of $c_v = 4.8\%$. We acknowledge that due to the varying rice cultivation practices around the world (Conen et al., 2010), the effects of rice paddy irrigation and the timing of fertilisation on C_μ cannot be captured by the DMCM approach.

To determine whether our derived values for C_μ and $\overline{\phi}$ are relevant to tropical ecosystems, we compare them against laboratory measurements of anaerobic decomposition of withered leaves from a wetland region in Narathiwat, Thailand (Miyajima et al., 1997). We simulate CH_4 production from C_μ at each model gridcell for a 200-day period without fresh carbon input (N_μ=0), and we use inundated fraction observations (Prigent et al., 2007) to determine the flux magnitude over flooded areas only. Figure 2 shows the cumulative CH_4 production over a 200-day period for (i) simulated decomposition from derived $\overline{\phi}$ and C_μ values over the Amazon, (ii) simulated decomposition from derived $\overline{\phi}$ and C_μ values over boreal wetlands, and (iii) upscaled withered leaf mineralisation rates by Miyajima et al. (1997) using a median of 17.5 Mg C ha^{-1} fine and coarse woody debris (Malhi et al., 2009). For boreal and tropical C_μ decomposition, the median cumulative CH_4 emissions, 68% confidence interval, and mean decay constants ($\overline{\phi}$) are shown. For the withered leaf mineralisation rates, we show the mean fitted decay constant ($\overline{\phi}$) and the range and median cumulative CH_4 emissions.

The top-down parameter estimation of $\overline{\phi}$ and C_μ suggest plant litter C_μ is a fundamental component of tropical CH_4 emission seasonality. Our top-down estimation of anaerobic decomposition rates for tropical wetland CH_4 emissions compare favourably with laboratory measurements of anaerobically produced CH_4: while the magnitude of tropical C_μ decomposition is more than a factor of two smaller than laboratory measurements (Miyajima et al., 1997), the mean decay constant $\overline{\phi}_{Amazon}$ = 0.017 day^{-1} compares well to $\overline{\phi}_{leaf}$ = 0.011 day^{-1} for withered leaf decomposition. The larger laboratory measurements (Miyajima et al., 1997) are partially explained by an incubation temperature of 35°C (cf. a mean surface temperatures in the Amazon basin of 23°C), and the lack of observations for coarse woody debris decomposition. As a result of relatively high $\overline{\phi}$ values, measured leaf decomposition and model CH_4 emissions both show a significant reduction of CH_4 emission rates throughout the 200-day period. In contrast, the boreal decay constant ($\overline{\phi}_{Boreal}$= 0.0003 day^{-1}) indicates relatively constant CH_4 emission rates throughout the 200-day period.

Table 1 shows a comparison between observed and model decay constants derived from a variety of methods. The range of $\overline{\phi}_{Amazon}$ values are within the order of magnitude of leaf and wetland macrophyte decay constants (Miyajima et al., 1997; Longhi et al., 2008; Wania et al., 2010). We believe that $\overline{\phi}_{Amazon}$ is an indicator for the cumulative decay constant of the rapid anaerobic de-

composition of root exudates, plant litter decomposition, and the contribution of recalcitrant carbon pools. For a more detailed $\overline{\phi}_{Amazon}$ comparison with observed and model decay constant values, an estimation of the overall $\overline{\phi}$ in wetland CH_4 production from bottom-up process-based models (e.g. Wania et al., 2010) is needed.

Figure 3 shows the total CH_4 flux over the central branch of the Amazon river (0°N–6°S, 80° W–40°W). The temporal changes in C_μ result in a significantly different timing for CH_4 emissions over the tropics in comparison to the Bloom et al. (2010) water volume and temperature dependence approach. While in the dry season the minimum CH_4 fluxes coincide with the lowest GRACE EWH, peak CH_4 fluxes occur during the rising water phase. The DMCM optimisation predicts that the accumulation of carbon in the dry season results in higher C_μ values at the onset of the wet season. This carbon pool is then rapidly depleted during the wet season. As a result, CH_4 emission rates begin to decrease before the peak water phase in the wet season. CH_4 oxidation within the water column has been proposed as a mechanism explaining reduced CH_4 emissions during the peak of the wet season (Mitsch et al., 2010), although this would result in a second CH_4 peak at the end of the wet season. The absence of this peak in our analysis suggests this process plays only a minor role in tropical wetland CH_4 emissions seasonality.

By globally integrating the DMCM method we estimated tropical wetlands emit 111.1 Tg CH_4 yr^{-1}, where Amazon wetlands account for 26.2 Tg CH_4 yr^{-1} (24%). Table 2 shows our estimates are within the range of other independent Amazon wetland emission CH_4 estimates. Figure 4 shows the zonal profile of our top-down approach with the associated uncertainty estimates. We capture three main features of global wetland and rice paddy emissions, i.e. peaks over the tropics, subtropics and lower mid-latitudes (mainly due to rice), and boreal latitudes, in agreement with previous studies (Bloom et al., 2010; Fung et al., 1991; Riley et al., 2011). In comparison to our previous work (Bloom et al., 2010) we find a slight reduction in boreal wetland emissions (3.2%), primarily due to the introduction of a gradual cut-off in methanogenesis rates under 0°C (section 2.3). During 2003-2008, the global change in CH_4 wetland emissions amounts to an increase 7.7 Tg CH_4 yr^{-1}, mostly as a result of boreal wetlands (3.1 Tg CH_4 yr^{-1}) and tropical wetlands (3.4 Tg CH_4 yr^{-1}), while there is also a significant increase of 1.1 Tg CH_4 yr^{-1} from mid-latitude wetlands. The increase in southern hemisphere extra-tropical wetland emissions (0.13 Tg CH_4 yr^{-1}) did not significantly contribute to the CH_4 wetland emissions growth during 2003–2008.

Finally, we use our wetland and rice CH_4 emission estimates to drive the GEOS-Chem global 3-D atmospheric chemistry and transport model (described and evaluated by Fraser et al., 2011) allowing us to test consistency between our emissions to surface measurements of CH_4 concentrations. We sample the model at the time and geographical location of the surface CH_4 measurements from the GasLab, AGAGE and ESRL networks (Francey et al., 1996; Prinn et al., 2000; Cunnold et al., 2002; Dlugokencky et al., 2009). Figure 5 shows model and observed CH_4 concentration anomalies (i.e., minus the mean trend) for the northern and southern hemispheres. We chose to remove the

interannual trend from all CH_4 concentrations to compare the seasonality of model and surface measurements of CH_4. We show that the DMCM approach better describes the observed seasonality in both hemispheres (r_{NH}=0.9, r_{SH}=0.9), and the amplitude of the southern hemisphere seasonality is largely improved in comparison to the GEOS-Chem runs using Fung et al. (1991) and Bloom et al. (2010) CH_4 emissions.

4 Concluding Remarks

Understanding the temporal controls of temperature, water volume and carbon content of wetlands is crucial in determining the global and regional seasonal cycle of wetland CH_4 emissions. We show that incorporating a temporally variable methanogen-available carbon pool, C_μ, in our top-down approach results in a significant improvement in describing the temporal behaviour of tropical and global CH_4 emissions.

By implementing our dynamic methanogen-available carbon model (DMCM) on a global scale we determine the effects of a seasonally variable C_μ on the seasonality of wetland CH_4 emissions in the Amazon river basin. We find a median decay constant of $\overline{\phi}_{Amazon}$ = 0.017 day^{-1} over the Amazon river basin. Seasonal changes in C_μ in the tropics largely explain the seasonal lag between SCIAMACHY observed CH_4 concentrations and GRACE equivalent water height. The relatively high seasonal variability in C_μ (mean c_v = 28%) over the Amazon river basin results in peak CH_4 emissions occurring mostly 1-3 months prior to the peak water height period: in contrast, the median boreal C_μ variability is $c_v < 0.1\%$. We show a substantial improvement in simulating surface concentrations when using the GEOS-Chem ACTM with our wetland and rice CH_4 emission estimates (r=0.9). These improvements in the magnitude and temporal dynamics of tropical CH_4 emissions will ultimately help constrain global inverse modelling efforts.

We anticipate that this work will lead to further and more detailed parameterisation of tropical wetland CH_4 emissions, and we expect our tropical wetland CH_4 emission parameterisation will reduce the uncertainty in forecasting future changes in wetland CH_4 emissions.

Acknowledgements. We thank Catherine Prigent for providing global inundated fraction data and Christian Frankenberg for providing the SCIAMACHY CH4 retrievals. The surface measurements were provided by the NASA AGAGE network, the NOAA ESRL network, and the CSIRO Marine and Atmospheric Research GASLab network. A.A.B. was supported by the UK Natural Environmental Research Council (NERC) studentship NE F007973 1 and funds from P.I.P.'s Philip Leverhulme Prize. A.C.F. was supported by the NERC Centre for Earth Observation.

References

Bianchini Jr., I., Cunha-Santino, M. B. d., Romeiro, F., and Bitar, A. L.: Emissions of methane and carbon dioxide during anaerobic decomposition of aquatic macrophytes from a tropical lagoon (São Paulo, Brazil), Acta Limnologica Brasiliensia (Online), 22, 157–164, 2010.

Bloom, A. A., Palmer, P. I., Fraser, A., Reay, D. S., and Frankenberg, C.: Large-Scale Controls of Methanogenesis Inferred from Methane and Gravity Spaceborne Data, Science, 327, 322–325, 2010.

Cao, M., Marshall, S., and Gregso, K.: Global carbon exchange and methane emissions from natural wetlands: Application of a process-based model, Journal of Geophysical Research, 101, 14 399–14 414, 1996.

Conen, F., Smith, K. A., and Yagi, K.: Methane and Climate Change, chap. Rice Cultivation, pp. 115–135, EarthScan, iSBN 9781844078233, 2010.

Cunnold, D. M., Steele, L. P., Fraser, P. J., Simmonds, P. G., Prinn, R. G., Weiss, R. F., Porter, L. W., O'Doherty, S., Langenfelds, R. L., Krummel, P. B., Wang, H. J., Emmons, L., Tie, X. X., and Dlugokencky, E. J.: In situ measurements of atmospheric methane at GAGE/AGAGE sites during 1985-2000 and resulting source inferences, Journal of Geophysical Research (Atmospheres), 107, 4225, doi:10.1029/2001JD001226, 2002.

Denman, K., Brasseur, G., Chidthaisong, A., Ciai, P., Cox, P., Dickinson, R., Hauglustaine, D., Heinze, C., Holland, E., Jacob, D., U.Lohmann, Ramachandran, S., da Silva Dias, P., Wofsy, S., and Zhang, X.: Couplings Between Changes in the Climate System and Biogeochemistry. In: Climate Change 2007: The Physical Science Basis. Contribution of Working Group I to the Fourth Assessment Report of the Intergovernmental Panel on Climate Change [Solomon, S., D. Qin, M. Manning, Z. Chen, M. Marquis, K.B. Averyt, M.Tignor and H.L. Miller (eds.)]., Cambridge University Press, Cambridge, United Kingdom and New York, NY, USA., 2007.

Dingemans, B., Bakker, E., and Bodelier, P.: Aquatic herbivores facilitate the emission of methane from wetlands, Ecology, 92, 1166–1173, 2011.

Dlugokencky, E. J., Lang, P., and Masarie, K.: Atmospheric Methane Dry Air Mole Fractions from the NOAA ESRL Carbon Cycle Cooperative Global Air Sampling Network, 1983-2007, Version: 2008-07-02, 2009.

Francey, R. L., Steele, L., Langenfelds, R., Lucarelli, M., Allison, C., Beardsmore, D., Coram, S., Derek, N., de Silva, F., Etheridge, D., Fraser, P., Henry, R., Turner, B., Welch, E., Spencer, D., and Cooper, L.: Global Atmospheric Sampling Laboratory (GASLAB): supporting and extending the Cape Grim trace gas programs. Baseline Atmospheric Program (Australia) 1993, edited by R.J. Francey, A.L. Dick and N. Derek, pp 8-29, Bureau of Meteorology and CSIRO Division of Atmospheric Research, Melbourne, Australia, 1996.

Frankenberg, C., Meirink, J. F., van Weele, M., Platt, U., and Wagner, T.: Assessing Methane Emissions from Global Space-Borne Observations, Science, 308, 1010–1014, 2005.

Frankenberg, C., Warneke, T., Butz, A., Aben, I., Hase, F., Spietz, P., and Brown, L. R.: Pressure broadening in the $2\nu_3$ band of methane and its implication on atmospheric retrievals, Atmospheric Chemistry & Physics, 8, 5061–5075, 2008.

Fraser, A., Miller, C. C., Palmer, P. I., Deutscher, N. M., Jones, N. B., and Griffith, D. W. T.: The Australian methane budget: Interpreting surface and train-borne measurements using a chemistry transport model, Journal of Geophysical Research, 116, D20 306, doi:10.1029/2011JD015964, 2011.

Fung, I., John, J., Lerner, J., Matthews, E., Prather, M., Steele, L. P., and Fraser, P. J.: Three-dimensional model synthesis of the global methane cycle, Journal of Geophysical Research, 96, 13 033–13 065, doi:

10.1029/91JD01247, 1991.

Gedney, N., Cox, P. M., and Huntingford, C.: Climate feedback from wetland methane emissions, Geophysical Research Letters, 31, L20 503, doi:10.1029/2004GL020919, 2004.

Hodson, E. L., Poulter, B., Zimmermann, N. E., Prigent, C., and Kaplan, J. O.: The El Niño-Southern Oscillation and wetland methane interannual variability, Geophysical Research Letters, 38, L08 810, doi: 10.1029/2011GL046861, 2011.

Joabsson, A., Christensen, T. R., and Wallen, B.: Vascular plant controls on methane emissions from northern peatforming wetlands, Trends in Ecology and Evolution, 14, 385–388, 1999.

Kalnay, E., Kanamitsu, M., Kistler, R., Collins, W., Deaven, D., Gandin, L., Iredell, M., Saha, S., White, G., Woollen, J., Zhu, Y., Leetmaa, A., Reynolds, R., Chelliah, M., Ebisuzaki, W., Higgins, W., Janowiak, J., K.C. Mo, C. R., Wang, J., Jennec, R., and Joseph, D.: The NCEP/NCAR 40-Year Reanalysis Project, Bulletin of the American Meteorological Society, 77, 437–471, 1996.

Lemoine, J.-M., Bruinsma, S., Loyer, S., Biancale, R., Marty, J.-C., Perosanz, F., and Balmino, G.: Temporal gravity field models inferred from GRACE data, Advances in Space Research, 39, 1620–1629, doi:10.1016/j.asr.2007.03.062, 2007.

Lewis, S. L., Brando, P. M., Phillips, O. L., van der Heijden, G. M. F., and Nepstad, D.: The 2010 Amazon Drought, Science, 331, 554, doi:10.1126/science.1200807, 2011.

Longhi, D., Bartoli, M., and Viaroli, P.: Decomposition of four macrophytes in wetland sediments: Organic matter and nutrient decay and associated benthic processes, Aquatic Botany, 89, 303 – 310, doi:10.1016/j.aquabot.2008.03.004, 2008.

Malhi, Y., Aragao, L. E. O. C., Metcalfe, D. B., Paiva, R., Quesada, C. A., Almeida, S., Anderson, L., Brando, P., Chambers, J. Q., Da Costa, A. C. L., Hutyra, L. R., Oliveira, P., Patino, S., Pyle, E. H., Robertson, A. L., and Teixeira, L. M.: Comprehensive assessment of carbon productivity, allocation and storage in three Amazonian forests, Global Change Biology, 15, 1255–1274, doi:10.1111/j.1365-2486.2008.01780.x, 2009.

Melack, J. M., Hess, L. L., Gastil, M., Forsberg, B. R., Hamilton, S. K., Lima, I. B. T., and Nova, E. M. L. M.: Regionalization of methane emissions in the Amazon basin with microwave remote sensing, Global Change Biology, 10, 530–544, 2004.

Mitsch, W., Nahlik, A., Wolski, P., Bernal, B., Zhang, L., and Ramberg, L.: Tropical wetlands: seasonal hydrologic pulsing, carbon sequestration, and methane emissions, Wetlands Ecology and Management, 18, 573–586, doi:doi:10.1007/s11273-009-9164-4, 2010.

Miyajima, T., Wada, E., Hanba, Y. T., and Vijarnsorn, P.: Anaerobic mineralization of indigenous organic matters and methanogenesis in tropical wetland soils, Geochimica et Cosmochimica Acta, 61, 3739–3751, doi:10.1016/S0016-7037(97)00189-0, 1997.

Neue, H., Wassmann, R., Kludze, H., Bujun, W., and Lantin, R.: Factors and processes controlling methane emissions from rice fields, Nutrient Cycling in Agroecosystems, 49, 111–117, 1997.

Oki, T. and Sud, Y. C.: Design of Total Runoff Integrating Pathways (TRIP) - A global river channel network, Earth Interactions, 2, 1–37, 1998.

Prigent, C., Papa, F., Aires, F., Rossow, W. B., and Matthews, E.: Global inundation dynamics inferred from multiple satellite observations, 1993-2000, Journal of Geophysical Research (Atmospheres), 112, D12 107, doi:10.1029/2006JD007847, 2007.

Prinn, R. G., Weiss, R. F., Fraser, P. J., Simmons, P. G., Cunnold, D. N., Alyea, F. N., O'Doherty, S., Salameh, P., Miller, B. R., Huang, J., Wang, R. H. J., Hartley, D. E., Harth, C., Steele, L. P., Sturrock, G., Midgley, P. M., and McCulloch, A.: A History of Chemically and Radiatively Important Gases in Air deduced from ALE/GAGE/AGAGE, J. Geophys. Res., 105, 17 751–17 792, 2000.

Riley, W. J., Subin, Z. M., Lawrence, D. M., Swenson, S. C., Torn, M. S., Meng, L., Mahowald, N. M., and Hess, P.: Barriers to predicting changes in global terrestrial methane fluxes: analyses using CLM4Me, a methane biogeochemistry model integrated in CESM, Biogeosciences, 8, 1925–1953, doi:10.5194/bg-8-1925-2011, 2011.

Ringeval, B., de NobletDucoudr, N., Ciais, P., Bousquet, P., Prigent, C., Papa, F., and Rossow, W. B.: An attempt to quantify the impact of changes in wetland extent on methane emissions on the seasonal and interannual time scales, Global Biogeochemical Cycles, 24, GB2003, 2010.

Sitch, S., Smith, B., Prentice, I. C., Arneth, A., Bondeau, A., Cramer, W., Kaplan, J. O., Levis, S., Lucht, W., Sykes, M. T., Thonicke, K., and Venevsky, S.: Evaluation of ecosystem dynamics, plant geography and terrestrial carbon cycling in the LPJ dynamic global vegetation model, Global Change Biology, 9, 161–185, doi:10.1046/j.1365-2486.2003.00569.x, 2003.

Tapley, B. D., Bettadpur, S., Ries, J. C., Thompson, P. F., and Watkins, M. M.: GRACE Measurements of Mass Variability in the Earth System, Science, 305, 503–506, doi:10.1126/science.1099192, 2004.

Walter, B. P., Heimann, M., and Matthews, E.: Modelling modern methane emissions form natural wetlands 1. Model description and results, Journal of Geophysical Research, 106, 34 189–34 206, 2001.

Wania, R., Ross, I., and Prentice, I. C.: Implementation and evaluation of a new methane model within a dynamic global vegetation model: LPJ-WHyMe v1.3.1, Geoscientific Model Development, 3, 565–584, doi:10.5194/gmd-3-565-2010, 2010.

Whalen, S. C.: Biogeochemistry of Methane Exchange between Natural Wetlands and the Atmosphere, Environmental Engineering Science, 22, 73–95, 2005.

	Decay Constant (yr^{-1})	Study
Amazon Wetlands ($\overline{\phi}_{Amazon}$)	2.6 - 9.6[a] (median=5.9)	**This Study**: Top-down wetland CH_4 emission parameter optimization
Withered Leaves (35°C)	4.0	**Miyajima et al. (1997)** Decay constant from anaerobic tropical leaf CH_4 mineralisation
Wetland Macrophyte Decomposition	1.0 - 5.5	**Longhi et al. (2008)**[b] : Measured decomposition rates in Paluda di Ostiglia, Italy
Soil Carbon Pool (10°C) Leaf Litter (10°C) Root Exudates (10°C)	0.001 - 0.03 0.35 13	**Wania et al. (2010)**: Bottom-up CH_4 Emissions from Northern Peatlands

[a]68% confidence interval
[b]Mass-loss decomposition rates

Table 1. Model and observed decay constants for organic matter decomposition in anaerobic environments

Study	Amazon Wetland CH_4 Emissions ($Tg\ CH_4\ yr^{-1}$)
Melack et al. (2004)	22
Fung et al. (1991)	5.3
Riley et al. (2011)	58.9 [a]
Bloom et al. (2010)	20.0
This study	**26.2 ± 9.8**

[a]High tropical fluxes by Riley et al. (2011) are a result of anomalously high predicted net primary productivity in the Community Land Model (CLM version 4)

Table 2. Estimates of total annual Amazon river basin wetland CH_4 emissions ($Tg\ CH_4\ yr^{-1}$)

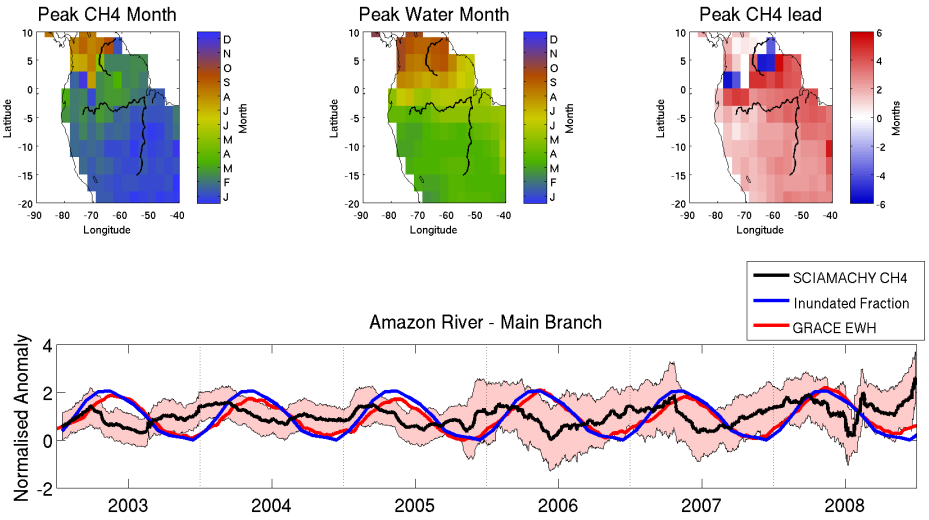

Fig. 1. Top: The timing (day of year) of peak CH_4 concentrations from SCIAMACHY (left), peak equivalent water height (EWH) from GRACE (middle), and the peak CH_4 concentration lead over tropical South America (right). Bottom: Normalised anomaly of GRACE EWH, mean flood fraction (Prigent et al., 2007) and mean CH_4 concentrations (including 1-standard deviation envelope) over the main branch of the Amazon river (0°–6°S, 40°–80°W).

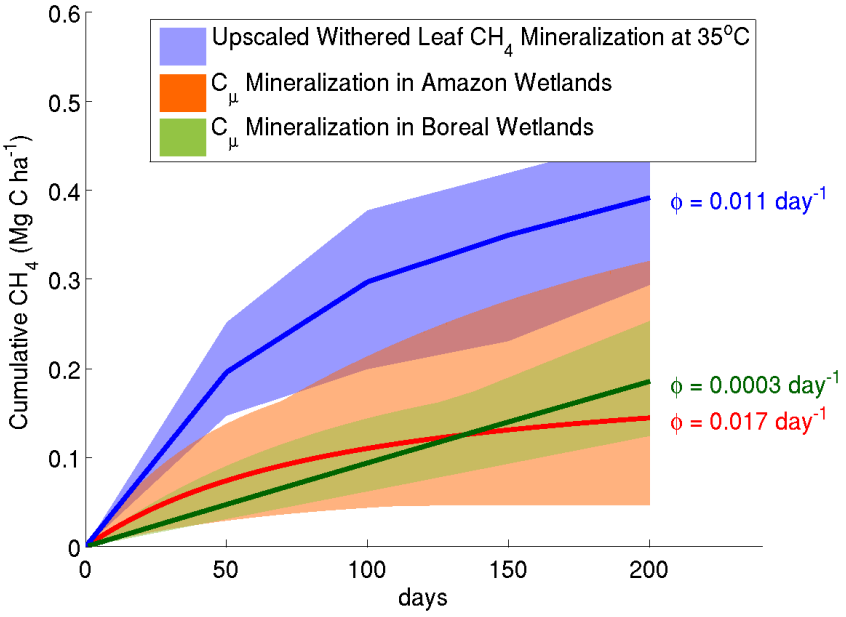

Fig. 2. Model and laboratory measurements of cumulative CH_4 emissions from withering leaves over a 200-day period. Blue: median and range of values from Miyajima et al. (1997). Red (green): median and 68% confidence interval range of CH_4 emissions from the Amazon river basin (boreal wetland) from C_μ and $\overline{\phi}$ values when N_μ = 0. A total litter stock of 17.5 Mg C ha^{-1} (Malhi et al., 2009) was used to upscale the Miyajima et al. (1997) CH_4 mineralisation rates.

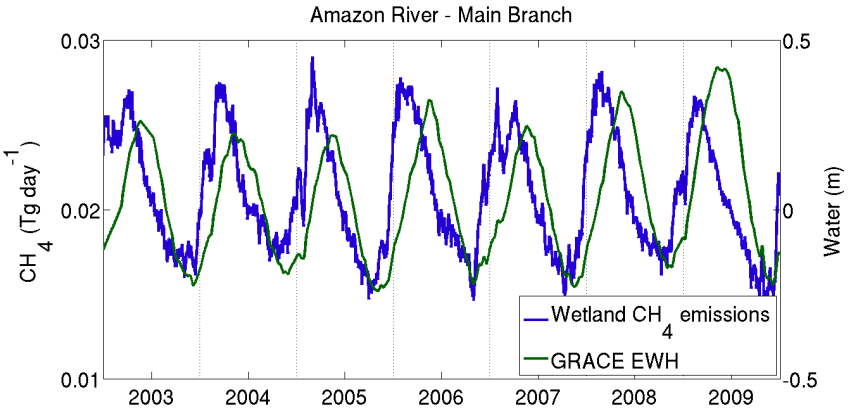

Fig. 3. Daily wetland CH_4 emissions for 2003–2009 (blue) and GRACE equivalent water height (green) over the central branch of the Amazon river (0°–6°S, 40°–80°W).

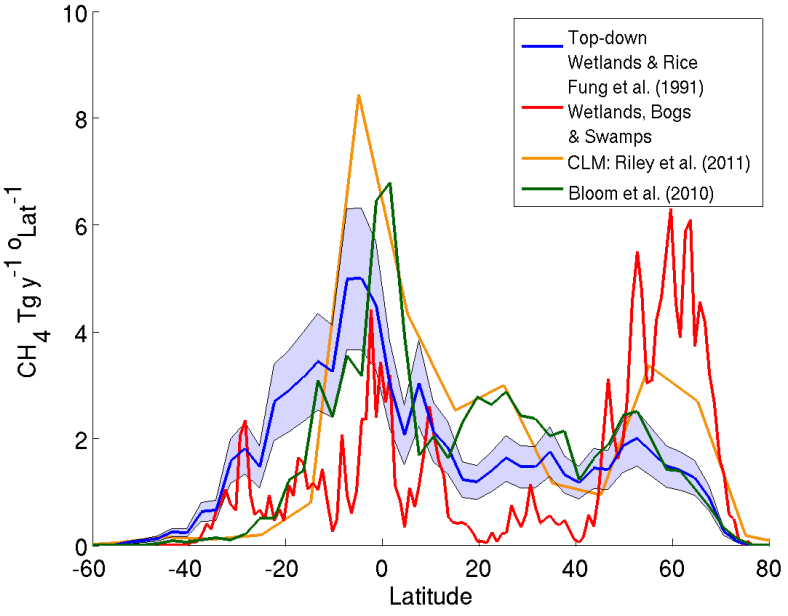

Fig. 4. Zonal profile of CH_4 emissions from wetlands and rice paddies: top-down approach (blue); Fung et al. (1991), wetlands only (red); Riley et al. (2011) wetland and rice paddy emissions (orange); Bloom et al. (2010) wetland and rice paddy CH_4 emissions (green). Riley et al. (2011) attribute their elevated tropical fluxes to anomalously high predicted net primary productivity in the Community Land Model (CLM version 4).

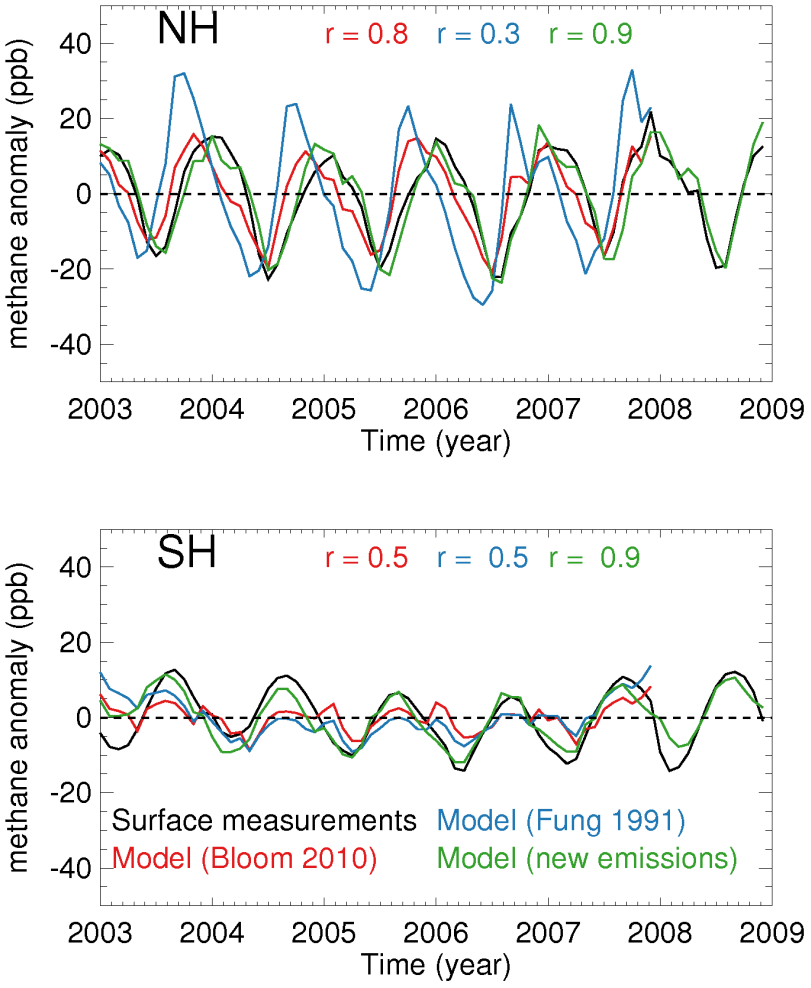

Fig. 5. Hemispheric mean observed and model methane anomalies from surface concentration measurements, 2003–2008. Surface concentration measurements (black) are from the GasLab, AGAGE and ESRL networks (Francey et al., 1996; Prinn et al., 2000; Cunnold et al., 2002; Dlugokencky et al., 2009). The GEOS-Chem global 3-D chemistry transport model (Fraser et al., 2011) is driven by wetland CH_4 emission estimates from Fung et al. (1991) (blue), Bloom et al. (2010) (red), and our new top-down approach (green).

Chapter 6

Discussion

The objective of this thesis has been to improve the current understanding of global biogenic CH_4 sources by using satellite data to test newly developed CH_4 source estimating methods. The main conclusions of my thesis are the following:

- CH_4 emissions from UV irradiation of foliar pectin at a global scale are a negligible source of CH_4.
- Global spaceborne CH_4 observations can be used to determine wetland CH_4 emission sensitivity to temperature and water availability.
- There is a strong indication that tropical CH_4 emissions are controlled by methanogenically available carbon on seasonal timescales.

As expected, my findings in turn pose new questions in the field of global CH_4 emissions. In addition to the discussion and conclusions in previous chapters, I will provide an overview the significance of my results in the global CH_4 source estimation, and will introduce main areas where a further understanding is needed to better quantify global-scale biogenic CH_4 emissions.

6.1 The Big Picture

On a global scale, the attribution of CH_4 to anaerobic and aerobic CH_4 production in natural environments remains challenging. Figure 6.1 shows the spatial overlap of fluxes across the atmosphere-biosphere boundary. As an example, in a partially flooded ecosystem, CH_4 is produced anaerobically in the flooded areas, and the wetland CH_4 source comprises of CH_4 fluxes through diffusion and ebullition to the atmosphere. In addition, Rice et al. (2010) find that up to 60 Tg CH_4 yr^{-1} of anaerobically produced CH_4 finds its way into the atmosphere through terrestrial vegetation in flooded soils. Methanotrophs in unsaturated aerobic soils consume CH_4, and amount to an overall sink of 20 - 45 Tg CH_4 yr^{-1}(Dutaur and Verchot, 2007). Finally, aerobically produced CH_4 spatially coincides with the above-mentioned sources and sinks.

In chapters 3, 4 and 5 I determined the global scale temporal behaviour of wetlands, which account for 100-231 Tg CH_4 yr^{-1} of the total CH_4 source. In chapter 2, I determined that one of the identified anaerobic CH_4 pathways, the UV irradiation of pectin, globally accounts for 0.2-1.0 Tg CH_4 yr^{-1} and is ultimately an insignificant source in terms of the global CH_4 budget, but may be potentially significant on a regional scale. Nonetheless, my upscaling of UV irradiated pectin emissions does not discard the possibility of an alternative, and potentially larger source of aerobically produced CH_4 (Keppler et al., 2009).

Therefore the presence of a globally significant aerobic CH_4 source from terrestrial vegetation is still plausible. From Keppler et al. (2006) it is expected that such a source is driven by UV radiation and therefore climatic feedbacks associated with surface UV irradiance and atmospheric chemistry (e.g. Paul, 2010) may significantly contribute to the overall radiative forcing of CH_4. In contrast, Niemi et al. (2002) find that an increase in UV-B irradiance correlates negatively with CH_4 emissions in the peatland microcosms, hence suggesting more complex feedbacks associated with future changes in global UV irradiance.

While sources and sinks of CH_4 can be identified by their isotopic weight, (e.g. Fung

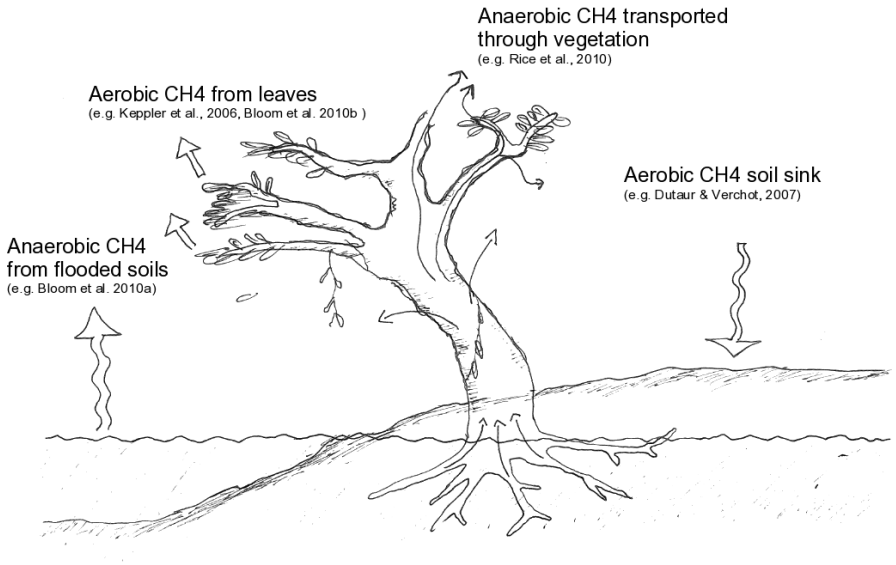

Figure 6.1: The overlapping CH_4 fluxes in a seasonally flooded ecosystem: wetland emissions, aerobic CH_4 emissions, transport of anaerobically produced CH_4 and the CH_4 soil sink.

et al., 1991; Keppler et al., 2006; Kai et al., 2011) the large volume of satellite observations of atmospheric CH_4 VMR cannot be isotopically deciphered, Process-based parameter optimisation, through which Bloom et al. (2010b) determined the magnitude and distribution of CH_4 emissions from wetlands, is an essential step in deciphering the mechanisms and ultimately the individual components of the global CH_4 cycle at a global scale. Global wetland CH_4 emission estimates are often characterised as either "top-down" or "bottom-up" estimates (see chapter 1). Nonetheless, the work carried out in chapters 3, 4 and 5 does not conceptually fit either category. The Bloom et al. (2010b) method is based on a process-based model, such as those used by bottom-up CH_4 estimates, but optimises the model parameters using a top-down optimisation approach. Examples of such approaches include global wetland CH_4 emission estimates by Gedney et al. (2004) and CO_2 uptake estimates by Nakatsuka and Maksyutov (2009). In contrast to top-down flux estimation (e.g Bousquet et al., 2006; Bergamaschi et al., 2009), the approach in Bloom et al. (2010b) is a top-down parameter optimization approach. Top-down parameter optimisation methods can be used to determine the wetland CH_4 emissions sensitivity to environmental variables at a global scale, and can be seen as complementary to the overall framework of global wetland CH_4 esti-

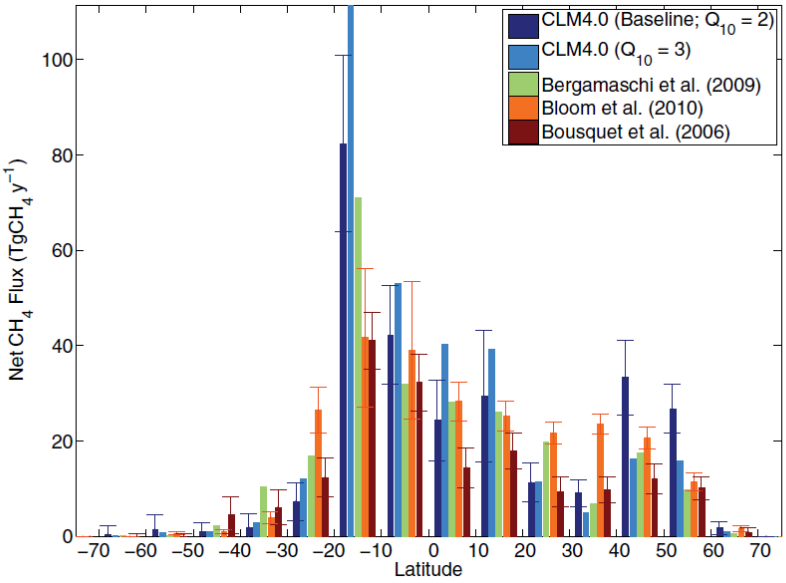

Figure 6.2: A comparison between global wetland CH_4 estimates by Riley et al. (2011), Bloom et al. (2010b), Bergamaschi et al. (2009) and Bousquet et al. (2006). Figure adapted from Riley et al. (2011).

mates. Hence, top-down parameter optimisation CH_4 emission estimates can inform top-down and bottom-up estimation process. Top-down flux estimation approaches often rely on a-priori estimates of CH_4 emissions (e.g. Bousquet et al., 2006; Bergamaschi et al., 2009), and the results from Bloom et al. (2010b) can be used as a-priori emission estimates in top-down approaches. Bottom-up emission estimates rely on global parameters relating to CH_4 emissions from wetlands, such as Q_{10} temperature dependence factor (e.g. Riley et al., 2011). Top-down parameter optimisation methods such as Bloom et al. (2010b) can provide globally optimised parameters to bottom-up emission estimates. Hence the work carried out in chapters 3, 4 and 5 can be seen as complementary to the global CH_4 wetland emission estimation effort. Figure 6.2 shows a comparison between global wetland and rice paddy CH_4 emission estimates by Riley et al. (2011), Bloom et al. (2010b), Bergamaschi et al. (2009) and Bousquet et al. (2006).

6.2 The Upcoming Challenges

The ever increasing volume of global atmospheric CH_4 observations data will inevitably result in uncertainty reduction of the estimates from Bloom et al. (2010b), and will help to constrain the global significance of the aerobic foliar CH_4 emissions (e.g. Bloom et al., 2010a). Nonetheless, some major challenges in quantifying CH_4 sources and sinks will persist regardless of the data volume. In this section I will discuss some of the most challenging aspects.

6.2.1 The Boreal Blind-Spot

Greenhouse gas observations from space rely on measurements of the reflected sunlight from the Earth's surface (e.g. Frankenberg et al., 2006). As a result, in the absence of reflected solar radiation, observations of CH_4 are impossible to achieve. When satellites are in nadir mode view (straight down) the poles are a continuous blind spot for all near polar orbiting satellites. A much greater seasonal "blind-spot" results from the lack of observations during boreal winter. Figure 6.3 shows the number of months during 2003-2004 throughout which no single value of SCIAMACHY CH_4 has been retrieved. While southern hemisphere near-polar CH_4 sources are less prominent in the global CH_4 cycle, a similar blind-spot will occur over the southern hemisphere.

While boreal summer-time CH_4 observations can be used to determine the temperature sensitivity of wetland CH_4 emissions, the absence of a year-round CH_4 cycle is a restricting factor for the Bloom et al. (2010b) method when determining (i) the onset of CH_4 emissions in spring; (ii) the decline in methanogenesis rates in autumn; and (iii) the overall atmospheric chemistry of boreal winter. Although the seasonal gap is incorporated in the uncertainty of the Bloom et al. (2010b) method, non-predictable biases may arise: for example, Mastepanov et al. (2008) have shown that increased CH_4 emissions from boreal ecosystems occur at the end of boreal summer due to the freezing of the ground. Although atmospheric chemistry and transport inversion estimates do not necessarily depend on overlying CH_4 observations, the complete lack of CH_4

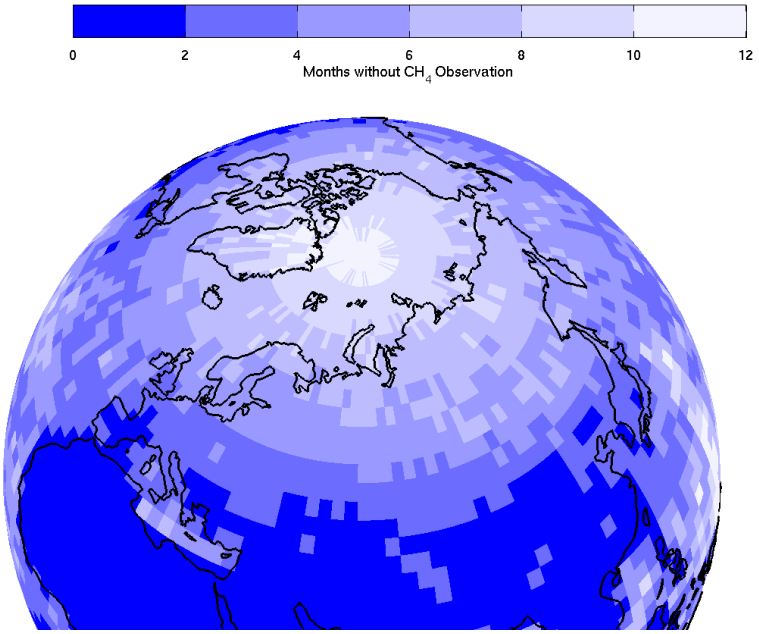

Figure 6.3: The satellite blind spot: maximum number of months without SCIAMACHY CH_4 observations at a 3° x 3° resolution.

observations during more than half a year will undoubtedly result in large uncertainties associated with boreal CH_4 emission estimates.

6.2.2 Gravity versus Innundated Fraction

While the Bloom et al. (2010b) method relied on global observations of gravity derived equivalent water height (Γ) from GRACE, other recent studies such as Ringeval et al. (2010) and Hodson et al. (2011) determine global wetland CH_4 emissions using multi-satellite-derived surface inundated fraction data by Prigent et al. (2007). In comparison to the GRACE Γ wetland volumetric constraint, the inundated fraction data provides a wetland area constraint. Papa et al. (2008) find that the GRACE and inundated fraction data co-vary over major river basins.

While the seasonal variability of temperate and tropical wetland areas can be observed with GRACE Γ, Bloom et al. (2010b) show that boreal CH_4 emissions from wetlands are driven by temperature. Nonetheless, GRACE gravity observations cannot distinguish between water and snow (Tapley et al., 2004). Therefore the observed Γ season-

ality does not reflect the seasonality of wetland depth and wetland extent.

Optimised values of $\frac{D}{\alpha}$ in boreal regions imply a temperature dependent wetland emissions (F_{CH_4}) seasonality (see chapter 3). Nonetheless, the presence of snow at high boreal latitudes throughout a significant part of the year implies a dual snow-water effect on the seasonality of Γ. Hence GRACE observations of Γ do not only represent saturated soil volume changes throughout the year, and the overall effect of wetland volume changes may be a significant factor in the seasonality of boreal wetland emissions.

6.2.3 The Tropical Carbon Cycle

Wetlands in the tropics are characterised by more rapid decomposition rates due to their distinct climatic setting. Moreover, as opposed to boreal ecosystems, temperature, net primary productivity and flooding do not seasonally coincide. The work from chapter 5 implies that the carbon cycle in tropical wetlands is a prominent factor in the seasonality of CH_4 emissions. Nonetheless, the process-based model devised in chapter 5 has assumed a constant influx of labile carbon in wetland ecosystems.

Plant litter is a significant contributor to the tropical wetland carbon stock. Litterfall varies significantly over seasonal timescales over the Amazon (Chave et al., 2010), and due to the high decay constants found for tropical wetlands any further approaches to the tropical CH_4 cycle need to address the significance of leaf litter seasonality on tropical wetland carbon stocks. The method in chapter 5 is a first order approximation of CH_4 bound carbon, and it is assumed that plant litter input is constant throughout the year. In order to determine the effects of plant litter seasonality on wetland CH_4 emissions, additional knowledge of plant litter seasonality must be incorporated into future estimates of seasonal CH_4 emission estimates from tropical wetlands. In addition to year-round observations of CH_4 fluxes in tropical wetlands, a combination of year-round tropical plant-litter rates (e.g. Chave et al., 2010), bottom-up CH_4 emission estimates from a dynamical vegetation model (e.g. Spahni et al., 2011), top-down determination of leaf litter seasonality (e.g. Caldararu et al., *in review*) is needed in order

to determine the overall effect of plant litter seasonality on wetland CH_4 emissions. Moreover, satellite observations of CH_4 are inherently biased to daytime cloud-free conditions. Therefore complementary CH_4 observations are essential in the effort to better constrain tropical wetland CH_4 fluxes.

6.2.4 Global Distinction between Wetlands and Rice Paddies

Wetland and rice paddy CH_4 emissions respond similarly to water availability and temperature on seasonal timescales. Although the sensitivity of these CH_4 emissions to environmental parameters is expected to be similar, major differences have to be considered when their emissions are extrapolated on a global scale. Rice paddy emissions will vary according to the type of agriculture implemented on a local and regional scale, and the drainage timing will affect the seasonality of CH_4 emissions (e.g. Zhang et al., 2011). Moreover, as rice paddy flooding is controlled, global changes in wetland water volume (GRACE) will not necessarily reflect the changes in rice paddy CH_4 emissions. Nonetheless, other datasets may be brought into the localisation and quantification CH_4 emissions from rice paddies, such as national inventories of rice agriculture and satellite observations of the growth cycle (e.g. Chen et al., 2011). The isotopic signatures of agricultural CH_4 (105-215‰) and wetland CH_4 (38-75‰) are distinct (Kai et al., 2011). Therefore by developing a method to incorporate isotope CH_4 surface measurements, the uncertainty in the distinction between wetlands and rice paddies can be reduced.

6.3 Future Prospects of Process-Based Wetland CH_4 Emissions Modelling

There is an increasing amount of global scale datasets relating to wetland and the subsequent CH_4 emissions. The ESA Gravity field and steady-state Ocean Circulation Explorer (GOCE) satellite retrieves the Earth's gravitational field at a spatial resolution of spherical harmonic degree and order 200 (approximately 200km resolution) and in conjunction with other datasets the observation accuracy of the Earth's geoid is

expected to be 1-3 cm (Rummel and Gruber, 2010). Atmospheric CH_4 VMR retrievals from the Greenhouse gases Observing SATellite (GOSAT) date from April 2009, and bear an unprecedented accuracy of 0.4-0.8% (Parker et al., 2011). These datasets can be used in conjunction with GRACE and SCIAMACHY observations in order to reduce the overall uncertainty of parameter optimisation using the Bloom et al. (2010b) method.

The top-down approach by Bloom et al. (2010b) can be developed and implemented (i) on other sources and sinks at a local, regional and global scale; and (ii) using a transport model to determine transport and loss of CH_4 in the atmosphere. Tall towers and aircraft CH_4 observations, eddy-covariance flux measurements (e.g. Dengel et al., 2011) and global flask networks (Dlugokencky et al., 2009) in conjunction with satellite CH_4 VMR can be used to optimise wetland model parameters. A transport model can be used to link the process-based model to the atmospheric CH_4 observations. For example, by combining an atmospheric transport model and a process-based model, Nakatsuka and Maksyutov (2009) have optimised maximum light-use efficiency and Q_{10} coefficients for 11 biomes on a global scale by minimising the differences between modelled and observed atmospheric CO_2. Finally, the parameters derived from top-down parameter optimisation wetland CH_4 emission estimates can be used to determine CH_4 emissions in future and past climates. For example, Bloom et al. (2010b) water-temperature dependence relationships can be used to determine future CH_4 wetland emissions if the process-based model is adapted to incorporate future climate scenarios, such as HadCM3 temperature and precipitation outputs for 2000-2100.

References

Bergamaschi, P., C. Frankenberg, J. F. Meirink, M. Krol, M. G. Villani, S. Houweling, F. Dentener, E. J. Dlugokencky, J. B. Miller, L. V. Gatti, A. Engel, and I. Levin, 2009: Inverse modeling of global and regional CH_4 emissions using SCIAMACHY satellite retrievals. *Journal of Geophysical Research (Atmospheres)*, **114**, D22301, doi:10.1029/2009JD012287.

Bloom, A. A., J. Lee-Taylor, S. Madronich, D. J. Messenger, P. I. Palmer, D. S. Reay, and A. R. McLeod, 2010a: Global methane emission estimates from ultraviolet irradiation of terrestrial plant foliage. *New Phytologist*, **187**, 417–425.

Bloom, A. A., P. I. Palmer, A. Fraser, D. S. Reay, and C. Frankenberg, 2010b: Large-Scale Controls of Methanogenesis Inferred from Methane and Gravity Spaceborne Data. *Science*, **327**, 322–325.

Bousquet, P., P. Ciais, J. B. Miller, E. J. Dlugokencky, D. A. Hauglustaine, C. Prigent, G. R. van der Werf, P. Peylin, E.-G. Brunke, C. Carouge, R. L. Langenfelds, J. Lathière, F. Papa, M. Ramonet, M. Schmidt, L. P. Steele, S. C. Tyler, and J. White, 2006: Contribution of anthropogenic and natural sources to atmospheric methane variability. *Nature*, **443**, 439–443, doi:10.1038/nature05132.

Chave, J., D. Navarrete, S. Almeida, E. Álvarez, L. E. O. C. Aragão, D. Bonal, P. Châtelet, J. E. Silva-Espejo, J.-Y. Goret, P. von Hildebrand, E. Jiménez, S. Patiño, M. C. Peñuela, O. L. Phillips, P. Stevenson, and Y. Malhi, 2010: Regional and seasonal patterns of litterfall in tropical South America. *Biogeosciences*, **7**, 43–55.

Chen, J., J. Huang, and J. Hu, 2011: Mapping rice planting areas in southern china using the china environment satellite data. *Mathematical and Computer Modelling*, **54**, 1037 – 1043, doi:10.1016/j.mcm.2010.11.033, mathematical and Computer Modeling in agriculture (CCTA 2010).

Dengel, S., P. E. Levy, J. Grace, S. K. Jones, and U. M. Skiba, 2011: Methane emissions from sheep pasture, measured with an open-path eddy covariance system. *Global Change Biology*, doi:10.1111/j.1365-2486.2011.02466.x.

Dlugokencky, E. J., P. Lang, and K. Masarie, 2009: Atmospheric methane dry air mole fractions from the NOAA ESRL carbon cycle cooperative global air sampling network, 1983-2007, version: 2008-07-02.

Dutaur, L. and L. V. Verchot, 2007: A global inventory of the soil CH_4 sink. *Global Biogeochemical Cycles*, **21**, GB4013, doi:10.1029/2006GB002734.

Frankenberg, C., J. F. Meirink, P. Bergamaschi, A. P. H. Goede, M. Heimann, S. Körner, U. Platt, M. van Weele, and T. Wagner, 2006: Satellite chartography of atmospheric methane from SCIAMACHY on board ENVISAT: Analysis of the years 2003 and 2004. *Journal of Geophysical Research (Atmospheres)*, **111**, D07303, doi:10.1029/2005JD006235.

Fung, I., J. John, J. Lerner, E. Matthews, M. Prather, L. P. Steele, and P. J. Fraser, 1991: Three-dimensional model synthesis of the global methane cycle. *Journal of Geophysical Research*, **96**, 13033–13065, doi:10.1029/91JD01247.

Gedney, N., P. M. Cox, and C. Huntingford, 2004: Climate feedback from wetland methane emissions. *Geophysical Research Letters*, **31**, L20503, doi:10.1029/2004GL020919.

Hodson, E. L., B. Poulter, N. E. Zimmermann, C. Prigent, and J. O. Kaplan, 2011: The El Niño-Southern Oscillation and wetland methane interannual variability. *Geophysical Research Letters*, **38**, L08810, doi:10.1029/2011GL046861.

Kai, F. M., S. C. Tyler, J. T. Randerson, and D. R. Blake, 2011: Reduced methane growth rate explained by decreased northern hemisphere microbial sources. *Nature*, **476**, 194–197.

Keppler, F., M. Boros, C. Frankenberg, J. Lelieveld, A. McLeod, A. M. Pirttil, T. Rckmann, and J. Schnitzler, 2009: *Environmental Chemistry*, **6**, 459–465.

Keppler, F., J. T. G. Hamilton, M. Braß, and T. Röckmann, 2006: Methane emissions from terrestrial plants under aerobic conditions. *Nature*, **439**, 187–191, doi:10.1038/nature04420.

Mastepanov, M., C. Sigsgaard, E. J. Dlugokencky, S. Houweling, L. Ström, M. P. Tamstorf, and T. R. Christensen, 2008: Large tundra methane burst during onset of freezing. *Nature*, **456**, 628–630, doi:10.1038/nature07464.

Nakatsuka, Y. and S. Maksyutov, 2009: Optimization of the seasonal cycles of simulated CO_2 flux by fitting simulated atmospheric CO_2 to observed vertical profiles. *Biogeosciences Discussions*, **6**, 5933–5957.

Niemi, R., P. J. Martikainen, J. Silvola, A. Wulff, S. Turtola, and T. Holopainen, 2002: Elevated uv-b radiation alters fluxes of methane and carbon dioxide in peatland microcosms. *Global Change Biology*, **8**, 361–371, doi:10.1046/j.1354-1013.2002.00478.x.

Papa, F., A. Güntner, F. Frappart, C. Prigent, and W. B. Rossow, 2008: Variations of surface water extent and water storage in large river basins: A comparison of different global data sources. *Geophysical Research Letters*, **351**, L11401, doi:10.1029/2008GL033857.

Parker, R., H. Boesch, A. Cogan, A. Fraser, L. Feng, P. I. Palmer, J. Messerschmidt, N. Deutscher, D. W. T. Griffith, J. Notholt, P. O. Wennberg, and D. Wuncha, 2011: Methane observations from the greenhouse gases observing satellite: Comparison to ground-based tccon data and model calculations. *Geophysical Research Letters*, **38**, L15807.

Paul, N. D., 2010: The sunny side of greenhouse gas emissions quantifying the contribution of aerobic methane production to global methane budgets. *New Phytologist*, **187**, 263–265, doi:10.1111/j.1469-8137.2010.03348.x.

Prigent, C., F. Papa, F. Aires, W. B. Rossow, and E. Matthews, 2007: Global inundation dynamics inferred from multiple satellite observations, 1993-2000. *Journal of Geophysical Research (Atmospheres)*, **112**, D12107, doi:10.1029/2006JD007847.

Rice, A. L., C. L. Butenhoff, M. J. Shearer, D. Teama, T. N. Rosenstiel, and M. A. K. Khalil, 2010: Emissions of anaerobically produced methane by trees. *Geophysical Research Letters*, **37**, L03807, doi:10.1029/2009GL041565.

Riley, W. J., Z. M. Subin, D. M. Lawrence, S. C. Swenson, M. S. Torn, L. Meng, N. M. Mahowald, and P. Hess, 2011: Barriers to predicting changes in global terrestrial methane fluxes: analyses using CLM4Me, a methane biogeochemistry model integrated in CESM. *Biogeosciences*, **8**, 1925–1953, doi:10.5194/bg-8-1925-2011.

Ringeval, B., N. de NobletDucoudr, P. Ciais, P. Bousquet, C. Prigent, F. Papa, and W. B. Rossow, 2010: An attempt to quantify the impact of changes in wetland extent on

methane emissions on the seasonal and interannual time scales. *Global Biogeochemical Cycles*, **24**, GB2003.

Rummel, R. and T. Gruber, 2010: Gravity and steady-state ocean circulation explorer goce. *System Earth via Geodetic-Geophysical Space Techniques*, F. M. Flechtner, T. Gruber, A. Gntner, M. Mandea, M. Rothacher, T. Schne, J. Wickert, L. Stroink, V. Mosbrugger, and G. Wefer, eds., Springer Berlin Heidelberg, Advanced Technologies in Earth Sciences, 203–212.

Spahni, R., R. Wania, L. Neef, M. van Weele, I. Pison, P. Bousquet, C. Frankenberg, P. N. Foster, F. Joos, I. C. Prentice, and P. van Velthoven, 2011: Constraining global methane emissions and uptake by ecosystems. *Biogeosciences Discussions*, **8**, 221–272, doi:10.5194/bgd-8-221-2011.

Tapley, B. D., S. Bettadpur, J. C. Ries, P. F. Thompson, and M. M. Watkins, 2004: GRACE Measurements of Mass Variability in the Earth System. *Science*, **305**, 503–506, doi:10.1126/science.1099192.

Zhang, Y., Y. Y. Wang, S. L. Su, and C. S. Li, 2011: Quantifying methane emissions from rice paddies in Northeast China by integrating remote sensing mapping with a biogeochemical model. *Biogeosciences*, **8**, 1225–1235, doi:10.5194/bg-8-1225-2011.